

**Mitochondrial Aspartyl-tRNA Synthetase (DARS2)
Deficiency and Tissue-Specific Consequences of
Defective Mitochondrial Translation**

Inaugural-Dissertation

zur

Erlangung des Doktorgrades

der Mathematisch-Naturwissenschaftlichen Fakultät

der Universität zu Köln



vorgelegt von

ŞÜKRÜ ANIL DOĞAN
aus Malatya, Türkei

Köln 2014

Berichterstatter: **Prof. Dr. Aleksandra Trifunovic**

Prof. Dr. Elena Rugarli

Tag der mündlichen Prüfung: 28.01.2014

To My Dear Family and Beloved Ones...

Table of Contents

| | |
|---|-----------|
| Table of Contents | iv |
| List of Figures | vii |
| List of Tables | ix |
| Abbreviations | x |
| Abstract | xiii |
| Zusammenfassung | xv |
| 1. Introduction..... | 1 |
| 1.1. Mitochondria..... | 2 |
| 1.2. Mitochondrial Diseases | 4 |
| 1.2.1 Mitochondrial genetics..... | 4 |
| 1.2.2 Mitochondrial diseases caused by mitochondrial DNA (mtDNA) mutations | 6 |
| 1.2.3 Mitochondrial diseases caused by nuclear DNA (nDNA) mutations | 10 |
| 1.3. (Mitochondrial) Aminoacyl-tRNA synthetases and -related diseases | 12 |
| 1.3.1 Aminoacyl-tRNA synthetases | 12 |
| 1.3.2 Mitochondrial aminoacyl-tRNA synthetase-related diseases | 16 |
| 1.4. Mitochondrial Stress Signaling | 19 |
| 1.4.1 Mitochondrial retrograde signaling..... | 20 |
| 1.4.2 Mitochondrial anti-oxidative response | 22 |
| 1.4.3 Mitochondrial unfolded protein response (UPR ^{mt})..... | 23 |
| 1.4.3.1 ‘Mitokines’ and Fibroblast growth factor 21 (FGF21) | 26 |
| 1.4.4 (Macro)Autophagy and Mitophagy | 27 |
| 1.5. Objectives | 29 |
| 2. Materials and Methods..... | 32 |
| 2.1 Mouse Experiments..... | 32 |
| 2.1.1 Animal Care | 32 |
| 2.1.2 Mouse handling and breeding..... | 32 |
| 2.1.3 Mice..... | 32 |
| 2.1.4 Blood collection and determination of blood glucose, non-esterified fatty acids and FGF21 levels..... | 33 |
| 2.1.5 Analysis of body composition (NMR)..... | 34 |
| 2.1.6 Perfusion..... | 34 |
| 2.2 Molecular biology | 35 |
| 2.2.1 Isolation of genomic DNA from mice tails..... | 35 |
| 2.2.2 Isolation of genomic DNA from mice tissues | 35 |
| 2.2.3 Isolation of total RNA from mice tissues | 36 |
| 2.2.4 Quantification of nucleic acids | 36 |
| 2.2.5 Polymerase chain reaction (PCR) | 36 |
| 2.2.6 Southern blot analysis for mitochondrial DNA (mtDNA) quantification..... | 38 |
| 2.2.7 Northern blot analysis for mRNA and tRNA levels | 39 |
| 2.2.8 Reverse transcriptase PCR (Gene expression analysis)..... | 40 |
| 2.3 Biochemistry | 41 |
| 2.3.1 Protein isolation from tissues | 41 |
| 2.3.2 Mitochondria isolation from tissues other than skeletal muscle..... | 42 |

| | | |
|------------|--|------------|
| 2.3.3 | Mitochondria isolation from skeletal muscle | 42 |
| 2.3.4 | Blue Native polyacrylamide gel electrophoresis (BN-PAGE) and in-gel activity of respiratory chain complexes I and IV..... | 43 |
| 2.3.5 | Western blot analysis | 44 |
| 2.3.6 | Citrate synthase activity and respiratory chain complex activity assays..... | 46 |
| 2.3.7 | Oxygen consumption rates | 46 |
| 2.3.8 | Analyses of de novo transcription and translation in isolated mitochondria | 46 |
| 2.3.9 | tRNA aminoacylation assay | 47 |
| 2.4 | Histological Analyses..... | 48 |
| 2.4.1 | Vibratome and cryostat sections..... | 48 |
| 2.4.2 | Transmission electron microscopy..... | 48 |
| 2.4.3 | Nissl Staining | 48 |
| 2.4.4 | COX-SDH staining..... | 49 |
| 2.4.5 | Hemotoxylin and Eosin staining (H&E Staining) | 49 |
| 2.4.6 | Masson's trichrome staining..... | 49 |
| 2.4.7 | TUNEL assay | 50 |
| 2.4.8 | Immunohistochemical and immunofluorescence analyses | 50 |
| 2.5 | Statistical analyses | 51 |
| 2.6 | Chemicals and biological material..... | 51 |
| 3. | Results | 54 |
| 3.1. | Mitochondrial aspartyl-tRNA synthetase (DARS2) is essential for embryonic development in the mouse | 54 |
| 3.2. | DARS2 +/- mice are haplosufficient..... | 55 |
| 3.3. | Tissue-specific disruption of <i>Dars2</i> | 57 |
| 3.4. | DARS2 deficiency leads to early pathological changes in heart and skeletal muscle..... | 57 |
| 3.5. | Defective mitochondrial translation gives rise to strong respiratory chain deficiency | 62 |
| 3.6. | Mitochondrial stress responses are activated exclusively in DARS2-deficient heart | 68 |
| 3.7. | Early disturbance in mitochondrial proteostasis triggers stress responses in heart independent of MRC deficiency..... | 72 |
| 3.8. | DARS2 deficiency in forebrain neurons, hippocampus and striatum..... | 79 |
| 3.9. | DARS2 deficiency in forebrain cause respiratory chain deficiency | 81 |
| 3.10. | DARS2 deficiency causes progressive neuronal degeneration | 86 |
| 3.11. | Corticohippocampal nerve cell loss was highly likely to be caused by apoptosis | 88 |
| 3.12. | Increased immune response and gliosis in DARS2-deficient mice | 91 |
| 4. | Discussion | 97 |
| 4.1. | Mitochondrial aspartyl-tRNA synthetase (DARS2) is essential for embryonic development and one copy of the gene is enough for survival in mouse | 99 |
| 4.2. | DARS2 deficiency in heart and skeletal muscle causes comparable mitochondrial dysfunction in both tissues but activates mitochondrial stress responses exclusively in heart..... | 100 |
| 4.3. | DARS2 deficiency in forebrain neurons, hippocampus and striatum causes progressive neuronal degeneration accompanied by an activation of inflammatory responses and reactive astrogliosis in an age- and region-dependent manner..... | 110 |
| 4.4. | Summary and perspectives | 117 |
| | References..... | 119 |
| | Acknowledgements | 136 |

| | |
|--------------------------------|------------|
| Erklärung | 140 |
| Teilpublikationen | 141 |
| Curriculum Vitae | 142 |

List of Figures

| | |
|---|----|
| Figure 1.1 Human mitochondrial DNA and related diseases..... | 7 |
| Figure 1.2 Aminoacylation reaction..... | 13 |
| Figure 1.3 The mitochondrial unfolded protein response (UPR ^{mt}) in <i>Caenorhabditis elegans</i> | 25 |
| Figure 3.1 Disruption of <i>Dars2</i> in the germline..... | 55 |
| Figure 3.2 Respiratory Chain Complexes in Heart, Skeletal Muscle (SkM) and Liver Mitochondria of 104-Week-Old wild type (+/+) and heterozygous (+/-) <i>Dars2</i> mice..... | 56 |
| Figure 3.3 Phenotypic characterization of tissue-specific DARS2-deficiency in heart and skeletal muscle..... | 58 |
| Figure 3.4 Molecular characterization of tissue-specific DARS2-deficiency in heart and skeletal muscle..... | 59 |
| Figure 3.5 Immunohistochemical characterization of heart and skeletal muscle. | 60 |
| Figure 3.6 Increased mitochondrial mass was observed only in DARS2-deficient cardiomyocytes..... | 61 |
| Figure 3.7 Characterization of mitochondrial dysfunction in 6-week-old DARS2- deficient heart and skeletal muscle..... | 63 |
| Figure 3.8 Deregulated protein synthesis and steady-state levels of mitochondrial ribosomal subunits..... | 65 |
| Figure 3.9 RNA-related assays (Northern blot, aminoacylation and <i>in organello</i> transcription)..... | 67 |
| Figure 3.10 Antioxidant responses in DARS2-deficient heart and skeletal muscle. | 69 |
| Figure 3.11 Mitochondrial unfolded protein response and autophagy in 6-week- old DARS2-deficient heart and skeletal muscle..... | 70 |
| Figure 3.12 Characterization of mitochondrial dysfunction and stress responses in 3-week-old DARS2-deficient heart and skeletal muscle..... | 72 |
| Figure 3.13 Proof on perturbed mitochondrial proteostasis in DARS2-deficient hearts..... | 74 |
| Figure 3.14 Fibroblast growth factor 21 (FGF21) levels and related adaptive systemic changes in DARS2 knockout mice..... | 76 |
| Figure 3.15 Western blots analysis of 1-week-old hearts..... | 78 |
| Figure 3.16 Phenotypic characterization of tissue-specific DARS2-deficiency in forebrain neurons, hippocampus and striatum..... | 80 |
| Figure 3.17 Characterization of mitochondrial dysfunction in 28- (and 23-) week- old DARS2-deficient cortex and unaffected cerebellum..... | 82 |

| | |
|--|-----|
| Figure 3.18 Further characterization of mitochondrial dysfunction by COX-SDH staining and TEM in 28/30-week-old mice..... | 85 |
| Figure 3.19 Neuronal degeneration in DARS2-deficient cortex and hippocampus. | 87 |
| Figure 3.20 TUNEL staining in DARS2-deficient cortical and hippocampal regions. | 90 |
| Figure 3.21 IBA1 staining in DARS2-deficient cortical and hippocampal regions. | 94 |
| Figure 3.22 GFAP staining in DARS2-deficient cortical and hippocampal regions. | 96 |
| Figure 4.1 Proposed model for the heart-mediated stress responses to perturbed protein homeostasis caused by DARS2 deficiency..... | 110 |

List of Tables

| | |
|--|----|
| Table 1.1 Diseases and affected organs due to the mutations in mitochondrial aminoacyl-tRNA synthetases..... | 18 |
| Table 2.1 Genotyping PCR primer sequences | 37 |
| Table 2.2 Primary antibodies used for Western blot analysis..... | 45 |
| Table 2.3 Chemicals used and suppliers | 52 |
| Table 3.1 Length of mitochondrial-encoded MRC subunits and the number, percentage and positions of aspartate residues..... | 66 |

Abbreviations

| | |
|--------------------|--|
| 3' | three prime end of DNA sequence |
| 5' | five prime end of DNA sequence |
| A | adenosine |
| ADP | adenosine diphosphate |
| ARS2 | mitochondrial aminoacyl-tRNA synthetase |
| ATP | adenosine triphosphate |
| Avertin | tribromoethyl alcohol and tert-amyl alcohol |
| BAT | brown adipose tissue |
| bp | base pairs |
| BN | blue native |
| C | cytosine |
| CA | cornu ammonis (hippocampus) |
| CaMKII α | calcium/calmodulin-dependent kinase II α |
| cDNA | complementary DNA |
| CNS | central nervous system |
| Cre | bacteriophage P1 derived site-specific recombinase |
| COX | cytochrome c oxidase |
| Da | Dalton |
| DAPI | 4,6-diamidino-2-phenylindole |
| DARS2 | mitochondrial aspartyl-tRNA synthetase |
| ddH ₂ O | double distilled water |
| DG | dentate gyrus (hippocampus) |
| DNA | desoxyribonucleic acid |
| dNTP | desoxyribonucleotide-triphosphate |
| EC | enzyme commission number |
| ECL | enhanced chemoluminescence |

| | |
|-------------------------------|---|
| EDTA | ethylenediamine tetraacetate |
| EGTA | ethylene glycol tetraacetic acid |
| ELISA | enzyme-linked immunosorbent assay |
| EtBr | ethidium bromide |
| ETC | Electron transport chain |
| EtOH | ethanol |
| g | gram |
| G | guanine |
| GFAP | glial fibrillary acidic protein |
| h | hour |
| H&E | hematoxylin/eosin |
| H ₂ O ₂ | hydrogen peroxide |
| HCl | hydrochloric acid |
| HEPES | N-2-hydroxyethylpiperazine-N-2-ethansulfonic acid |
| i.e. | <i>id est</i> |
| i.p. | intraperitoneal |
| IBA1 | ionized calcium-binding adapter molecule |
| IRES | internal ribosomal entry site |
| k | kilo |
| KCl | potassium chloride |
| ko | knockout |
| KOH | potassium hydroxide |
| l | liter |
| L | loxP flanked |
| lacZ | gene encoding β -galactosidase |
| m | milli |
| M | molar |
| MgCl ₂ | magnesium chloride |
| min | minute |
| mtDNA | mitochondrial DNA |

| | |
|----------------------------------|---|
| mRNA | messenger RNA |
| NaCl | sodium chloride |
| NaF | sodium fluoride |
| NaH ₂ PO ₄ | monosodium phosphate |
| NaHCO ₃ | sodium bicarbonate |
| NaOH | sodium hydroxide |
| PAGE | polyacrylamide gel electrophoresis |
| PBS | phosphate buffered saline |
| PCR | polymerase chain reaction |
| RNA | ribonucleic acid |
| RNase | ribonuclease |
| Rpm | revolutions per minute |
| RT | room temperature |
| rtPCR | reverse transcription polymerase chain reaction |
| SDS | sodiumdodecylsulfate |
| sec | second |
| SEM | standard error of the mean |
| TBE | tris-borate-EDTA buffer |
| TE | tris-EDTA buffer |
| Tris | 2-amino-2-(hydroxymethyl)-1,3-propanediol |
| tRNA | transfer RNA |
| TWEEN | polyoxethylene-sorbitan-monolaureate |
| U | units |
| V | volt |
| v/v | volume per volume |
| w/v | weight per volume |
| WAT | white adipose tissue |
| WT | wild type |
| β-me | β-mercaptoethanol |
| μl | microliter |

Abstract

Cells try to counteract mitochondrial respiratory chain deficiencies via various kinds of largely unknown compensatory mechanisms, which play a central role in determining the extent of tissue-specific defects leading to disease phenotypes. In this study, we directly disrupted mitochondrial protein synthesis in mice by deleting the mitochondrial aspartyl-tRNA synthetase (*Dars2*) gene in a tissue-specific manner. We generated DARS2 deficiency in three different tissues (heart, skeletal muscle and forebrain neurons) and followed the dynamics and extent of pathological changes that occurred.

Deficiency of this essential protein leads to severe deregulation of mitochondrial protein synthesis in both heart and skeletal muscle. Yet, mitochondrial stress responses, like increased biogenesis, decreased autophagy, upregulation of mitochondrial unfolded protein response and mitokine FGF21, are only observed in DARS2-deficient cardiomyocytes. Surprisingly, the initiation of these stress responses is stemming from perturbed mitochondrial proteostasis, rather than the respiratory deficiency. Skeletal muscle, on the other hand, has intrinsic protective mechanisms that make it better equipped for folding and turnover of mitochondrial proteins, as well as slow turnover of mitochondrial transcripts that is coupled with possible upregulation of muscle regeneration. As a result, skeletal muscle is able to cope with increased levels of unassembled proteins better.

Although DARS2 depletion leads to very strong, deleterious respiratory deficiency in heart and skeletal muscle, causing animals to die within 7-8 weeks, its deficiency in forebrain neurons seems to have a milder effect that takes much longer time to develop. Defective mitochondrial translation in forebrain neurons caused abnormal behavior, and severe forebrain atrophy, which is caused by neuronal cell apoptosis and accompanied by activation of inflammatory responses such as microgliosis and reactive astrogliosis. Surprisingly, neurodegeneration occurred in an age-dependent manner and affected cortex and hippocampal regions differently.

Zusammenfassung

Zellen kompensieren Defekte der mitochondrialen Atmungskette mit Hilfe verschiedener oftmals noch weitgehend unbekannter Mechanismen, welche eine zentrale Rolle dabei spielen, in welchem Ausmaß gewebe-spezifische Defekte zu einem Krankheitsphänotyp beitragen.

In dieser Arbeit wurde mit Hilfe eines konditionalen Mausmodells gewebe-spezifisch die mitochondriale Protein-Synthese durch die Deletion des mitochondrialen Asprtyl-tRNA-Synthase (Dars2) Gens zerstört. Die Dynamik und das Ausmaß der hierdurch verursachten pathologischen Veränderungen wurden dabei einerseits im Herz- und Skelettmuskel sowie den Neuronen des Vorderhirns untersucht.

Der Verlust dieses essenziellen Proteins führt zu einer schweren Dysregulation der mitochondrialen Proteinsynthese sowohl im Herzen wie auch im Skelettmuskel. In DARS2-defizienten Kardiomyozyten konnten mitochondriale Stressreaktionen wie vermehrte Biogenese, verminderte Autophagie, die Hochregulierung der mitochondriale *unfolded protein response* und des Mitokins FGF21 nachgewiesen werden. Überraschenderweise werden diese Stressreaktionen jedoch weniger durch die auftretende respiratorische Fehlfunktion als vielmehr durch eine gestörte Protein-Homöostase hervorgerufen.

Im Skelettmuskel wiederum scheinen intrinsisch protektive Mechanismen zu existieren, welche die Faltung und Stabilität mitochondrialer Proteine erhöhen. Darüberhinaus weist der Skelettmuskel eine geringere Abbaurate mitochondrialer Transkripte auf, was möglicherweise in Zusammenhang mit einer erhöhten Muskel-Regeneration steht.

Im Gegensatz zu dem starken Phänotyp in Herz- und Skelettmuskel, bei dem die Mäuse innerhalb der ersten 7-8 Lebenswochen sterben, hat der Verlust von DARS2 spezifisch in Vorderhirn-Neuronen einen milderen Effekt, der deutlich länger für eine Entwicklung braucht. Defekte in der mitochondrialen Translation in diesem Gewebe verursacht abnormales Verhalten der Mäuse, eine schwere Atrophie des Vorderhirns, welche durch Apoptose der Neuronen hervorgerufen wird und die Aktivierung inflammatorischer Prozesse wie Mikrogliose and reaktive Astrogliose. Erstaunlicherweise tritt diese Neurodegeneration in altersabhängiger Weise auf und betrifft den Cortex und Hippocampus Regionen in unterschiedlicher Weise.

1. Introduction

Chinese philosophy explains the basis of nature through yin and yang, opposing forces, interdependent and able to exist only in relation to each other. The cell and the mitochondria have a very similar story. It is a tale of two enemies, who later became friends and allies. On this particular day, an ancient bacterium has invaded a single cell organism and instead of killing its host -as it happened many times before- it has found a safe haven and decided to stay within. Why not? The available nutrients were more than sufficient and the host offered shelter from the hostile environment of the ancient world. As for the single cell, beside the fact that it has survived the attack, benefits have also been great. Finally, it was granted a way to fight the poisonous oxygen in the surrounding and moreover, a new, more efficient energy form was suddenly available. This random encounter, which happened around 1-2 billion years ago to give rise to a synergically superior eukaryote, is described by the 'endosymbiotic theory' (Margulis, 1975). We now believe that the bacterium became integrated into the recipient cell and evolved into an organelle, the mitochondrion. Whether the random encounter was an invasion, infection or an unwilling indigestion event, the yin -the anaerobic cell- and the yang -the aerobic mitochondrion- left their differences behind and cooperated. The story, which started almost as a horror movie, turned into a romantic comedy in the end; or did it? Does the initial invasion of the bacteria continue even if it lost its ability to live independently? Is the mitochondrion abusing its powers in the cell and waiting a suitable time for revenge like a smart serial killer? A number of different disorders and diverse disease manifestations, as well as mitochondrial involvement in age-associated diseases, seem to prove this (Dogan and Trifunovic, 2011).

1.1. Mitochondria

Mitochondria are small organelles found in almost every eukaryotic cell. They form a very dynamic network, with constant fusion and fission, and occupy roughly one fifth of its total volume (McBride et al., 2006). The mitochondrion comprises of two membranes, the outer (OMM) of which is separated from the inner (IMM) one by the intermembrane space (IMS). The inner membrane exhibits a folded structure, named cristae, to maximize its surface. The innermost compartment of the mitochondria is called the mitochondrial matrix, and contains the mitochondrial genome, ribosomes, transfer RNAs (tRNAs), and various proteins and enzymes required for mitochondrial function. Mitochondria are unique because they are the only organelles in animal cells containing their own DNA, mitochondrial DNA (mtDNA).

The main function of the mitochondria is to use oxygen to generate the cell's major energy source, adenosine triphosphate (ATP). Thus, mitochondria are the powerhouses of the cell, generating ATP through the process of oxidative phosphorylation (OXPHOS). The proteins mediating electron transport and OXPHOS reside in the inner mitochondrial membrane. Moreover, mitochondria are very important for other cellular processes such as the first step of iron-sulfur (Fe-S) cluster biosynthesis, pyruvate decarboxylation and tricarboxylic acid cycle (TCA cycle), programmed cell death (apoptosis), steroid synthesis, calcium homeostasis and reactive oxygen species (ROS) formation.

The redox reactions in the cell feed the electron transport chain (ETC), which couples the electron transfer between an electron donor (NADH and FADH₂) and acceptor (oxygen) with the transfer of protons across the inner membrane. ETC has four macromolecular complexes: complex I (CO I - NADH:ubiquinone oxidoreductase, EC 1.6.5.3), complex II (CO II - Succinate dehydrogenase, EC

1.3.5.1), complex III (CO III - Ubiquinol cytochrome-c reductase, EC 1.10.2.2) and complex IV (CO IV or COX - cytochrome c oxidase, COX, EC 1.9.3.1). ETC catalyzes the electron transfer from reducing equivalents to molecular oxygen. Electrons are carried from CO I and CO II to CO III by coenzyme Q (CoQ or ubiquinone), linking TCA cycle to the process. Other sources of electrons, such as glycolysis, fatty acid oxidation, pyrimidine biosynthesis, choline and amino acid oxidation, exist that can donate electrons to CoQ (Vafai and Mootha, 2012). The electron transport from CO III to CO IV is mediated by soluble electron carrier cytochrome c. The synthesis of ATP from ADP and P_i in mitochondria is catalyzed by Complex V (or ATP synthase) (CO V, EC 3.6.3.14), which is powered by the proton gradient generated.

The organization of the OXPHOS system is more intricate than separately assembled complexes that are arranged in sequence in the inner mitochondrial membrane. Two models have been proposed for the organization of the mitochondrial respiratory chain: (i) the “fluid-state” or “random collision” model, where all OXPHOS complexes diffuse individually in the membrane and electron transfer depends on the random collision of the complexes and electron carriers (Hackenbrock et al., 1986); (ii) the “solid-state” model, which was proposed over 50 years ago, where the complexes together form large, rigid supramolecular structures termed respirasomes (Hatefi et al., 1962). The most plausible scenario, however, is a combination of these two models: the “plasticity” model. In this model, single complexes (“fluid-state” model) and different types of supercomplexes (“solid-state” model) coexist in the inner membrane. Complex I, for instance, is mainly found in association with complex III in various supercomplexes that additionally contain the electron carriers coenzyme Q and cytochrome c, complex IV, and sometimes complex II or V, and are able to respire. On the other hand, most of the complexes II and IV are present as individual entities. How the supercomplexes are assembled is currently not

known, but the significance of this arrangement for the stability of the different complexes is certain (Acin-Perez et al., 2008).

1.2. Mitochondrial Diseases

Mitochondrial diseases are one of the most common inborn errors of metabolism with a frequency of ~ 1 in 5000 (Schaefer et al., 2004). The term “mitochondrial encephalomyopathies” is often used since the affected organs/tissues are mostly brain and skeletal muscle (Shapira et al., 1977). Nowadays, the term “mitochondrial diseases” is almost exclusively used to describe diseases caused by defects in mitochondrial oxidative phosphorylation (OXPHOS) and not regarding the defects in numerous other cellular processes within mitochondria. Even within these boundaries, the classification of the mitochondrial diseases became quite complicated because mutations in either mtDNA or nuclear DNA (nDNA) genes coding for mitochondrial proteins lead to major and catastrophic diseases in humans. The first patient suffering from a mitochondrial disorder was identified in 1962 (Luft et al., 1962). Since then, thousands of patients have been diagnosed with different kinds of mitochondrial diseases. Due to the complexity of mitochondrial diseases, a new way of classification is embraced, one that is using the diseases’ genetic defect rather than clinical manifestation.

1.2.1 Mitochondrial genetics

Human mitochondrial DNA (mtDNA) is a small (16,569 basepair long), circular, double-stranded molecule (Figure 1.1). mtDNA only encodes 13 respiratory chain subunits, 22 tRNAs and 2 rRNAs, which are essential for mitochondrial translation (Larsson, 2010). During the course of evolution, mtDNA lost more than 99% of its original genes, thus now depends on nDNA for all its basic functions such as synthesis and assembly of most respiratory chain subunits,

synthesis of the phospholipids of the inner mitochondrial membrane and the necessary aids for its DNA's replication, transcription, and translation (Vafai and Mootha, 2012).

A couple of unique features of mtDNA genetics and inheritance make it very difficult to predict the course of the disease, prenatal diagnosis and/or genetic counseling in everyday clinical practice (Dogan and Trifunovic, 2011):

- mtDNA does not follow the Mendelian rules of inheritance while it is maternally inherited. Therefore, a mother carrying an mtDNA mutation can transmit it to her children, but only her daughters can further transmit it to the next generation. As each cell contains ~10,000 copies of mtDNA, a pathogenic mutation could be present in all of them or just few of copies of the molecule. Existence of two or more different populations of mtDNA in a single cell is called '*heteroplasmy*', in contrast to '*homoplasmy*' where all mtDNA molecules are identical.
- Threshold effect represents the minimal critical level of a pathogenic mutation in mtDNA that should be present in the cell or tissue to have a deleterious effect. A certain proportion of mutant mtDNA must be present before reduction in OXPHOS activity is observed, and the threshold seems to be lower in tissues that are more dependent on oxidative metabolism. It has been shown that there are different thresholds for different types of mtDNA mutations, 60% for large mtDNA deletions (Bourgeron et al., 1993) to 90% for some tRNA mutations (Chomyn et al., 1992; Hanna et al., 1995).
- The last but not least problem of mtDNA genetics is the mitotic segregation. Random distribution of mtDNA molecules during cell

division can lead to increased amounts of mutant mtDNA molecules in one of the daughter cells. This can lead to a cell carrying low levels of mutated molecules giving rise to one of relatively high levels, which in turn will affect OXPHOS in that cell.

1.2.2 Mitochondrial diseases caused by mitochondrial DNA (mtDNA) mutations

About 200 mtDNA point mutations and numerous single large-scale partial deletions have been associated with human diseases, most of which affect the nervous system (Wallace, 2005). Although genetically distinct, most mtDNA diseases share common features such as lactic acidosis, mosaic pattern of cells deficient in cytochrome c oxidase (COX) activity and massive mitochondrial proliferation in muscle resulting in ragged-red fibers (DiMauro et al., 1985). The more mtDNA-related diseases are identified, the more it became clear that mitochondrial diseases commonly have a delayed onset and progressive course.

Mutations in mtDNA are divided into two groups: (i) mtDNA point mutations and (ii) mtDNA rearrangements. A depiction of human mitochondrial DNA and the most common diseases can be found in Figure 1.1 (DiMauro and Schon, 2008). Diseases and the genes, the mutations in which cause the disease, are labeled with the same color.

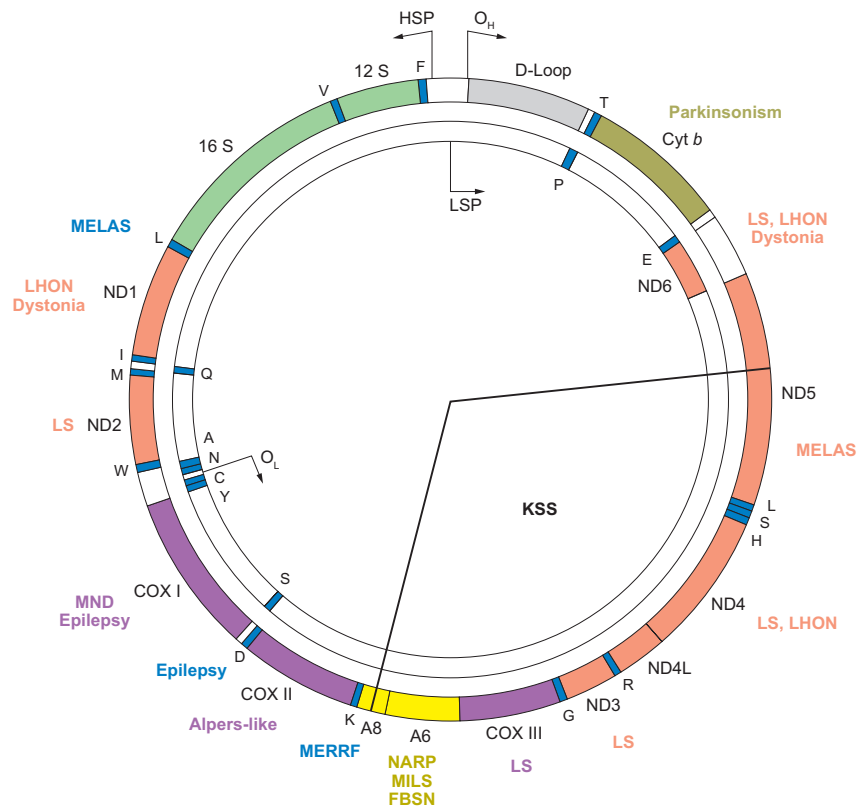


Figure 1.1 Human mitochondrial DNA and related diseases.

Human mitochondrial DNA. Names of the common mitochondrial diseases -caused by point mutations and/or rearrangements- are indicated on the figure. The disease manifestations and the related mutations are color-coded (DiMauro and Schon, 2008). LS, Leigh syndrome; MELAS, mitochondrial myopathy, encephalopathy, lactic acidosis, and stroke-like episodes; MERRF, myoclonic epilepsy and ragged red fibres; MILS, maternally inherited Leigh syndrome; NARP, neurogenic weakness, ataxia, and retinitis pigmentosa; PS, Pearson syndrome.

(i) mtDNA point mutations:

Most human mtDNA point mutations occur in tRNA genes, thus the most common mtDNA-related disorders are caused by mutations in those genes:

Mitochondrial encephalomyopathy, lactic acidosis and stroke-like episodes (MELAS) is a multisystem disorder that is often fatal in childhood or in young adulthood. The disease principally affects muscle, brain and the endocrine system. Stroke-like episodes are experienced before the patients are 40 years old. Most people with MELAS have a buildup of lactic acid in their bodies. Less commonly, people with MELAS may experience involuntary muscle spasms (myoclonus), impaired muscle coordination (ataxia), hearing loss, heart and kidney problems, diabetes, and hormonal imbalances (Kaufmann et al., 2011). Although the most common mutation is A3243G in tRNA^{Leu(UUR)}, other mutations (in protein coding genes, as well as tRNAs) have been found to be associated with the disease.

Myoclonus epilepsy and ragged red fibres (MERRF) is almost exclusively a result of mutations in tRNA^{Lys}. MERRF is characterized by muscle twitches, myopathy, and spasticity. Affected individuals sometimes have short stature and heart abnormalities (cardiomyopathy) (Moraes et al., 1993). Gomorri Trichrome staining of the muscle cells reveals clumps of diseased mitochondria accumulation in the subsarcolemmal region of the muscle fiber, which appear as 'rough' or so-called 'Ragged Red Fibers'. As in MELAS, the disease affects translational efficiency via failure in tRNA modification with taurine (Suzuki et al., 2011).

Additionally, missense mutations in mtDNA protein coding genes can also result in an array of clinical manifestations:

A mutation in the mtDNA ATP6 gene is associated with ***neurogenic muscle weakness, ataxia, and retinitis pigmentosum (NARP)*** when present at lower percentages of mutant (~40%) (Holt et al., 1990) and ***lethal childhood Leigh syndrome*** when present at higher percentages (~95%) of mutant (Tatuch et al., 1992).

Leber's hereditary optic neuropathy (LHON), the most common mtDNA-related disease, causes severe visual loss in both eyes. LHON, mostly an early-onset disease, is usually caused by homoplasmic mutations in one of three genes encoding complex I subunits (G11778A in NADH dehydrogenase 4 (ND4), G3460A in ND1 and T14484C in ND6). A significant percentage of people with a mutation that causes LHON do not develop any features. Specifically, more than 50 percent of males with a mutation and more than 85 percent of females with a mutation never experience vision loss or related medical problems (Man et al., 2002).

(ii) mtDNA rearrangements:

Systemically distributed mtDNA rearrangement mutations, mostly deletions, can be either inherited or spontaneous. Deletions usually result in a spectrum of symptoms. The nature and severity of the symptoms from mtDNA deletion rearrangements is usually due to the tissue distribution of the rearranged mtDNAs (Wallace, 2005).

Kearns–Sayre syndrome (KSS) is defined by the onset before age 20 of ophthalmoplegia (paralysis of the muscles that move the eyeballs), ptosis (droopy eyelids), pigmentary retinopathy (Kearns and Sayre, 1958). In this multisystemic disorder, partially deleted mtDNAs are present in all examined tissues. In chronic progressive external ophthalmoplegia (CPEO) deleted mtDNAs are found only in muscle (Moraes et al., 1989). In Pearson's syndrome, which is characterized by sideroblastic anaemia and exocrine pancreas dysfunction, deleted mtDNAs are initially abundant in haematopoietic cells (Pearson et al., 1979).

1.2.3 Mitochondrial diseases caused by nuclear DNA (nDNA) mutations

Mitochondrial diseases caused by a mutation in nuclear encoded genes are a very heterogeneous group. Not only are most of the ~80 structural proteins of the OXPHOS system encoded by nDNA, but all the proteins needed for their import from the cytoplasm and assembly in mitochondria are also encoded by the nucleus. Defects in any of these proteins could lead to functionally impaired OXPHOS and therefore to mitochondrial disease. Furthermore, defects in any protein affecting stability, expression and/or integrity of mtDNA could lead to the same deleterious effect.

Mitochondrial diseases caused by mutations in nDNA can be divided into four categories (DiMauro and Schon, 2008):

- 1) Mutations in genes encoding respiratory chain subunits
- 2) Mutations in genes encoding ancillary proteins
- 3) Mutations in genes affecting the lipid milieu of respiratory chain
- 4) Mutations in genes encoding for mtDNA maintenance, replication, transcription and translation

1) Mutations in genes encoding respiratory chain subunits: A severe autosomal-recessive neurological disease, clinical features of which includes psychomotor retardation with extrapyramidal signs, restlessness, global dementia, severe defects in verbal communication, and mild axial hypotonia has been found in 2008 (Barel et al., 2008). Mutations in nuclear-encoded UQCRQ, encoding ubiquinol-cytochrome c reductase, CO III subunit VII, are found to be the main reason for the observed phenotypes. In most of the cases, the mitochondrial-encoded subunit of CO III (cytb) is the main cause of disease phenotypes (CO III is composed of ten nuclear-encoded subunits and one mitochondrial-encoded subunit). So far, one other nuclear mutation in protein coding genes of respiratory chain has been identified: the UQCRB gene (ubiquinol-cytochrome c reductase

binding protein), encoding subunit VI of CO III (De Meirleir et al., 2003). One patient with this mutation is shown to have CO III dysfunction with clinical hypoglycemia and lactic acidosis (Haut et al., 2003).

2) Mutations in genes encoding ancillary proteins: Leigh syndrome (LS), or subacute necrotizing encephalomyelopathy, is a neurodegenerative disorder characterized by predominant involvement of the central nervous system (CNS) (Leigh, 1951). LS is an early-onset and progressive disease. This condition is characterized by progressive loss of mental and movement abilities (psychomotor regression) and typically results in death within a couple of years, usually due to respiratory failure (Finsterer, 2008). Mutations in both nuclear and mitochondrial genes have been identified in LS patients. However, mutations in the nuclear *Surf1* gene, coding for a putative CO IV assembly factor are one of the main cause of LS. In these patients, SURF1p mutations or depletions cause a reduction in the fully assembled COX (Tiranti et al., 1999).

3) Mutations in genes affecting the lipid milieu of respiratory chain: Cardiolipin is the major component of the inner mitochondrial membrane and it has been shown to participate in the formation of supercomplexes in yeast (Zhang et al., 2005). This fact exemplifies the importance of cardiolipin in proper respiratory function. Barth syndrome, an X-linked recessive disease manifesting cardiomyopathy, causes underdeveloped skeletal musculature and muscle weakness, growth delay, 3-methylglutaconic aciduria, and altered composition of cardiolipin. Mutations in the *TAZ* gene, encoding for tafazzin, is found to be responsible for the disease (Schlame and Ren, 2006). Tafazzin, a phospholipid acyltransferase, is involved in cardiolipin remodelling and mutations in the *TAZ* gene cause defects in mitochondrial architecture and function.

4) Mutations in genes encoding for mtDNA maintenance, replication, transcription and translation: The most common nuclear mutations associated with mitochondrial diseases are found in the gene encoding mitochondrial DNA polymerase γ . Around 70 disease manifestations related to the mutations in the gene coding for the polymerase have been reported: such as progressive external ophthalmoplegia (PEO) (Van Goethem et al., 2001), Alpers syndrome (Naviaux and Nguyen, 2004), mitochondrial neurogastrointestinal encephalomyopathy (MNGIE) (Van Goethem et al., 2003) or sensory ataxic neuropathy, dysarthria and ophthalmoparesis (SANDO) (Van Goethem et al., 2003).

One class of housekeeping genes encoded by nuclear genome, namely mitochondrial aminoacyl-tRNA synthetases, has also been implicated in various diseases. Before going deeper with the disease phenotypes caused by aminoacyl-tRNA synthetases, we will have a closer look to these fascinating enzymes.

1.3. (Mitochondrial) Aminoacyl-tRNA synthetases and -related diseases

1.3.1 Aminoacyl-tRNA synthetases

One of the first steps during translation is aminoacylation: the covalent ‘charging’ of a tRNA with its cognate amino acid, a two-step process that uses ATP (Delarue, 1995). tRNA charging is performed by a highly specialized subgroup of enzymes, the aminoacyl-tRNA synthetases (ARSs). ARSs are ubiquitously expressed and highly conserved enzymes, which can be found in a range of species. In the first step, the amino acid and a molecule of ATP is bound via a specific ARS for that amino acid (Figure 1.2). Following the formation of an aminoacyl adenylate intermediate, a pyrophosphate molecule is released. The second step starts with the binding of the cognate tRNA molecule to the ARS.

After the binding of tRNA molecule, the amino acid is transferred to the tRNA and an adenosine monophosphate (AMP) molecule is released. After the releasing of the charged tRNA molecule and ARS is free for another aminoacylation reaction. Typically, ARSs have a catalytic domain and an anticodon-binding domain but some also have an editing domain for deacylating mischarged amino acids. The anticodon binding domain as well as the editing domain, which only some ARSs contain, is very important for specificity of the ARSs, as well as serves as a quality control mechanism of protein synthesis (Ling et al., 2009).

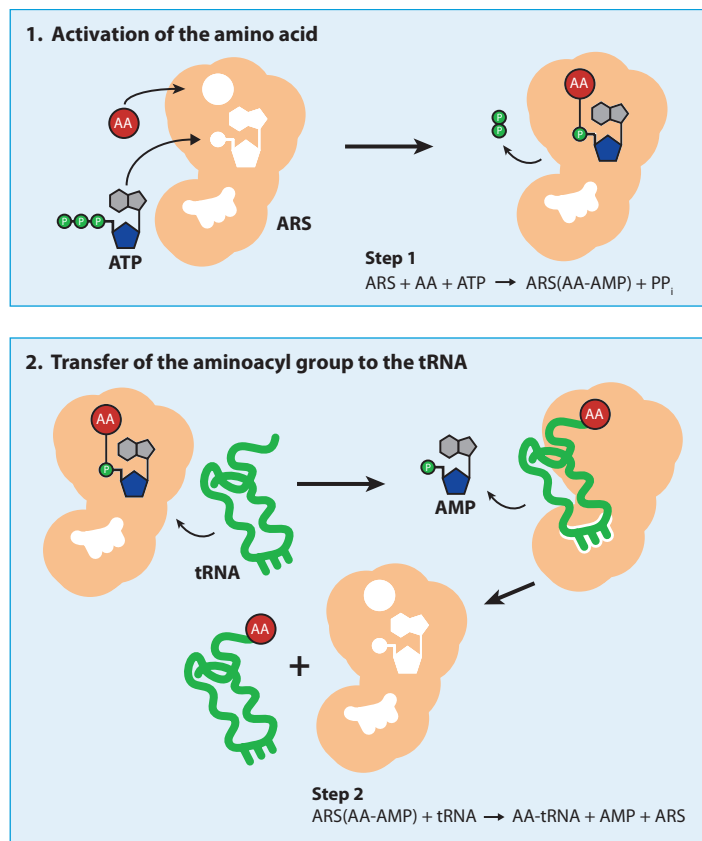


Figure 1.2 Aminoacylation reaction.

The two-step aminoacylation reaction catalyzed by aminoacyl-tRNA synthetases (ARSs) (Antonellis and Green, 2008). AA: aminoacid; PP_i: pyrophosphate; ATP: adenosine triphosphate; AMP: adenosine monophosphate.

Different criteria can be used for categorizing the ARSs. First, they can be grouped according to their place of action: (i) cytoplasmic, (ii) mitochondrial, and (iii) bifunctional. If we consider humans, there are 36 aminoacyl-tRNA synthetases; 17 cytoplasmic, 17 mitochondrial and 2 bifunctional. If we add up cytoplasmic/mitochondrial and bifunctional ones, we achieve the number 19, still one less than the total number of amino acids. This is due to the fact that one ARS, glutamyl-prolyl-tRNA synthetase, is responsible for charging tRNA^{Glu} and tRNA^{Pro} in the cytoplasm (Berthonneau and Mirande, 2000). Mammalian mitochondria have no enzyme corresponding to glutaminyl-tRNA synthetase so glutamine (Gln)-tRNA^{Gln} is synthesized indirectly via misacylated glutamic acid (Glu)-tRNA^{Gln} through transamidation (Nagao et al., 2009). The nomenclature for ARSs also differs according to where they are active. Cytoplasmic ARSs use the single-letter amino acid code followed by ARS: the gene symbol for cytoplasmic aspartyl-tRNA synthetase is, therefore, DARS. In the case of mitochondrial specific ARSs, a '2' is added to the end, thus, the symbol for mitochondrial aspartyl-tRNA synthetase is DARS2.

Another method of categorizing ARSs is via their distinct structural motifs: Class I and II. Class I ARSs have a characteristic ATP binding region, a parallel β -sheet nucleotide-binding domain, namely Rossmann fold. Class II ARSs contain three structural motifs (motif 1, 2, and 3) (Ibba and Soll, 2000). Class I synthetases attach the charged amino acid at the 2' OH and, class II synthetases at the 3' OH, on the ribose of the acceptor end of the tRNA.

Why do we have two different sets of ARSs? The co-existence of cytoplasmic and mitochondrial translation apparatus results also in two sets of distinct ARSs. Interestingly, it was shown that at least some mitochondrial ARSs can aminoacylate the corresponding cytoplasmic tRNAs but not vice versa (Buck and Nass, 1969). Of course, one of the reasons for that phenomenon can be explained with differences in the mitochondrial tRNA structures. The mammalian

mitochondrial genomes contain one gene for each tRNA, with the exceptions of tRNA^{Leucine} and tRNA^{Serine} for which two genes are present. Whereas the vast majority of eukaryotic cytosolic and prokaryotic tRNAs share a canonical structure, mt-tRNAs can be very different, or even be called ‘bizarre’ (Wolstenholme et al., 1987). Whereas most of these tRNAs have cloverleaf-like structures (except tRNA^{Ser(AGY)}, where the D-arm is completely absent), large variations in D-, and especially T-loop sizes are seen. Moreover, in mammalian mitochondria, the genetic code diverges from the universal one by the use of AUA for Methionine, UGA for Tryptophan, and AGA/AGG for a stop codon.

Some ARSs have been shown to have secondary, non-canonical functions. In humans, these functions includes, but not limited to, promoting rRNA biogenesis (for MARS) (Ko et al., 2000), inhibition of apoptosis (for QARS) (Ko et al., 2001), and promoting angiogenesis (for YARS and WARS) (Wakasugi et al., 2002a; Wakasugi et al., 2002b). Moreover, nine of the cytoplasmic synthetases are shown to be tightly bound together in a large multisynthetase complex (MSC), which also include three ‘aminoacyl tRNA synthetase-interacting multifunctional proteins’ (AIMPs): 1, 2, and 3 (Robinson et al., 2000; Han et al., 2003). Although there is still some ambiguity about the stoichiometry and total number of components, the synthetases found in those MSC are: EP-ARS, IARS, LARS, MARS, QARS, RARS, KARS and DARS. It was proposed that formation of MSCs increases the efficiency of tRNA charging by “channeling” substrates to the ribosome or to regulate the secondary functions of ARSs (Park et al., 2005). One of the open questions is whether mitochondria also contain MSCs. So far, there is only one example: it has been proposed that human mitochondrial tyrosyl-tRNA synthetase (YARS2) and bifunctional glycyl-tRNA synthetase (GARS) function as part of a high-molecular-weight complex (Sasarman et al., 2012).

1.3.2 Mitochondrial aminoacyl-tRNA synthetase-related diseases

The first case, in which mutations in a mitochondrial aminoacyl-tRNA synthetase gene cause a human genetic disease, was reported in 2003 (van der Knaap et al., 2003). Leukoencephalopathy with brain stem and spinal cord involvement and lactate elevation (LBSL) was first defined by characteristic magnetic resonance imaging (MRI) and spectroscopic findings. LBSL is a childhood or juvenile-onset disorder clinically characterized by slowly progressive cerebellar ataxia and spasticity with dorsal column dysfunction (decreased position and vibration sense). Among limbs, legs are affected more than the arms. Difficulty in articulation develops as the cognitive decline and learning problems occur. The disease causes the patients to be wheelchair dependent, usually during their teenager times. The MRI pattern shows differences from the other defined leukoencephalopathies, therefore giving a diagnostic tool for the disease. MRIs of the affected individuals show signal abnormalities in the cerebral white matter and specific brain stem and spinal cord tracts. Magnetic resonance spectroscopy (MRS) shows increased lactate in the abnormal white matter in almost all affected individuals (van der Knaap et al., 2003; Linnankivi et al., 2004). Involvement of other organs than the nervous system has never been reported.

Four years after the disease is characterized, the mutation responsible was discovered: LBSL is caused by mutations in the DARS2 gene, which encodes for the mitochondrial aspartyl-tRNA synthetase (Scheper et al., 2007). Most mapped mutations are predicted to affect splicing of exon 3, which causes a frameshift and truncation of the protein. These mutations are 'leaky', leading to an ablated, but not absent, expression of full-length DARS2 (van Berge et al., 2012). As being a rare disease, only 54 cases have been reported, and just 29 of these have been described clinically (Tzoulis et al., 2011). Majority (43/45) of the genetically confirmed cases were compound heterozygous for DARS2 mutations, which in most cases (41/43) included a frameshift-causing mutation in intron 2. Except the

‘common’ mutation, different types of mutations have been found in the other allele of *DARS2*, such as deletions, nonsense, splice site, and missense mutations (van Berge et al., 2013).

Previous reports hypothesized that homozygous *DARS2* mutations might not be compatible with life. However, two homozygous *DARS2* mutations were observed (Miyake et al., 2011; Synofzik et al., 2011). The mechanisms how these homozygous mutations are compatible with life need further addressing.

Since the initial discovery of an *ARS2*-mutation-leading-to-a-disease, last six years witnessed a number of *ARS2* mutations as being the sole cause of some diseases. Mutations in cytoplasmic and bifunctional *ARSs* share phenotypic and genotypic features, whereas diseases phenotypes caused by mutations in the corresponding mitochondrial enzymes are clinically more variable. Table 1.1 summarizes the diseases and the affected organs due to the mutations in different mitochondrial *ARS2s*.

Table 1.1 Diseases and affected organs due to the mutations in mitochondrial aminoacyl-tRNA synthetases.

| Gene | Disease | Affected organ | References |
|-------|---|----------------|----------------------------|
| DARS2 | Leukoencephalopathy with brain stem and spinal cord involvement and lactate elevation (LBSL) | Brain | Scheper et al., 2007 |
| RARS2 | Pontocerebellar Hypoplasia type 6 (PCH6) | Brain | Edvardson et al., 2007 |
| YARS2 | Myopathy, Lactic Acidosis, and Sideroblastic Anemia (MLASA) | Muscle | Riley et al., 2010 |
| SARS2 | Hyperuricemia, Pulmonary hypertension, Renal failure in infancy, and Alkylosis (HUPRA) | Kidney | Belostotsky et al., 2011 |
| HARS2 | Perrault syndrome with progressive sensorineural hearing loss and ovarian dysgenesis | Cochlea, ovary | Pierce et al., 2011 |
| AARS2 | Infantile mitochondrial cardiomyopathy | Heart | Gotz et al., 2011 |
| MARS2 | Autosomal Recessive Spastic Ataxia with Leukoencephalopathy (ARSAL) | Brain | Bayat et al., 2012 |
| FARS2 | Fatal epileptic mitochondrial encephalopathy | Brain, muscle | Elo et al., 2012 |
| EARS2 | Early-onset Leukoencephalopathy with Thalamus and Brainstem Involvement and High Lactate (LTBL) | Brain | Steenweg et al., 2012 |
| LARS2 | Premature Ovarian Failure and Hearing Loss in Perrault Syndrome | Cochlea, ovary | Pierce et al., 2013 |
| GARS | Charcot-Marie-Tooth (CMT) disease and distal spinal muscular atrophy type V | Nerve | Seburn et al., 2006 |
| KARS | Intermediate Charcot-Marie-Tooth (CMT) disease | Nerve | Santos-Cortez et al., 2013 |

In addition, synthetases for glycine (GARS) and lysine (KARS) have been associated with diseases of peripheral neuropathy. GARS mutations cause Charcot-Marie-Tooth (CMT) disease and distal spinal muscular atrophy type V (Seburn et al., 2006; Dubourg et al., 2006), whereas KARS mutations have been described in an unusual combination of intermediate CMT (Santos-Cortez et al., 2013). In contrast to the recessive ARS2 diseases, GARS mutations are dominantly inherited and toxicity in peripheral neurons due to the mutant GARS has been experimentally observed (Motley et al., 2011). GARS and KARS are the bifunctional synthetases that are ‘charging’ their respective amino acids both in cytoplasm and mitochondria. Thus, the question whether these diseases are the

results of defective mitochondrial or cytoplasmic translation has to be investigated.

Currently, the tissue specificity and diverse clinical presentations of the ARS2s are one of the most puzzling questions in the field. To exemplify, LBSL and PCH6 involve specific progressive central nervous system dysfunction, whereas MLASA causes sideroblastic anemia; HUPRA is a multisystemic disorder involving progressive renal failure. Interestingly, reduced synthetase activity and/or decreased mitochondrial translation leading to a lower activity of OXPHOS complexes harboring mtDNA encoded-subunits have been observed in some, but not all diseases. However, a general feature that is common for all diseases caused by mutations in ARS2 genes is still missing. To investigate those diseases in detail, mouse models mimicking the disease mutations should be generated and studied.

1.4. Mitochondrial Stress Signaling

What happens to the mitochondria during 'dysfunctional/disease state'? Do they accept their fate and wait for the inevitable or do they strike back? You are not expecting the mitochondria to be the silent victims in a drama, are you? They behave as the last survivor in a teen slasher (like Sydney Prescott in the genre-redefining Wes Craven movie 'Scream') who tries to find clever ways to defeat the evil serial killer, and to achieve that they use every possible way imaginable – even evoking responses from the local authorities.

Many different stress responses have been described in mitochondria that involves diverse nuclear and mitochondrial signaling pathways. As mentioned before, mitochondria encode only 13 proteins that are components of mitochondrial respiratory complexes (MRC) and the rest of its protein pool (~1500 proteins) is

encoded by the nuclear genome. Therefore, responses to different stresses require coordination of those two genomes and in great need of cross talk between the nucleus and mitochondria. Mitochondria evokes those responses in order to (i) increase their biogenesis (their number or volume), (ii) enhancing the expression or activity of the OXPHOS subunits, (iii) send out signals to the nucleus and even to other organelles/organs to get more help, (iv) induce apoptosis, and (v) fight with oxidative damage. The well-defined signaling cascades include retrograde signaling leading to upregulation of mitochondrial biogenesis, anti-oxidative response and more recently, mitochondria specific unfolded protein response (UPR^{mt}). Respiratory deficiency, causing a decreased production of ATP, is considered to be the primary activator of most of these adaptive responses in the course of mitochondrial diseases. However, we have very limited knowledge about signaling cascade involved in these responses, while the mechanisms that regulate tissue specificity are basically not known.

1.4.1 Mitochondrial retrograde signaling

Mitochondrial retrograde signaling is a pathway of communication from mitochondria to the nucleus that influences many cellular and organismal activities under both normal and pathophysiological conditions. In budding yeast, *Saccharomyces cerevisiae*, it is used as a sensor of mitochondrial dysfunction that initiates readjustments of carbohydrate and nitrogen metabolism (Butow and Avadhani, 2004). In higher organisms retrograde response is much less understood and is commonly linked to increased mitochondrial biogenesis/proliferation.

Patients with mitochondrial dysfunction in muscle, show a phenotype called 'ragged-red fibers'. Those fibers can be seen when muscle is stained with Gomori Trichrome staining as a result of high subsarcolemmal accumulation of abnormal

mitochondria due to increased biogenesis. As discussed before, ragged-red fibers are seen in MERRF (myoclonic epilepsy associated with ragged-red fibers) syndrome patients, who have decreased mitochondrial translation and ETC defects (Zeviani et al., 1993). Those defects cause the retrograde signaling to the nucleus to increase mitochondrial mass (Wallace, 2005).

Mitochondrial biogenesis is regulated by specific set of transcription factors including: nuclear respiratory factors 1 and 2 (NRF1 and NRF2, estrogen related receptor α (ERR α), the cAMP response element (CREB) and ying yang 1 transcription factor (YY1) (Scarpulla et al., 2012). NRF1 and NRF2 also directly regulate mitochondrial transcription factor A (TFAM), which packages and maintains mtDNA, and is important for mitochondrial transcription and replication (Kukat and Larsson, 2013). Transcriptional control of nuclear genes encoding mitochondrial enzymes and proteins is also dependent on the members of the nuclear receptor superfamily, namely the peroxisome proliferator-activated receptor (PPAR) family that includes PPAR α , PPAR β (also known as PPAR δ) and PPAR γ .

How do these transcription factors control mitochondrial biogenesis? The clues led to the identification of peroxisome-proliferator-activated receptor coactivator-1 α (PGC-1 α) as a master regulator of mitochondrial biogenesis (Puigserver et al., 1998). PGC-1 α is a member of a family of transcriptional coactivators that includes PGC-1 β (Lin et al., 2002) and PRC (PGC-1 related coactivator) (Kelly and Scarpulla, 2004). It was shown that the level of PGC-1 α in cells is closely correlated with the number of mitochondria (Kelly and Scarpulla, 2004). Tissue-specificity is a hallmark of PGC-1 α . For example, cold exposure leads to the activation of PGC-1 α in brown adipose tissue (Puigserver et al., 1998), whereas long-term exercise in skeletal muscle, leading to mitochondrial biogenesis (Zong et al., 2002). PGC-1 α overexpression causes increases in mitochondrial content, in agreement with its role in mitochondrial biogenesis (Lehman et al., 2000).

However, loss of PGC-1 α in mice causes disturbances only upon stress exposure, e.g. PGC-1 α deficient mice are unable to maintain their body temperature upon cold exposure and they exhibit reduced exercise tolerance and abnormalities in the muscle fiber composition (Scarpulla, 2012). These results indicate that PGC-1 α is indeed essential for mitochondrial-biogenesis on-demand, but seems not to be needed to maintain normal levels of mitochondria in the cell.

1.4.2 Mitochondrial anti-oxidative response

Mitochondrial respiratory chain is the main site of reactive oxygen species (ROS) production. Electrons can leak from the electron transport chain directly to oxygen, producing free radicals such as superoxide anion (O_2^-) (Droge, 2002). Superoxide anion is converted into hydrogen peroxide either spontaneously or via manganese superoxide dismutase (MnSOD or SOD2), a nuclear encoded primary antioxidant enzyme localized exclusively in the mitochondrial matrix (Weisiger and Fridovich, 1973). Membrane-permeable hydrogen peroxide can be diffused within the cell and can be scavenged via antioxidant systems such as catalase, glutathione peroxidase, and thioredoxin peroxidase (Nordberg and Arner, 2001). These are the sophisticated defense mechanisms evolved to limit the cellular damage that ROS can implement on lipids, proteins and nucleic acids, causing oxidative damage. One point that should not be neglected is the fact that ROS are also important signaling molecules in cell proliferation (Clement and Pervaiz, 1999) or cell death (Burdon, 1996).

1.4.3 Mitochondrial unfolded protein response (UPR^{mt})

Mitochondria have dedicated molecular chaperones and proteases that promote proper protein folding, complex assembly and quality control. All mitochondrial proteins that are translated in the cytoplasm should take a great journey to be functional in mitochondria. They have to pass through the double membrane of mitochondria, not to mention the unfolding, cleavage and refolding they have to go through. Mitochondrial dysfunction accumulates with increasing age and it is not surprising that increased levels of unfolded and/or misfolded proteins also escalate. Mitochondria respond to the accumulation of unfolded proteins by activating stress responses, which further upsurge the level of molecular chaperones and proteases, involved in protein quality control. Some of these stress responses are the well-documented ER unfolded protein response (UPR^{ER}) (Mori et al., 1993) and mitochondrial unfolded protein response (UPR^{mt}) (Zhao et al., 2002; Yoneda et al., 2004). The UPR^{mt} activates the transcription of nuclear-encoded mitochondrial chaperone genes to promote protein homeostasis within the organelle. Mitochondrial unfolded protein response is very specific and different from signaling cascades that are activated by heat-shock, endoplasmic reticulum stress or oxidative stress response (Haynes et al., 2013).

Matrix-localized chaperones are required for protein import and facilitate protein folding, whereas proteases localized in the inner membrane and matrix degrade proteins that fail to fold or assemble correctly (Tatsuta and Langer, 2008). The targeting of many mitochondrial proteins synthesized in cytosol requires molecular chaperones such as cytosolic Hsp70 and Hsp90 (Young et al., 2003). Mitochondrial Hsp70 (mtHsp70) is required within the mitochondrial matrix for the import of unfolded protein across the inner membrane and with the help of chaperonins Hsp60/10, they fold the imported and mitochondrially-synthesized proteins (Ryan et al., 1997). MRC complexes are assembled and embedded into the inner mitochondrial membrane and possess their own quality control system:

two ATP-dependent metalloproteases (AAA protease). According to where their catalytic sides reside, they are named as the intermembrane space (i-AAA) or matrix side (m-AAA) proteases. Mitochondrial matrix harbors two major proteases, namely LON and CLPXP. LON protease is shown to preferentially degrade oxidized proteins (e.g. aconitase) and to regulate mtDNA copy number and transcription by selective degradation of mitochondrial transcription factor A (TFAM) (Ngo and Davies, 2007; Matsushima and Kaguni, 2012). CLPXP seems to be the main matrix protease that is dealing with unfolded and/or misfolded proteins (Zhao et al., 2002).

The UPR^{mt} has extensively been studied in *C. elegans*, where it acts by upregulating the expression of *hsp-60* and *hsp-6* (Hsp60 and mtHsp70, respectively). There are different hypothesis (and some proof) on how UPR^{mt} signals are sensed and transported into the nucleus (Figure 1.3). CLPXP recognizes and degrades misfolded proteins into peptides of 8-20 residues (Choi and Licht, 2005). Those peptides accumulating in the mitochondrial matrix are extruded via an ABC (ATP Binding Cassette) transporter called HAF-1. This efflux of peptides is believed to activate bZIP transcription factor ATFS-1 in *C. elegans*, which further activates downstream UPR^{mt} signaling targets (Haynes et al., 2010). ATFS-1 harbors both a nuclear localization sequence and a mitochondrial targeting sequence. Under physiological conditions, ATFS-1 is imported into mitochondria and degraded by Lon protease. However, during mitochondrial stress, import efficiency is reduced and ATFS-1 accumulates in the cytosol and nucleus where it activates genes coding for mitochondrial chaperones (Nargund et al., 2012). It has also been proposed ATFS-1 import to mitochondria can be slowed by peptide efflux via HAF-1, which occurs when the mitochondrial chaperone capacity is exceeded by unfolded proteins. But the mechanism of this attenuation in protein import is not fully understood and it is being hypothesized to be evolved independently of the UPR^{mt} (Haynes et al., 2013).

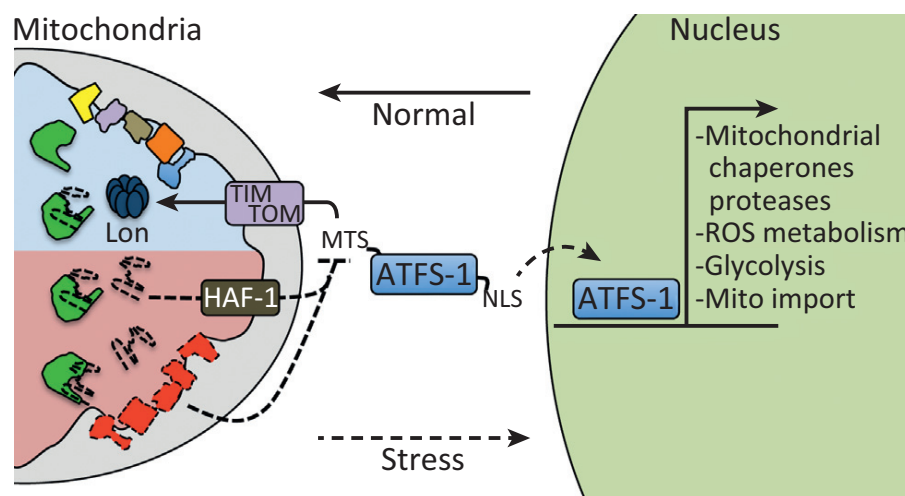


Figure 1.3 The mitochondrial unfolded protein response (UPR^{mt}) in *Caenorhabditis elegans*.

Mitochondrial unfolded protein response is activated during mitochondrial stress and it upregulates the transcription of mitochondrial chaperones, proteases, genes necessary for ROS metabolism, glycolysis and mitochondrial protein import machinery (Haynes et al., 2013). In normal conditions, Activating Transcription Factor associated with Stress-1 (ATFS-1) is imported into mitochondria and degraded by LON protease. However, during mitochondrial stress, import efficiency was reduced and ATFS-1 accumulates in the cytosol and nucleus where it activates genes coding for mitochondrial chaperones. Moreover, ATFS-1 import to mitochondria can be slowed by peptide efflux via HAF-1. TIM: Translocase of the Inner Membrane; TOM: Translocase of the Outer Membrane.

In mammals, UPR^{mt} is less understood. Still, the upregulation of Hsp60 and mtHsp70 is observed, similar to UPR^{mt} response in *C. elegans*. The activation of the nuclear genes as a result of UPR^{mt} seems through the heterodimerization of the transcription factors C/EPB β (CCAAT enhancer-binding protein β) and CHOP (C/EBP homology protein). These transcription factors are activated via JUN transcription factor that binds to an AP-1 (activator protein-1) element in the promoter of both genes. There is evidence that JNK2 (c-Jun N-terminal kinase 2) can be also involved in this signalling pathway (Aldridge et al., 2007). Several genes encoding mitochondrial protein quality control proteins that are responsive to mitochondrial unfolded protein stress, as well as 15 nuclear genes encoding other mitochondrial proteins, also contain a CHOP-binding element in their promoter region (Horibe and Hoogenraad, 2007). Interestingly, CHOP gene itself

seems to be upregulated by the accumulation of unfolded proteins in mitochondria (Zhao et al., 2002). It has been proposed that UPR^{mt} can be a two-stage regulatory process (Ryan and Hoogenraad, 2007). First, the unfolded proteins in mitochondria are sensed and via the retrograde signaling to the nucleus, they activate CHOP (and possibly other) genes. Second, CHOP, in cooperation with C/EBP β , then binds to target promoters and activates the transcription of mitochondrial-responsive genes. CHOP, also a part of induction of UPR^{ER}, have a promoter with separate mitochondrial and ER UPR elements and that is the way it can differentially upregulate responsive genes for either UPR^{mt} or UPR^{ER} (Horibe and Hoogenraad, 2007).

1.4.3.1 ‘Mitokines’ and Fibroblast growth factor 21 (FGF21)

In the movie Scream, in the dawn of one-year anniversary of Sidney Prescott’s mother’s murder, new killings start to take place in Woodsboro. At first, not-so-bright Deputy sheriff Dewey Riley tries to provide shelter and protection for Sidney, which turns out not to be so effective. Local authorities cannot always protect you from the vicious serial killers. At that point, signaling to the national forces, such as FBI, becomes more crucial.

Mitochondria adopted a similar signaling pathway, which became apparent very recently, to send mayday signals to the remote tissues/organs. It has been proposed that neuronal cells experiencing mitochondrial dysfunction could produce a mitochondrial signal for the upregulation of UPR^{mt} (Durieux et al., 2011). The interesting thing is those cells can generate an extracellular signal, a ‘mitokine’, which can be transmitted to the distal cells, in their case intestinal cells of *C. elegans*. This cell-nonautonomous signal can induce UPR^{mt} in those distal, far away tissues.

In 2010, a report identified the first mammalian mitokine known-to-date, FGF21. It has been experimentally proven that mitochondrial dysfunction activates *Fgf21* transcription in skeletal muscle in a dose-dependent manner (Tynjismaa et al., 2010). FGF21 is produced mainly from liver and circulating FGF21 in the bloodstream comes from this organ. However, adipocytes and skeletal muscle have also been shown to be able to secrete FGF21, which then acts through autocrine or paracrine signaling (Potthoff et al., 2012). Fibroblast growth factor (FGF) 21 is a well-known hormone/cytokine, often described as “starvation-hormone”, which has regulatory roles in glucose, lipid, phosphate and bile acid metabolism (Kharitononkov et al., 2005). Sometimes it is also seen as a potential ‘miracle hormone/cytokine’ due to the fact that its systemic administration causes reductions in body weight, fat mass, and the levels of blood glucose and insulin (Xu et al., 2009).

In the beginning of 2013, another report strengthened the role of FGF21 as a mitokine (Kim et al., 2013). The authors showed that autophagy deficiency in skeletal muscle induced expression of *Fgf21* through activating transcription factor 4 (*Atf4*), which leads to increased β -oxidation and browning of WAT, and finally to protection from high fat diet (HFD)-induced insulin resistance (Kim et al., 2013). Thus it seems that we laid our hands on the first-ever-identified mammalian mitokine.

1.4.4 (Macro)Autophagy and Mitophagy

What if your normal FBI agents also fail in protecting you from our everyday serial killer? The logical next step is to employ better FBI agents, not the normal, just-out-of-Quantico ones, but agents like experienced Fox Mulder and Dana Scully. They will search ‘the truth out there’ by invoking every possible help

source they can lay their hands on, even from the evil 'Cancer Man'. But, do not be fooled: this could also lead to your demise!

The lysosome and the proteasome are the two major degradation systems in eukaryotes (Mizushima and Komatsu, 2011). Proteasomal degradation has high selectivity and recognizes only ubiquitinated substrates. On the other hand, lysosomal degradation does not necessarily have this selectivity and uses autophagy for delivery of to-be-recycled products. (Macro)Autophagy (the other kinds of autophagy, namely microautophagy, and chaperone-mediated autophagy, are not in the scope of this thesis), 'self-eating' in Greek, is an evolutionary conserved mechanism in which the cytoplasmic constituents, which also includes organelles, are destined to the lysosomes inside double-membrane vesicles (Yang and Klionsky, 2010). Autophagy exists in order to (i) get rid of misfolded proteins, damaged organelles and/or microorganisms, (ii) during starvation, to provide building blocks for biosynthesis, (iii) remodel the cell to cellular stress. Autophagy deploys 'autophagosomes', basically a small part of the cytoplasm in an isolation membrane, which fuses with the lysosome to give rise to autolysosome and degrade the materials contained (Mizushima et al., 2010). Molecules that were subjected to autophagic degradation are sent back to the cytoplasm and used for recycling or production of energy. Autophagy is a dynamic process that is up- or downregulated as a response to cellular stress. The best example of induced autophagy is as a result of nutrient starvation. Autophagy suppression, is on the other hand, is a phenomenon seen in various diseases and aging (Mizushima et al., 2010).

In yeast, multiple autophagy-related (ATG) proteins govern autophagosome formation (Yang and Klionsky, 2010). In mammalian cells, most of the Atg proteins are observed on isolation membranes (i.e., ULK1/2, Atg13, FIP200,

Atg101, Beclin 1, Atg14, LC3, Atg12, Atg16L1) (Longatti and Tooze, 2009); the only exception being LC3 (microtubule-associated protein light chain 3), which is also available on autophagosomes (Mizushima et al., 2004). That is the reason it is the most commonly used marker for autophagy.

Basal autophagy acts as the quality-control machinery for cytoplasmic components. There is also increasing evidence indicating selective autophagy for specific proteins, organelles, and invading bacteria. Recent studies have described a specialized form of autophagy that acts solely on damaged mitochondria, mitophagy. It utilizes the same machinery as autophagy; however, the process becomes selective through the participation of Atg32, which tags mitochondria for elimination (Okamoto et al., 2009). Much of our knowledge about mitophagy comes from *in vitro* studies and currently there is very little, if any, support for the role of mitophagy as a quality control mechanism *in vivo*. Actually, a recent *in vivo* study showed that depolarized mitochondria do not recruit Parkin in dopamine neurons (Sterky et al., 2011). Thus, many questions remain as a secret about mitophagy and its role as a quality control mechanism and we need more *in vivo* studies to fully understand this process.

1.5. Objectives

Mitochondrial disorders are very heterogeneous from a clinical, genetical, biochemical and molecular point of view (Schaefer et al., 2004). Certain tissues such as heart, brain, and skeletal muscle are very dependent on the OXPHOS for energy production; therefore, these tissues are more involved in mitochondrial diseases (Dogan and Trifunovic, 2011). However, this cannot explain the diverse manifestations of mutations that would be predicted to have similar effects. The mechanisms that regulate the tissue-specific consequence of mitochondrial disease

are still largely unknown. In fact, the different patterns of energy crisis are perhaps the most puzzling dilemma in the field.

Mutations in nuclear encoded proteins that obey the laws of Mendelian genetics and therefore have the same type of defect in all different cell types, often have tissue or organ specific presentation. One class of enzymes that fall into that category is mitochondrial aminoacyl-tRNA synthetases. The first described pathological mitochondrial synthetase mutation was in the *DARS2* gene, which encodes for the mitochondrial aspartyl-tRNA synthetase (Scheper et al., 2007). Eased by advantages in whole genome sequencing, large number of mutation in other synthetase genes quickly followed. Strikingly, the mutations in different mitochondrial synthetase genes often gave rise to clinically diverse diseases and organ involvement. However, we cannot really observe a general aspect that is common in all of those diseases that can explain this phenomenon. To investigate those diseases in detail, mouse models may be useful tools but to date none have been reported.

For this PhD thesis, we wanted to generate a novel mouse model that does not mimic the clinical presentations of a disease but having a strong respiratory chain deficiency as observed in majority of mitochondrial diseases. As no such model was available so far, we generated one by deleting *Dars2* gene encoding for mitochondrial aspartyl-tRNA synthetase, thus directly disrupting mitochondrial protein synthesis. With this model, we aimed to analyze tissue specific consequences of defective mitochondrial translation. We specifically wanted to compare effects of DARS2 depletion on heart and skeletal muscle -tissues of common origin that are often affected in mitochondrial diseases-, and with another mouse model in forebrain neurons: three of the high energy demanding tissues.

Cells have developed various kinds of compensatory mechanisms in response to mitochondrial respiratory chain deficiency that could play a central role in determining the extent of tissue-specific defects. We wanted to study those mechanisms, as well as mitochondrial stress signaling pathways, in order to find a mechanism for tissue-specific activation of adaptive responses during the development of mitochondrial diseases.

2. Materials and Methods

2.1 Mouse Experiments

2.1.1 Animal Care

Care of all animals was within institutional animal care committee guidelines. All animal procedures were conducted in compliance with protocols and approved by local government authorities (Bezirksregierung Köln, Cologne, Germany) and were in accordance with NIH guidelines. Animals were housed in groups of 3 - 5 mice per cage at an ambient temperature of 22 – 24 °C and kept at a 12-hour light / 12-hour dark cycle. Mice were sacrificed by cervical dislocation; the only exceptions were the brain-specific knockout and wild type animals, for which lethal CO₂ anesthesia was used.

2.1.2 Mouse handling and breeding

General handling and breeding of mice was performed according to Silver (Silver, 1995).

2.1.3 Mice

Mitochondrial aspartyl-tRNA synthetase (*Dars2*) gene targeting was carried out as part of the International Knockout Mouse Consortium (KOMP), in the JM8.N4 embryonic stem cell line on a C57BL/6N genetic background. The targeted *Dars2*^{tm1a(KOMP)WTSI} allele carried a gene-trap DNA cassette, inserted into the second

intron of the gene, consisting of a splice acceptor site, an internal ribosome entry site, and a β -galactosidase reporter, followed by a neomycin resistance marker expressed from an independent β -actin promoter (further information available at <http://www.knockoutmouse.org>, Project ID: 41773). Full body knockout mice were generated by mating the $Dars2^{+/tm1a(KOMP)WTSI}$ animals with transgenic mice ubiquitously expressing the Cre recombinase. Heart and skeletal muscle specific knockout mice were generated by mating $Dars2^{loxP/loxP}$ animals with transgenic mice expressing cre recombinase under the control of muscle creatine kinase promoter (*Ckmm-cre*) (Larsson et al., 1998). Forebrain specific knockout mice were generated by mating $Dars2^{loxP/loxP}$ animals with transgenic mice expressing cre recombinase under the control of CaMKII α promoter (*CaMKII-cre*) (Xu et al., 2000).

The animals were maintained in the pathogen-free animal facility of the CECAD/Max Planck Institute for Biology of Aging.

2.1.4 Blood collection and determination of blood glucose, non-esterified fatty acids and FGF21 levels

Tail bleeding of mice was performed as described (Silver, 1995). Venous blood samples were stored on ice for 15 minutes and subsequently centrifuged at 13.000 rpm for 20 minutes. Resulting serum was stored at -80 °C. Determination of metabolite levels and collection of blood samples from control and knockout mice were performed side-by-side in the morning to avoid intra-group deviations due to circadian variations.

Fed blood glucose concentrations were measured after tail-vein incision using glucose strips, which were read for absorbance in a reflectance meter (ACCU-CHEK AVIVA, Roche, Mannheim, Germany).

Serum Non-esterified fatty acids (NEFA) levels were determined using an acyl-CoA oxidase based colorimetric kit (WAKO NEFA-C; WAKO Life Sciences, Inc., Richmond, USA). NEFA standard solutions were used for the linear regression plot and absorbency measured at 550 nm in a Paradigm plate reader (Molecular Devices, Sunnyvale, USA).

Serum FGF21 concentrations were measured with a Mouse/Rat FGF-21 Quantikine ELISA Kit (R&D Systems, Minneapolis, USA) according to according to the manufacturer's instructions.

2.1.5 Analysis of body composition (NMR)

Nuclear magnetic resonance (NMR) was employed to determine the body fat content of live animals using the NMR Analyzer Minispec mq7.5 (Bruker Optik, Ettlingen, Germany).

2.1.6 Perfusion

Mice were anesthetized with 20 µl/g body weight of Avertin (2,2,2-tribromoethyl alcohol with tert-amyl alcohol), given subcutaneously intraperitoneal. Afterwards, perfusion is performed intracardially with phosphate buffered saline (PBS) followed by 4% paraformaldehyde (PFA) in 0.1M PBS (pH 7.4). Isolated brains were post-fixed in 4% PFA at 4 °C (for Transmission Electron Microscopy analysis, post-fixed in 2% Glutaraldehyde at 4 °C) overnight and then stored at 4 °C in 0.05% Sodium azide-PBS (NaN₃-PBS) until further analysis.

2.2 Molecular biology

2.2.1 Isolation of genomic DNA from mice tails

Mice tail biopsies were incubated overnight in lysis buffer (100 mM Tris-HCl pH 8.5, 5 mM EDTA, 0.2% (w/v) SDS, 0.2 M NaCl, 500 mg/ml Proteinase K) in a thermoshaker (Eppendorf, Hamburg, Germany) at 55 °C. DNA was precipitated by adding an equivalent volume of 2-Propanol (100%) and centrifuging at maximum speed for 20 minutes in a benchtop centrifuge. After removing the supernatant, the pellet was washed with 70% (v/v) ice-cold ethanol and centrifuged at maximum speed for 15 minutes. Then, the samples were pulsed down and DNA pellets were resuspended in 100 µl dH₂O by shaking at 37 °C for 1 h.

2.2.2 Isolation of genomic DNA from mice tissues

Shock-frozen mice tissues (about 3 mm³) were incubated overnight in lysis buffer (50 mM Tris-HCl pH 8.0, 2.5 mM EDTA, 0.5% (w/v) SDS, 0.1 M NaCl, 500 mg/ml Proteinase K) in a thermoshaker (Eppendorf, Hamburg, Germany) at 55 °C. DNA was precipitated by adding 75 µl of 8 M potassium acetate and 0.5 ml chloroform, and centrifuging at maximum speed for 10 minutes in a benchtop centrifuge. The upper, aqueous phase (not the lower chloroform phase) was transferred to a new 1.5 ml eppendorf tube. 1 ml of 95% ethanol was added to the samples, which were further inverted several times. The samples were centrifuged at maximum speed for 10 minutes. The pellet is, then, rinsed with 70% (v/v) ice-cold ethanol and centrifuged for an additional 5 minutes. Afterwards, the samples were pulsed down and DNA pellets were resuspended in 100 µl ddH₂O.

2.2.3 Isolation of total RNA from mice tissues

Total RNA was isolated either using the ToTALLY RNA Total RNA isolation kit (Ambion, Life Technologies GmbH, Darmstadt, Germany) or TRIzol reagent (Life Technologies GmbH, Darmstadt, Germany). To start with, 50-100 mg tissues were dissected and placed into Precellys (Bertin Technologies, Versailles, France) 1.5 ml tubes with beads (500 µl of denaturing buffer (ToTALLY RNA kit) or 500 µl of TRIzol reagent). The tissues were homogenized by a Precellys 24 (Bertin Technologies, Versailles, France) fast-prep machine at 5500 rpm for 2x30 seconds. Afterwards, manufacturer's instructions' were followed.

2.2.4 Quantification of nucleic acids

DNA and RNA concentrations were quantified by measuring the sample absorption at 260 nm and 280 nm with a NanoDrop ND-1000 UV-Vis spectrophotometer (Peqlab, Erlangen, Germany). A ratio greater than 2 of absorptions at 260 nm (DNA/RNA) divided by the absorption at 280 nm (protein) was used as an index of purity of DNA/RNA.

2.2.5 Polymerase chain reaction (PCR)

PCR reactions were used to detect whether the mouse genome contains floxed (LoxP flanked) exons (wt) –for full body knockout mice giving only wt band and for tissue-specific mice two bands corresponding to LoxP regions and wt band-, full body knockout (ko) –for full body knockout mice-, and cre-recombinase gene (cre) with primers described in Table 2.1.

Reactions were performed in a Veriti Thermal Cycler (Applied Biosystems, Life Technologies GmbH, Darmstadt, Germany). All amplifications were performed in a total reaction volume of 20 µl. For wt and ko PCR, 12.35 µl of dH₂O, 4 µl of 5x

GoTaqBuffer (Promega), 1 μ l of dNTPs (1.25 mM each), 0.8 μ l of each primer (10 μ M), and 0.05 μ l of GoTaq (5 U/ μ l, Promega) were added to 1 μ l of sample DNA. For cre PCR, 10.5 μ l of dH₂O, 4 μ l of 5x GoTaqBuffer, 3.2 μ l of dNTPs (1.25 mM each), 0.6 μ l of each primer (10 μ M) and 0.1 μ l of GoTaq (5 U/ μ l) were added to 1 μ l of sample DNA. Bands were determined by visualization of PCR products using 1% agarose gel with ethidium bromide.

Table 2.1 Genotyping PCR primer sequences

| Primer | Sequence |
|------------------------|-----------------------|
| Forward ^{wt} | ATGAATTCTAGGCCAGCCAC |
| Reverse ^{wt} | TGGCAATCTCTTAGGACTAAG |
| Forward ^{ko} | CGCTACCATTACCAGTTGGT |
| Reverse ^{ko} | TGACTGGCTATAATGCTGAAG |
| Forward ^{cre} | CACGACCAAGTGACAGCAAT |
| Reverse ^{cre} | AGAGACGGAAATCCATCGCT |

PCR programs for wt and ko PCR started with 5 minutes of denaturation at 95 °C, followed by 30 cycles consisting of denaturation at 95 °C for 30 seconds, annealing at 60 °C for 30 seconds and elongation at 72 °C for 45 seconds, and a final elongation step at 72 °C for 7 min.

PCR programs for cre PCR started with 5 minutes of denaturation at 95 °C, followed by 35 cycles consisting of denaturation at 95 °C for 30 seconds, annealing at 53 °C for 30 sec and elongation at 72 °C for 30 sec, and a final elongation step at 72 °C for 5 min.

2.2.6 Southern blot analysis for mitochondrial DNA (mtDNA) quantification

After DNA isolation from mice tissues (as mentioned before), 10 µg DNA was digested by *SacI* restriction enzyme (New England Biolabs, Ipswich, USA) overnight at 37 °C. DNA was precipitated by addition of 20 µl 5M NaCl and 500 µl 99.5% EtOH to the digestions. After mixing, the samples were left at -80 °C for 30 minutes. Further, the samples were centrifuged at maximum speed for 20 minutes in a benchtop centrifuge, washed with 1 ml 70% EtOH, air-dried and resuspended in 20 µl dH₂O and 6 µl 6X DNA loading dye (Fermentas, St. Leon-Rot, Germany). Samples were run on a 0.7% agarose gel at 1V/cm for 16-20 hours. Next day, the gel is denatured by shaking twice for 15 minutes in denaturation solution (1.5 M NaCl and 0.5 M NaOH). After rinsing shortly with dH₂O, the gel was neutralized by shaking twice for 20 minutes in neutralization solution (1.5 M NaCl and 1 M Tris-HCl pH 7.5). The gel was blotted overnight by sandwiching two long, bridging Whatman papers -presoaked in 20X saline-sodium citrate (SSC) (3M NaCl and 300 mM sodium citrate)-, two short Whatman papers, gel (surrounded tightly with plastic wrap to circumvent shortcuts), Hybond N+ nylon membrane (GE Healthcare, Munich, Germany), two short Whatman papers, about 10-15 cm of paper staple and a weight of 600 g on top. After disassembling of the blot, the membrane was UV-crosslinked with Stratalinker UV Crosslinker (Agilent Technologies, Waldbronn, Germany) twice at 200000 Joule/cm². Afterwards, the membrane was placed in a glass hybridization bottle and prehybridized for 60 minutes at 65 °C in 10 ml rapid-hyb buffer (GE Healthcare, Munich, Germany). In the meantime, the probe, PAM1 – for the whole mouse mitochondrial genome- was labelled with Prime-It II Random Primer Labeling Kit (Agilent Technologies, Waldbronn, Germany) and α-³²P-dCTP for 15 minutes. After denaturation of the probe, it was added to the glass hybridization bottle and hybridized for 2 hours at 65 °C. The membrane is washed in 2X SSC/0.1% SDS for 20 minutes at room temperature, in 1X

SSC/0.1% SDS for 20 minutes at 65 °C and finally in 0.1X SSC/0.1% SDS for for 20 minutes at 65 °C. The membrane, wrapped in a plastic bag, exposed to Amersham Hyperfilm (GE Healthcare, Munich, Germany) overnight.

2.2.7 Northern blot analysis for mRNA and tRNA levels

After RNA isolation (as mentioned above), 2 µg total RNA was taken and topped up to 10 µl with nuclease-free H₂O. 10 µl Ambion RNA Loading dye (Life Technologies GmbH, Darmstadt, Germany) was added to the samples, which were heated to 70 °C for 10 minutes. The agarose gel was prepared by addition of 72 ml DEPC H₂O, 1.2 g Agarose (Agarose-LE from Ambion, Life Technologies GmbH, Darmstadt, Germany). After heating up this mixture in the microwave, 10X MOPS Running Buffer (Ambion, Life Technologies GmbH, Darmstadt, Germany) and 18 ml formaldehyde solution (Sigma Aldrich, Seelze, Germany) were added with clean pipettes. The gel was run in 1X MOPS Buffer for 2 hours at 130 V. The gel was shaken three times for 15 minutes with clean, nuclease-free H₂O and for 20 minutes in 20X SSC solution. The gel was blotted overnight by the same sandwiching technique mentioned in Southern blot analysis. After disassembling of the blot, the membrane was UV-crosslinked with Stratalinker UV Crosslinker (Agilent Technologies, Waldbronn, Germany) twice at 200000 Joule/cm². Afterwards, the membrane was placed in a glass hybridization bottle and prehybridized for 60 minutes at 65 °C in 10 ml rapid-hyb buffer (GE Healthcare, Munich, Germany). The probes for mitochondrial-encoded protein coding genes were prepared with Prime-It II Random Primer Labeling Kit (Agilent Technologies, Waldbronn, Germany) and α-³²P-dCTP exactly as in Southern blot analysis. The probes for tRNAs were prepared by mixing 10 pmol of the probe, with 2 µl of 10X T4 Polynucleotide Kinase Reaction Buffer (New England Biolabs, Ipswich, USA), 1 µl T4 Polynucleotide Kinase (New England Biolabs, Ipswich, USA), 12 µl dH₂O and 40 µCi γ-³²P-dATP. After denaturation

of the probe, it was added to the glass hybridization bottle and hybridized for 2 hours at 65 °C (for mRNAs) or 42 °C (for tRNAs). The membrane is washed in 2X SSC/0.1% SDS for 20 minutes at room temperature, in, again, 2X SSC/0.1% SDS for 20 minutes at 65/42 °C and finally in 0.2X SSC/0.1% SDS for for 20 minutes at 65/42 °C. The membrane, wrapped in a plastic bag, exposed to Amersham Hyperfilm (GE Healthcare, Munich, Germany) overnight. The probes used for Northern blot analysis can be found in Park et al. (2007).

2.2.8 Reverse transcriptase PCR (Gene expression analysis)

Isolated total RNA was treated with DNase (DNA-free Kit, Ambion, Life Technologies GmbH, Darmstadt, Germany) and subsequently reversely transcribed with the High capacity reverse transcription kit (Applied Biosystems, Life Technologies GmbH, Darmstadt, Germany). Probes for target genes were from TaqMan Assay-on-Demand kits (Applied Biosystems, Life Technologies GmbH, Darmstadt, Germany). The only exceptions are *Nppa* and *Nppb* (Natriuretic peptide precursor type A and B) (Riehle et al., 2011), and mitochondrial and nuclear encoded MRC subunits (Karamanlidis et al., 2013) , where Brilliant III Ultra-Fast SYBR Green QPCR Master Mix (Agilent Technologies, Waldbronn, Germany) was used. Real-time PCR analysis was performed on an ABIPRISM 7700 Sequence detector (Applied Biosystems, Life Technologies GmbH, Darmstadt, Germany). Samples were adjusted for total RNA content by Hypoxanthine-guanine phosphoribosyltransferase (HPRT). Relative expression of mRNAs was determined using a comparative method ($2^{-\delta\delta CT}$) according to the ABI Relative Quantification Method. The TaqMan probes used and their accession numbers are: Trim63 - Muscle RING-finger protein 1 (MuRF1 - Mm01185221_m1), Atrogin 1/Fbxo32 - Fbxo32 – F-box protein 32 (Mm00499523_m1), Myod1 - Myogenic differentiation 1 (Mm00440387_m1), Myf5 - Myogenic factor 5 (Mm00435125_m1), Ddit3/chop

(Mm00492097_m1), Fgf21 (Mm00840165_g1), Atf4 (Mm00515324_m1), ATF5 (Mm00459515_m1), Pdk4 (Mm00443325_m1), Cpt1b (Mm00487200_m1), Ppar- α (Mm00440939_m1), Ppar- δ (Mm01305434_m1), Ppar-Y (Mm00440945_m1), Pgc-1 α (Mm00447180_m1).

2.3 Biochemistry

2.3.1 Protein isolation from tissues

Proteins from brain were isolated by *RIPA* buffer (50 mM Tris-HCl, pH 7.4, 150 mM NaCl, 5 mM EDTA, 1% Triton X-100, 1% sodium deoxycholate, 0.1% SDS, dH₂O and one tablet of protease inhibitor (Roche, Mannheim, Germany). Proteins from other mice tissues were isolated by *organ lysis buffer* (50 mM HEPES, pH 7.4, 50 mM NaCl, 10 mM EDTA, 1% Triton X-100, 10 mM sodium orthovanadat, 100 mM NaF, 0.1% SDS, dH₂O and one tablet of protease inhibitor (Roche, Mannheim, Germany).

To start with, 3 mm³ tissues were dissected and placed into Precellys (Bertin Technologies, Versailles, France) 1.5 ml tubes with beads (300 μ l of RIPA buffer or 500 μ l of organ lysis buffer). The tissues were homogenized by a Precellys 24 (Bertin Technologies, Versailles, France) fast-prep machine at 6500 rpm for 2x20 seconds. After incubation on ice for 10 minutes, the samples were centrifuged at 13000 rpm for 45 minutes at 4 °C. The supernatant was transferred to a new tube and the protein concentrations were measured by Bradford reagent (Sigma Aldrich, Seelze, Germany) according to the manufacturer's instructions. Later on, proteins were stored at -80 °C until used.

2.3.2 Mitochondria isolation from tissues other than skeletal muscle

After the mice were sacrificed, the tissues were transferred into a 50 ml falcon tube which includes 20 ml of mitochondria isolation buffer (MIB: 100 mM sucrose, 50 mM KCl, 1 mM EDTA, 20 mM TES, 0,2% BSA free from fatty acids, pH 7.2). After the blood was removed, the tissues were transferred onto a petri dish and cut into small pieces with razor. The pieces were transferred into a glass homogenizer tube (at this step, 1 mg/ml of Subtilisin A was added only for heart). The pieces were homogenized by hand until the solution became homogeneous. Later, the homogenate was transferred into 50 ml Falcon tube and centrifuged at 8500 g for 5 minutes at 4 °C. The supernatant, with floating fat, was discarded and the pellet was resuspended by shaking in 30 ml MIB. Another centrifugation step (at 800 g for 5 minutes at 4 °C) was performed and this time the supernatant, comprising of mitochondria, was transferred into a new 50 ml tube. The supernatant was then centrifuged at 8500 g for 5 minutes at 4 °C to pellet mitochondria. The supernatant was decanted and the remaining pellet in resuspended in 50 µl MIB without BSA. The concentrations were measured by Bradford reagent (Sigma Aldrich, Seelze, Germany) according to the manufacturer's instructions.

2.3.3 Mitochondria isolation from skeletal muscle

After the mice were sacrificed, the tissues were transferred into a 50 ml falcon tube that includes 10 ml of ice-cold PBS supplemented with 10 mM EDTA. After the hairs/blood were removed, the tissues were transferred onto a petri dish and cut into small pieces with razor. The pieces were transferred into a 50 ml Falcon tube including ice-cold PBS/10 mM EDTA and 0.05% trypsin was added. After 30 minutes of incubation on ice, the samples were centrifuged at 200 g for 5 min at 4 °C. The supernatant was discarded and the pellet was resuspended in IMB1 (67 mM Sucrose, 50 mM KCl, 50 mM Tris-HCl pH 8, 10 mM EDTA, 0,2% BSA

free from fatty acids, pH 7.4). The pieces were transferred into a glass homogenizer tube and were homogenized by hand until the solution became homogeneous. Later, the homogenate was transferred into 50 ml Falcon tube and centrifuged at 700 g for 10 minutes at 4 °C. The supernatant, comprising of mitochondria, was transferred into a new 50 ml tube and was centrifuged at 8000 g for 10 minutes at 4 °C to pellet mitochondria. The supernatant was decanted and the remaining pellet in resuspended in 5 µl of MIB2 (250 mM sucrose, 0.3 mM EGTA-Tris, 10 mM Tris-HCl, pH 7.4). After decanting of the supernatant, the pellet was resuspended in 100 µl of MIB2. The concentrations were measured by Bradford reagent (Sigma Aldrich, Seelze, Germany) according to the manufacturer's instructions.

2.3.4 Blue Native polyacrylamide gel electrophoresis (BN-PAGE) and in-gel activity of respiratory chain complexes I and IV

BN-PAGE was carried out using the Novex Bis-Tris system (Life Technologies GmbH, Darmstadt, Germany) according to the manufacturer's specifications. CO I *in-gel* activity was measured by incubating BN-PAGE gel in NADH 0.1 mg/ml nitro tetrazolium blue (NTB) 2.5 mg/ml in 5mM Tris (pH 7.4) for 1 hour. CO IV *in-gel* activity was measured by incubating BN-PAGE gel at 37 °C in 0.24 unit/ml catalase, 10% Cytochrome C and 0.1% Diaminobenzidine tetrahydrochloride (DAB) in 50 mM Tris (pH 7.4) for 1 hour. One set of samples was transferred to PVDF membrane using iBlot™ system (Life Technologies GmbH, Darmstadt, Germany) and immunodetection of mitochondrial protein complexes was performed.

2.3.5 Western blot analysis

Frozen protein extracts were thawed and 50 µg of proteins were separated by NuPAGE Bis-Tris Gel 4-12% system (Life Technologies GmbH, Darmstadt, Germany) according to the manufacturer's instructions. The proteins were blotted to nitrocellulose membranes in a dry-transfer manner by iBlot™ system (Life Technologies GmbH, Darmstadt, Germany). Membranes were incubated with 5% Milk-PBST for 1 hour for blocking purposes. Subsequently, primary antibodies (Table 2.2), diluted in 5% Milk-PBST were applied for overnight at 4 °C. Afterwards, the membrane was washed 3 x 5 minutes with PBST. The secondary antibody (all secondary antibodies were purchased from Sigma Aldrich, Seelze, Germany and the dilution used was 1:2000) was diluted in 5% Milk-PBST and applied for 1 hour at room temperature. The membrane was again washed 3 x 5 minutes with PBST and ECL solution (GE Healthcare, Munich, Germany) was applied. The membranes were developed by using ImageQuant LAS4000 (GE Healthcare, Munich, Germany). Western blot quantification was performed with ImageJ software as intensity per mm². Average protein expression of control mice was set to 100% and compared to protein expression of knockout animals unless stated otherwise.

Table 2.2 Primary antibodies used for Western blot analysis

| Antigen | Distributor | Dilution |
|----------------|--|-----------------|
| AFG3L2 | Polyclonal antisera made by Prof. Elena I. Rugarli | 1:1000 |
| MRPL-13 | Polyclonal antisera made by Prof. Nils-Göran Larsson | 1:200 |
| MRPS-27 | Polyclonal antisera made by Prof. Nils-Göran Larsson | 1:200 |
| COXII | Polyclonal antisera made by Prof. Nils-Göran Larsson | 1:200 |
| TFAM | Polyclonal antisera made by Prof. Nils-Göran Larsson | 1:1000 |
| Porin | Calbiochem (Merck, Darmstadt, Germany) | 1:2000 |
| ATP5a1 | Mitosciences (Abcam, Cambridge, UK) | 1:1000 |
| COXIV | Invitrogen (Karlsruhe, Germany) | 1:1000 |
| UQCRC2 | Invitrogen (Karlsruhe, Germany) | 1:1000 |
| SDHA | Invitrogen (Karlsruhe, Germany) | 1:10000 |
| NDUFA9 | Invitrogen (Karlsruhe, Germany) | 1:1000 |
| COX5B | Invitrogen (Karlsruhe, Germany) | 1:1000 |
| COXIII | Invitrogen (Karlsruhe, Germany) | 1:1000 |
| HSP60 | StressMarq (Victoria, Canada) | 1:1000 |
| DNP | Millipore (Merck, Darmstadt, Germany) | 1:150 |
| MnSOD | Millipore (Merck, Darmstadt, Germany) | 1:500 |
| MRPS-35 | Proteintech (Chicago, USA) | 1:1000 |
| DARS2 | Proteintech (Chicago, USA) | 1:1200 |
| Actin | Santa Cruz (Dallas, USA) | 1:5000 |
| HSC70 | Santa Cruz (Dallas, USA) | 1:10000 |
| PGC-1 α | Santa Cruz (Dallas, USA) | 1:1000 |
| CLPP | Sigma Aldrich, Seelze, Germany | 1:1000 |
| mtHSP70 | Abcam (Cambridge, UK) | 1:1000 |
| ND5 | Abcam (Cambridge, UK) | 1:1000 |
| MRPL-12 | Abcam (Cambridge, UK) | 1:500 |
| LON | Abcam (Cambridge, UK) | 1:1000 |
| LC3B | Cell Signaling, Danvers, USA | 1:1000 |
| Ubiquitin | Cell Signaling, Danvers, USA | 1:1000 |
| Beclin | Cell Signaling, Danvers, USA | 1:1000 |
| ATG7 | Cell Signaling, Danvers, USA | 1:1000 |
| ATG12 | Cell Signaling, Danvers, USA | 1:1000 |
| p62/SQSTM1 | Abnova (Taipei, Taiwan) | 1:1000 |

2.3.6 Citrate synthase activity and respiratory chain complex activity assays

The measurements of respiratory chain enzyme complex activities and citrate synthase activity were performed as previously described (Wibom et al., 2002).

2.3.7 Oxygen consumption rates

Oxygen consumption rates were measured with OROBOROS Oxygraph-2k for high-resolution respirometry (Oroboros Instruments, Vienna, Austria). In short, mitochondrial CO I activity was measured with 0.1 mg of heart mitochondria, with addition of 1 mM ADP, 5 mM pyruvate, 2 mM malate, 10 mM glutamate. Mitochondrial coupling was then evaluated by inhibition of ATP synthase by adding 1.5 µg/ml oligomycin, and uncoupling by a multiple-step FCCP titration. After inhibition of CO I by 0.5 µM rotenone, respiratory capacity with substrates for CO II alone were measured with 10 mM succinate as a substrate. Mitochondrial respiration was also measured in saponin-permeabilized fibers isolated from skeletal muscle as described (Kuznetsov et al., 2008).

2.3.8 Analyses of de novo transcription and translation in isolated mitochondria

In organello transcription assay was performed as previously described (Park et al., 2007). In brief, after mitochondria isolation, 1 mg mitochondria was resuspended in transcription incubation buffer (25 mM sucrose, 75 mM sorbitol, 100 mM KCl, 10 mM K₂HPO₄, 50 µM EDTA, 5 mM MgCl₂, 1 mM ADP, 10 mM glutamate, 2.5 mM malate, 10 mM Tris-HCl pH 7.4 and 1 mg/ml BSA), supplemented with 50 µCi of α-³²P-UTP. The samples were incubated for 1 hour at 37 °C with gentle rotation for pulse or without radioactivity for 3 and 6 hours of 'cold chase'. After incubation, mitochondria were washed twice with 1 ml of

washing buffer (10% glycerol, 10 mM Tris-HCl pH 6.8 and 0.15 mM MgCl₂) and resuspended in 1 ml of TRIzol reagent (Life Technologies GmbH, Darmstadt, Germany) for RNA isolation. Isolated RNA was analyzed by Northern blotting and radiolabeled transcripts were visualized by autoradiography.

In organello translation was performed as previously described in mitochondria from heart and liver (Edgar et al., 2009). Skeletal muscle mitochondria were incubated in translation buffer containing 25 mM sucrose; 75 mM sorbitol; 100 mM KCl; 1 mM MgCl₂; 0.05 mM EDTA; 10 mM Tris-HCl; and 10 mM K₂HPO₄, pH 7.4 with addition of 10 mM glutamate, 2.5 mM malate, 1 mM ADP, and 1 mg/ml fatty acid-free bovine serum albumin (BSA). In organello proteins synthesis was performed for 1 hour in presence of ³⁵S-met at 37°C. After this period, one-third of mitochondria was isolated by incubation in the SDS-PAGE loading buffer, while the other two-thirds were washed and incubated for additional 3 or 6 hours for the “cold-chase” experiment in a translation buffer containing all amino acids, including methionine. Translation products were separated by SDS-PAGE, the gel was stained with Coomassie Brilliant Blue R-250 incubated in Amplify solution (GE Healthcare, Munich, Germany), dried and newly synthesized polypeptides were detected by autoradiography.

2.3.9 tRNA aminoacylation assay

For analysis of the tRNA aminoacylation, total RNA was isolated with TRIzol reagent as described before. Total RNA was resuspended in 0.3 M NaOAc (pH 5.0) and 1 mM EDTA. Aminoacylation status was determined by acid-urea PAGE, using 6.5% (19:1) polyacrylamide, 8 M urea gels in 0.1 M NaOAc (pH 5.0) buffer. Gels were run for 48 hours at 4°C with regular buffer changes. tRNAs were detected using specific γ -³²P-dATP labeled oligonucleotide probes (Park et al., 2007).

2.4 Histological Analyses

2.4.1 Vibratome and cryostat sections

After perfusion, coronal sections were cut on a Leica VT1200S with a thickness of 30 - 40 μm . Free floating sections were kept at 4 °C in 0.05% NaN_3 -PBS.

For cryostat sections, brains were directly isolated after sacrificing the animals, directly embedded in Tissue-Tek (Sakura, Alphen aan den Rijn, The Netherlands) and placed onto dry ice until the Tissue-Tek froze. Afterwards, brains were stored at -80 °C. Coronal sections were cut on a Leica CM1850 cryostat with a thickness of 7 μm . Sections were directly mounted onto microscope slides and stored at -20 °C.

2.4.2 Transmission electron microscopy

Semithin and ultrathin sections, as well as transmission electron microscopy were prepared and visualized by Shuaiyu Wang as described previously (Almajan et al., 2012).

2.4.3 Nissl Staining

Vibratome sections were mounted on a microscope slide with cromalin solution (5% gelatine w/v, 2mM $\text{KCr}(\text{SO}_4)_2 \cdot 12 \text{H}_2\text{O}$ in water) and dried at 37 °C for 30 minutes. Sections were incubated 45 seconds with Nissl solution (0.04 N NaOH, 0.2 Acetic acid, 8.7 mM thionin acetate), washed shortly in dH_2O , dehydrated with increasing ethanol concentration (50%, 70%, 80%, 90 %, 95%, 100%, each step 30 seconds) and incubated in Xylene for 4 minutes.

2.4.4 COX-SDH staining

COX-SDH staining was performed on cryosections. The sections were air-dried for 1 h, surrounded with a PAP pen, incubated in a humid chamber for 40 minutes at 37 °C in COX solution (0.8 ml 3,3 diaminobenzidine tetrahydrochloride, 0.2 ml 500 µM cytochrome c, a few grains of catalase), and then washed in PBS. Later on, sections were incubated in SDH solution (0.8 ml 1.875 mM Nitroblue tetrazolium, 0.1 ml 1.3 M sodium succinate, 0.1 ml 2 mM Phenazine methosulphate, 0.01 ml 100 mM Sodium azide) for 90 minutes at 37 °C in a humid chamber. Sections were washed in PBS, dehydrated with increasing ethanol concentration (75% for 2 minutes, 95% for 2 minutes, 100% for 10 minutes), air dried, and mounted in D.P.X. (VWR, Darmstadt, Germany).

2.4.5 Hemotoxylin and Eosin staining (H&E Staining)

H&E staining was applied to cryosections. The sections were incubated for 1 minute in tap water, 6 minutes in Mayer's Hematoxylin solution (Sigma Aldrich, Seelze, Germany), and again with tap water, this time for 15 minutes. Afterwards, the samples were further incubated in 1 minute in dH₂O and 1 minute in Eosin. Following, the sections were washed several times with tap water, and then dehydrated with ethanol (75% for 1 min, 96% for 1 min, 100% for 1 min) and Xylene for 1 min. The final mounting was done with Entellan (Millipore, Merck, Darmstadt, Germany).

2.4.6 Masson's trichrome staining

Masson's trichrome staining was performed on cryosections using a staining kit (Sigma Aldrich, Seelze, Germany), according to the manufacturer's instructions.

2.4.7 TUNEL assay

Terminal deoxynucleotidyl transferase dUTP nick end labeling (TUNEL) assay was performed on 30 mm vibratome sections with ApopTag Plus Peroxidase In Situ Apoptosis Detection Kit (Millipore, Merck, Darmstadt, Germany) according to the manufacturer's protocol. Briefly, sections were fixed in PFA 4% in PBS for 10 minutes at room temperature. After post-fixation and permeabilization steps, sections were washed, incubated in proteinase K (20 mg/ml in PBS) for 15 minutes, washed in PBS and then quenched in 3% H₂O₂ in PBS for 5 minutes. Sections were then pre-incubated for 15 seconds in equilibration buffer and then in working strength TdT enzyme for 1 hour at 37°C. After the reaction was stopped, sections were washed in water, dehydrated with increasing ethanol concentration and Xylene.

2.4.8 Immunohistochemical and immunofluorescence analyses

Free-floating sections were washed extensively and pretreated for 30 minutes in 2% Triton X-100/PBS to remove cryoprotectant. Subsequently, the sections were treated with 0.3% H₂O₂ in PBS for 20 minutes to quench endogenous peroxidase activity. Sections were permeabilized and blocked in 0.4% Triton X-100, 10% goat serum in PBS for 1 hour at room temperature. Primary antibodies [GFAP (1:2000, NeoMarkers, Fremont, USA), IBA1 (1:3000, WAKO Life Sciences, Inc., Richmond, USA), p62 (SQSTM -Sequestosome 1 – for heart sections only) (1:200, Abnova, Taipei, Taiwan)] were incubated overnight in 0.4% Triton X-100, 5% goat serum in PBS at 4 °C. After 3x 5 minutes washing with PBS, secondary antibodies [anti-mouse Alexa Fluor 488 (1:2000, Invitrogen, Karlsruhe, Germany), anti-rabbit Alexa Fluor 546 (1:2000, Invitrogen, Karlsruhe, Germany)] were applied in 5% goat serum in PBS for 2 hours. Finally, the sections were washed in PBS and mounted using FluorSave Reagent (Calbiochem, Merck, Darmstadt, Germany).

Light microscopy images were acquired by a Leica SCN400 slide scanner (Leica Microsystems, Wetzlar, Germany). Evaluation and processing was done with SlidePath Gateway Client software (version 2.0). Fluorescent images were acquired by an Axio-Imager M2 microscope equipped with Apotome 2 (Zeiss, Jena, Germany). Images were processed with AxioVision software (version 4.8.2).

2.5 Statistical analyses

A two-tailed unpaired student's t-test was used to determine statistical significance. All p values below 0.05 were considered significant. Error bars represent standard error of the mean (S.E.M.). * $p < 0.05$; ** $p < 0.01$; *** $p < 0.001$; **** $p < 0.0001$.

2.6 Chemicals and biological material

Size markers for agarose gel electrophoresis (Gene Ruler DNA Ladder Mix) and for SDS-PAGE (Page Ruler Prestained Protein Ladder Mix) were obtained from Fermentas, St. Leon-Rot, Germany. GoTaq® Green Master Mix and DNA Polymerase were purchased from Promega, Mannheim, Germany. Chemicals used in this work are listed in table 2.3. Solutions were prepared with double distilled water.

Table 2.3 Chemicals used and suppliers

| Chemical | Supplier |
|-------------------------------------|---------------------------------------|
| β -mercaptoethanol | Applichem, Darmstadt, Germany |
| 2,2,2-Tribromoethanol (Avertin) | Sigma-Aldrich, Seelze, Germany |
| 2-Methyl-2-Butanol | Sigma-Aldrich, Seelze, Germany |
| Acetic Acid | Merck, Darmstadt, Germany |
| Acetone | KMF Laborchemie, Lohmar, Germany |
| Acrylamide | Roth, Karlsruhe, Germany |
| Agarose | Sigma-Aldrich, Seelze, Germany |
| Agarose (Ultra Pure) | Life Technologies, Darmstadt, Germany |
| Ammonium Acetate | Merck, Darmstadt, Germany |
| Ammoniumpersulfat (APS) | Sigma-Aldrich, Seelze, Germany |
| Bovine serum albumin (BSA) | Sigma-Aldrich, Seelze, Germany |
| Bromophenol | Merck, Darmstadt, Germany |
| Calcium Chloride | Merck, Darmstadt, Germany |
| Chloroform | Merck, Darmstadt, Germany |
| Deoxynucleotides (dNTPs) | Sigma-Aldrich, Seelze, Germany |
| Dimethylsulfoxide (DMSO) | Merck, Darmstadt, Germany |
| di-Natriumhydrogenphosphate | Merck, Darmstadt, Germany |
| Enhanced chemiluminescence (ECL) | GE Healthcare, Munich, Germany |
| Ethanol, absolute | Applichem, Darmstadt, Germany |
| Ethidium bromide | Sigma-Aldrich, Seelze, Germany |
| Ethylendiamine tetraacetate (EDTA) | Applichem, Darmstadt, Germany |
| Glycine | Applichem, Darmstadt, Germany |
| HEPES | Applichem, Darmstadt, Germany |
| Hydrochloric acid (37%) | Applichem, Darmstadt, Germany |
| Hydrogen peroxide | Sigma-Aldrich, Seelze, Germany |
| Isopropanol (2-propanol) | Roth, Karlsruhe, Germany |
| Magnesium chloride | Merck, Darmstadt, Germany |
| Methanol | Roth, Karlsruhe, Germany |
| Nitrogen (liquid) | Linde, Pullach, Germany |
| Paraformaldehyde (PFA) | Sigma-Aldrich, Seelze, Germany |
| Phenylmethylsulfonylfluoride (PMSF) | Sigma-Aldrich, Seelze, Germany |
| Phosphate buffered saline (PBS) | Gibco BRL, Eggenstein, Germany |
| Potassium chloride | Merck, Darmstadt, Germany |
| Potassium hydroxide | Merck, Darmstadt, Germany |
| Protease Inhibitor Cocktail Tablets | Roche, Basel, Switzerland |
| Sodium acetate | Applichem, Darmstadt, Germany |
| Sodium azide | Sigma-Aldrich, Seelze, Germany |
| Sodium chloride | Applichem, Darmstadt, Germany |
| Sodium citrate | Merck, Darmstadt, Germany |

| | |
|-------------------------------------|--------------------------------|
| Sodium dodecyl sulfate | Applichem, Darmstadt, Germany |
| Sodium fluoride | Merck, Darmstadt, Germany |
| Sodium hydroxide | Applichem, Darmstadt, Germany |
| Sodium orthovanadate | Sigma-Aldrich, Seelze, Germany |
| Sucrose | Applichem, Darmstadt, Germany |
| Tetramethylethylenediamine (TEMED) | Sigma-Aldrich, Seelze, Germany |
| Trishydroxymethylaminomethane(Tris) | Applichem, Darmstadt, Germany |
| Triton X-100 | Applichem, Darmstadt, Germany |
| Tween 20 | Applichem, Darmstadt, Germany |

3. Results

3.1. Mitochondrial aspartyl-tRNA synthetase (DARS2) is essential for embryonic development in the mouse

To determine the *in vivo* function of mitochondrial aspartyl-tRNA synthetase (DARS2) in mammals and to unravel the consequences of DARS2 deficiency, we have generated a novel mouse model whose part of 2nd intron and 3rd exon of the DARS2 gene is floxed, allowing Cre-recombinase mediated excision and conditional disruption of DARS2 gene (Figure 3.1A). The targeting vector, which is obtained as sperm from the Knockout Mouse Project (KOMP) Repository, presents itself as 'Knockout-first allele' (Testa et al., 2004), having the ability to cause frame-shift to create a null allele without the need for Flp- or Cre-mediated excision. Nevertheless, we first mated the mice heterozygous for the targeting allele with mice carrying Flp recombinase under the control of the human beta-actin promoter, thus excising the neomycin selection cassette (Figure 3.1A). Afterwards, *Dars2*^{+/*loxP*} mice were mated with mice expressing cre recombinase under the control of the β -actin promoter (ACTB-cre) to generate heterozygous DARS2 knockout mice (*Dars2*^{+/-}) (Figure 3.1A and 3.1B). Following the removal of the floxed region, transcript is predicted to produce a truncated protein product, which can be subjected to non-sense, mediated decay (NMD). Intercrossing of *Dars2*^{+/-} mice produced no viable homozygous knockouts (*Dars2*^{-/-}), whereas the other two genotypes were recovered at expected Mendelian proportion (total pups n=79; *Dars2*^{+/+} n=25, *Dars2*^{+/-} n=54). We then analyzed embryos derived from intercrossing of *Dars2*^{+/-} mice at embryonic day (E) 8.5 and found that ~25% embryos had a mutant appearance (Figure 3.1C). Genotyping confirmed that all mutant embryos were homozygous knockouts (*Dars2*^{-/-}) (Figure 3.1B). These results show that loss of DARS2 causes embryonic lethality at ~E8.5.

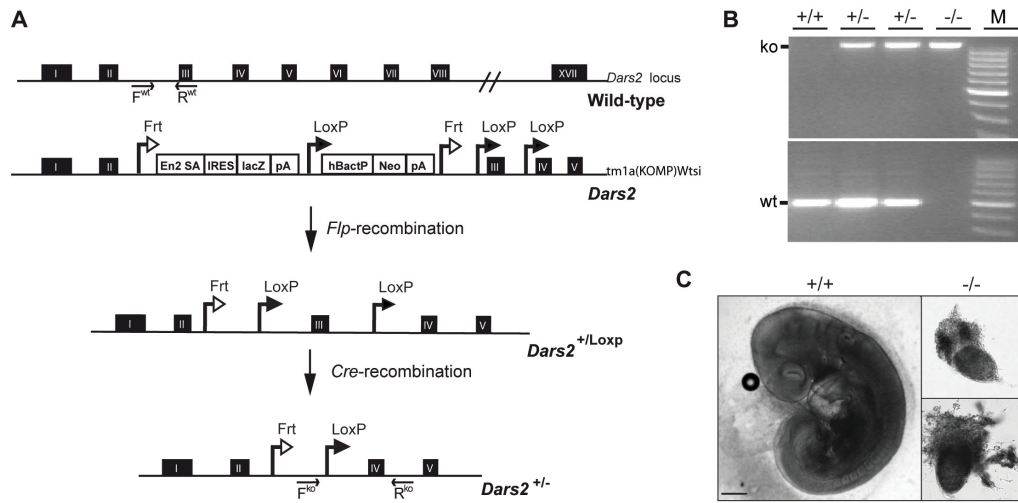


Figure 3.1 Disruption of *Dars2* in the germline.

(A) Targeting strategy for the conditional disruption of *Dars2* gene. EN2-SA - Splice acceptor of mouse homeobox protein engrailed-2 exon 2; IRES - Internal ribosome entry site from encephalomyocarditis virus; lacZ - lacZ gene; pA - SV40 polyadenylation site; hBactP - Human beta actin promoter; neo - Neomycin selection cassette. Depicted by arrows are the PCR primers used for genotyping of the alleles. (B) Genotyping PCR for one wild-type (+/+), two heterozygous (+/-), or one homozygous knockout (-/-) *Dars2* animals. DNA fragments corresponding to the wild type (wt – 475 bp), and knockout (ko – 1100 bp) *Dars2* loci are indicated. Marker (M) used is Generuler 100 bp (Fermentas). (C) Morphology of a wild-type ($DARS2^{+/+}$) and two homozygous knockout ($DARS2^{-/-}$) embryos at day ~E8.5. Scale bar, 100 μ m.

3.2. $DARS2^{+/-}$ mice are haplosufficient

We next analyzed heterozygous $Dars2^{+/-}$ mice to determine if one copy of the gene is sufficient to maintain proficient mitochondrial protein synthesis. Heterozygous $Dars2^{+/-}$ mice were born in expected Mendelian proportions, developed normally, and displayed no obvious phenotype even at 24 months of age. In order to assess the effect of loss of one *Dars2* allele, we analyzed steady-state levels of the mitochondrial respiratory chain (MRC) complexes in $Dars2^{+/-}$ mice. Mitochondrial proteins isolated from liver, heart and skeletal muscle were separated on n-dodecyl- β -D-maltoside-based blue native polyacrylamide electrophoresis (BN-PAGE) (Figure 3.2A), followed by Western blot analysis

with antibodies raised against different subunits of each of the five respiratory complexes (Figure 3.2B). We did not observe any reduction in steady-state levels of different OXPHOS complexes in mitochondrial extracts from *Dars2*^{+/-} mice (Figure 3.2A and 3.2B), suggesting that one copy of the gene is sufficient to sustain proficient mitochondrial protein synthesis. Consequently, *in gel* activities of complex I (NADH:ubiquinone oxidoreductase, COI, EC 1.6.5.3) and complex IV (cytochrome c oxidase, COX – COIV, EC 1.9.3.1) were also not changed in *Dars2*^{+/-} mitochondria (Figure 3.2C and 3.2D, respectively).

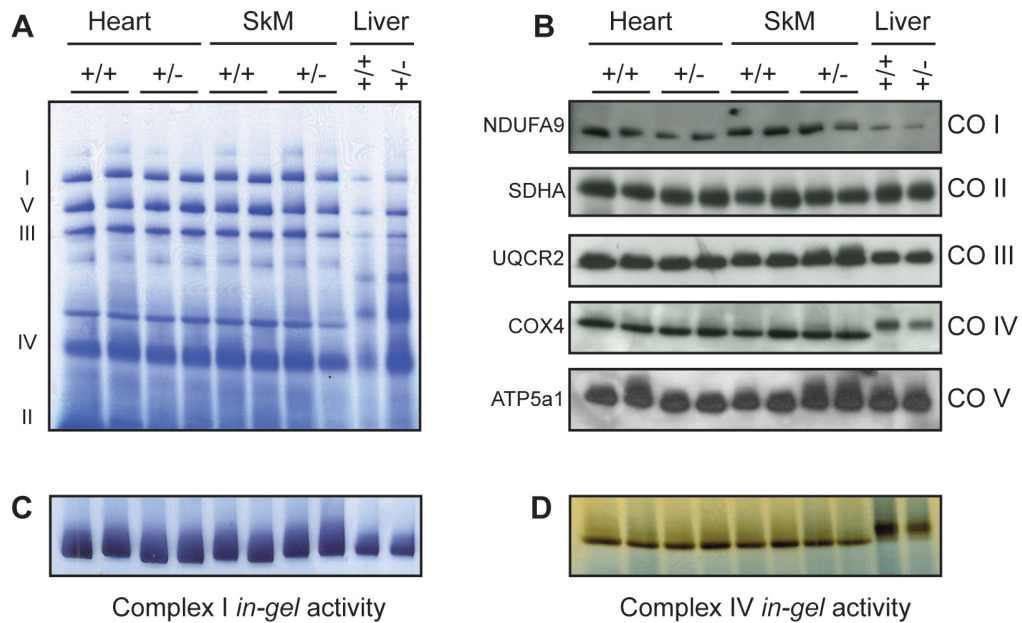


Figure 3.2 Respiratory Chain Complexes in Heart, Skeletal Muscle (SkM) and Liver Mitochondria of 104-Week-Old wild type (+/+) and heterozygous (+/-) *Dars2* mice.

(A) Coomassie brilliant blue stained BN-PAGE, (B) Western blots, (C) *In gel* activity of CO I and (D) *In gel* activity of CO IV performed after BN-PAGE.

3.3. Tissue-specific disruption of *Dars2*

In order to shed more light on the consequences of DARS2 deficiency in different tissues and to unravel their coping mechanisms against this deficiency, we decided to generate two different tissue specific mice models:

- (i) by disrupting the gene by breeding *Dars2*^{loxP/loxP} (from now on denoted as L/L) mice with transgenic mice expressing cre-recombinase from the muscle creatine kinase promoter (Ckmm-cre), and
- (ii) by mating L/L mice with mice expressing the cre-recombinase under the control of the Ca²⁺/calmodulin-dependent kinase II alpha promoter (CaMKII α -Cre).

By creating different models, we wanted to see how these different tissues (heart, skeletal muscle and brain), the most commonly affected ones in various mitochondrial diseases, react to defective mitochondrial protein synthesis and whether they activate mitochondrial stress signals.

3.4. DARS2 deficiency leads to early pathological changes in heart and skeletal muscle

DARS2 deletion in heart and skeletal muscle was mediated by cre-recombinase under the muscle creatine kinase promoter to produce *Dars2*^{L/L, +/Ckmm-cre} (hereafter denoted as L/L, cre) mice. The muscle creatine kinase promoter is fully active in heart and skeletal muscle after embryonic day 15.5 (E15.5) (Lyons et al., 1991). We first confirmed the complete loss of DARS2 in both targeted tissues at 6 weeks of age (Figure 3.3A). Liver extracts were used as a negative control throughout the experiments.

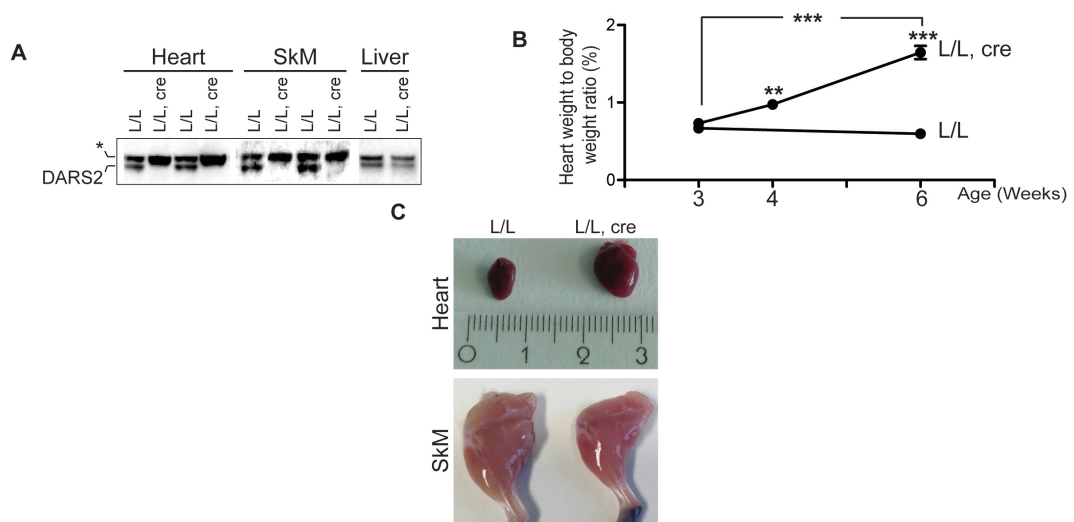


Figure 3.3 Phenotypic characterization of tissue-specific DARS2-deficiency in heart and skeletal muscle.

(A) Western blot analysis of DARS2 protein levels in heart, skeletal muscle (SkM) and liver of control (L/L) and *Dars2* tissue-specific knockout mice (L/L, cre). * Unspecific protein. (B) Heart-weight to body-weight ratio in mice at 3, 4 and 6 (n=5-9) weeks of age. (C) Heart and SkM morphology of 6-week-old mice.

Bars represent mean \pm S.E.M. Asterisks indicate level of statistical significance (Student's t-test, ** $p < 0.01$; *** $p < 0.001$).

The maximal lifespan of the DARS2-deficient mice was shortened only to 6-7 weeks. Out of 210 mice, only nine were observed to live until they are 8-week-old. The knockout mice had hypertrophied hearts and atrophied skeletal muscles. Moreover, we detected a decrease of body weight from 4 weeks of age accompanied by progressive cardiomyopathy characterized by a strong increase in heart size with increasing age (Figures 3.3B and 3.3C).

Does the observed phenotypes also coincide with the molecular clues? To answer that question, we checked hypertrophy, atrophy and myogeny markers. We detected clear signs of degeneration in both tissues at 6 weeks of age, as measured by the increased expression of hypertrophy markers *Nppa* and *Nppb* in heart, and

atrophy markers *MuRF1* and *Atrogin1* in skeletal muscle (Figure 3.4A). Although we found no change in expression of myogenic markers *Myod1* and *Myf5*, increased number of cells with centrally positioned nuclei suggests a possible upregulation of skeletal muscle regeneration in DARS2-deficient mice (Figure 3.4B).

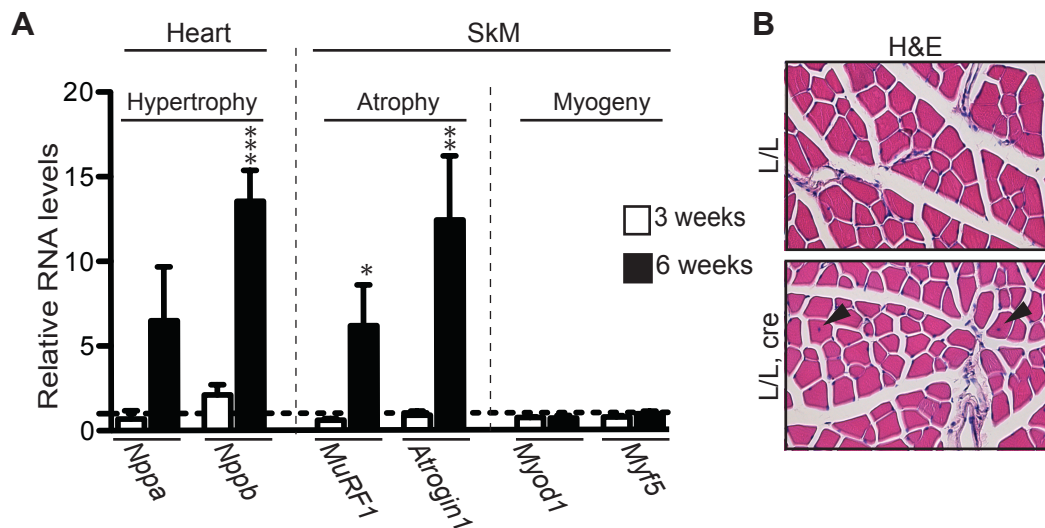


Figure 3.4 Molecular characterization of tissue-specific DARS2-deficiency in heart and skeletal muscle.

(A) Relative expression levels of cardiac hypertrophy markers (*Nppa* and *Nppb*), muscle atrophy markers (*MuRF1* and *Atrogin-1*) and myogenic factors (*Myod1* and *Myf5*) in 3- and 6-week-old mice. (n=6) **(B)** Hematoxylin & Eosin (H&E) staining of muscle sections from 6-week-old mice. Arrowheads indicate fibers with centrally located nuclei. (Scale bar: 100 μ m).

Bars represent mean \pm S.E.M. Asterisks indicate level of statistical significance (Student's t-test, *p<0.05, **p<0.01; ***p<0.001).

The ultrastructural analysis showed disruption of myocardial organization with accumulation of mitochondrial mass in 6-week-old DARS2-deficient hearts (Figure 3.5). Abnormally shaped mitochondria were also available in hearts. Surprisingly, we only seldom observed long, fused mitochondria, with no increase in mitochondrial mass, or major changes in fiber organization. COX-SDH

staining revealed a very strong and comparable respiratory chain deficiency in both tissues. Formation of excess fibrous connective tissue (fibrosis) was exemplified in both tissues via Masson's Trichrome staining. Ragged-red fibers were not apparent (data not shown).

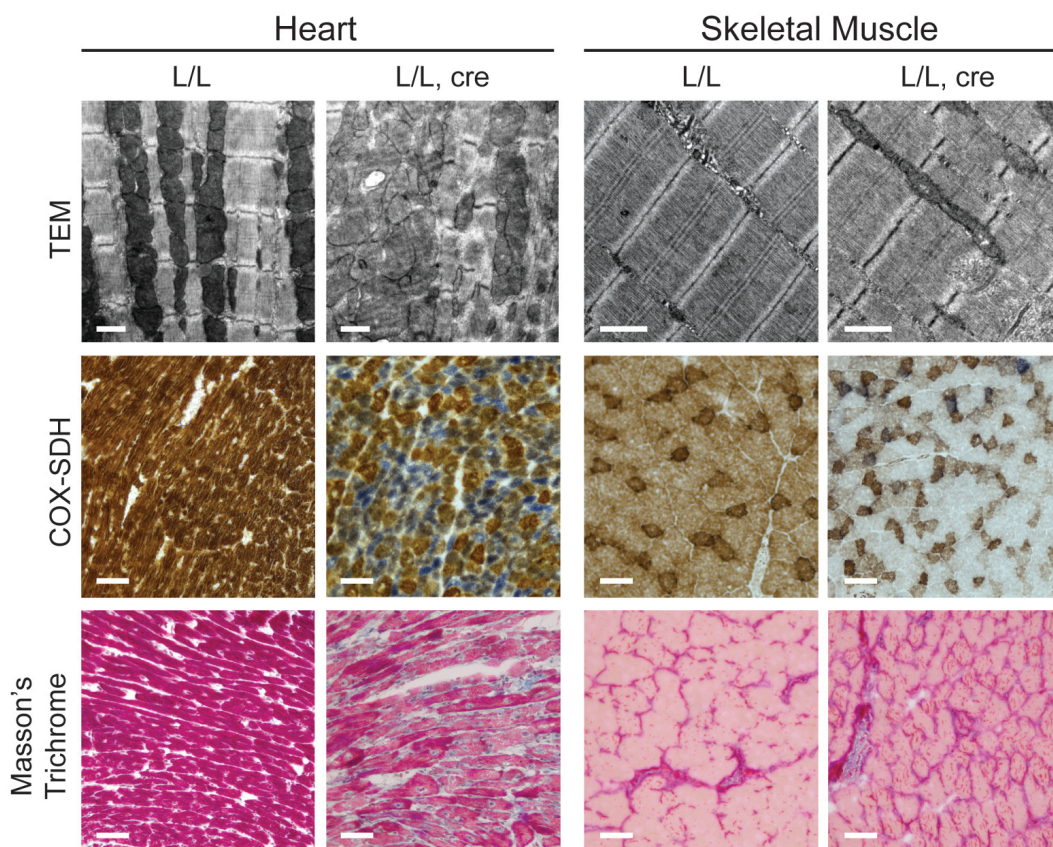


Figure 3.5 Immunohistochemical characterization of heart and skeletal muscle.

TEM – Transmission Electron Micrographs (Scale bar: 1 μ m), COX-SDH - Enzyme histochemical double staining for COX and SDH activities and Masson's Trichrome staining (Scale bars: 100 μ m) (n=4).

As mentioned above, we observed increased mitochondrial mass in Transmission Electron Micrographs (TEM) of heart only. Moreover, COX-deficient cardiomyocytes showed also high succinate dehydrogenase (SDH) activity (blue

staining), consistent with this observed mitochondrial mass increase (Figure 3.5). Even if TEM did not reveal any mitochondrial biogenesis in skeletal muscle, we wanted to employ other additional experimental methods to search for signs of increased mitochondrial mass. We measured citrate synthase activity, as this is one of the most commonly used markers of mitochondrial biogenesis. This enzymatic assay proved that mitochondrial mass was only increased in DARS2-deficient hearts (Figure 3.6A).

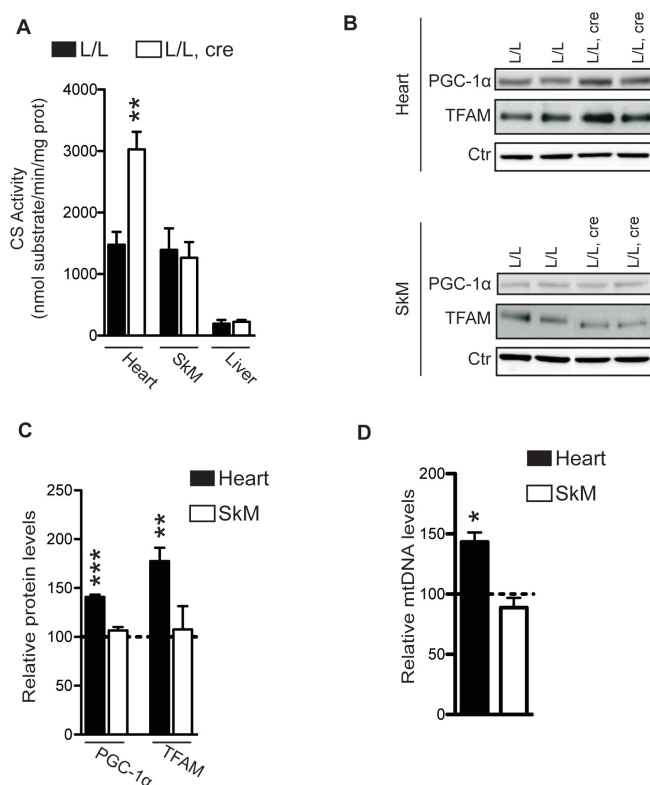


Figure 3.6 Increased mitochondrial mass was observed only in DARS2-deficient cardiomyocytes.

(A) Citrate synthase enzyme activity in heart, skeletal muscle (SkM) and liver of control (L/L) and DARS2-deficient mice (L/L, cre). (B-C) Western blot analysis (B) and corresponding quantification (C) of PGC-1 α and TFAM levels in total protein extracts from heart and SkM. (D) Relative mtDNA levels presented as percentage of control.

Moreover, PGC-1 α and TFAM levels were only up in cardiomyocytes (Figure 3.6B-C). As a last proof, we performed Southern blotting to detect mitochondrial DNA (mtDNA) levels and found out that mtDNA was also significantly upregulated in heart but not in skeletal muscle (Figure 3.6D). These data suggest that mitochondrial biogenesis is occurring only in cardiomyocytes, and other pathways could be involved in adaptive responses in DARS2-deficient skeletal muscle.

3.5. Defective mitochondrial translation gives rise to strong respiratory chain deficiency

To analyze biochemical consequences of DARS2 deficiency in heart and skeletal muscle, we first measured the levels of MRC enzyme activities (Figure 3.7A). A dramatic decrease in all complexes (except nuclear DNA-encoded CO II) was apparent in heart and skeletal muscle. Further, oxygen consumption measurements were performed in isolated heart mitochondria (Figure 3.7B) and skeletal muscle fibers (Figure 3.7C) and a general reduction in all inducible respiratory states was observed.

BN-PAGE analysis revealed reduction in the amount of fully assembled CO I, CO III and CO IV in both heart and skeletal muscle (Figure 3.7D), the latter being the most affected. The Western blots to detect the MRC subunits from the corresponding BN-PAGE analysis also showed a similar pattern (i.e. CO IV is nearly absent in knockout mice) (Figure 3.7E). Reduction of CO I and CO IV levels was mirrored by the decrease in *in-gel* activity in both tissues (Figure 3.7F and 3.7G, respectively). Furthermore, the Western blots from the total protein extracts revealed a strong decrease in the steady-state levels of CO IV subunits and a moderate reduction in the levels of CO I and CO III subunits in both tissues (Figure 3.7H).

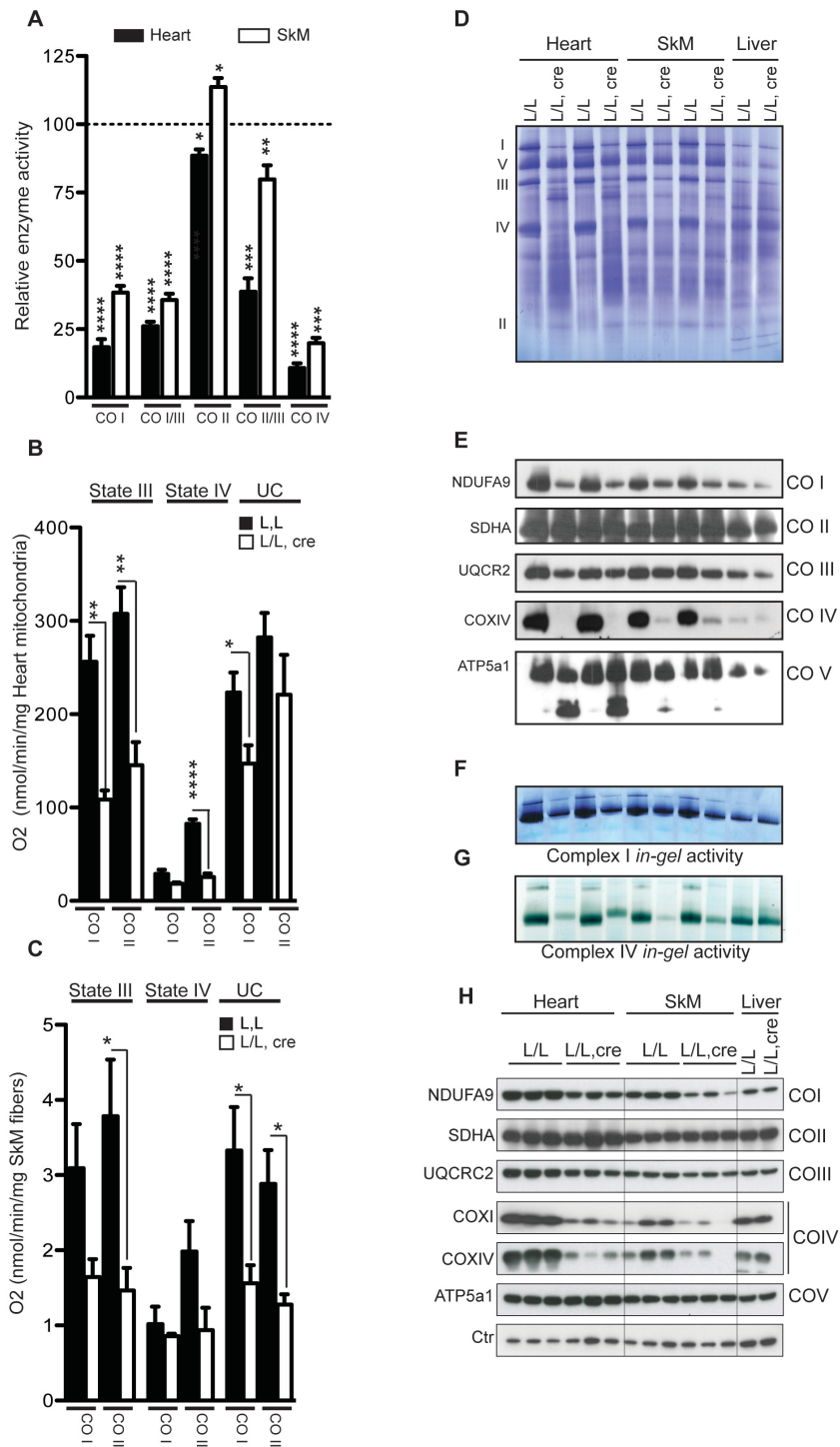


Figure 3.7 Characterization of mitochondrial dysfunction in 6-week-old DARS2-deficient heart and skeletal muscle.

(A) Relative MRC complex activities in isolated heart and SkM mitochondria of DARS2-deficient mice (L/L, cre) presented as a percentage of control (L/L) (n=5). (B-C) Measurement of substrate-dependent oxygen consumption of (B) isolated heart mitochondria and (C) permeabilized skeletal muscle fibers from L/L and L/L, cre mice. CO I-specific substrates (pyruvate, malate, glutamate); CO II-specific substrate (succinate). State III - ADP-stimulated oxygen consumption rate; State IV – respiration rate after addition of oligomycin; UC – oxygen consumption rate in the presence of an uncoupler. Bars represent mean \pm S.E.M. Asterisks indicate level of statistical significance (*p \leq 0.05; **p \leq 0.01; ****p $<$ 0.0001; Student's t-test; n=5). (D) Coomassie Brilliant Blue staining of BN-PAGE with indicated position of specific complexes. (E) Western blots for MRC complexes. Antibodies against individual MRC subunits (indicated on the left) and used to detect MRC complexes (indicated on the right). (F) *In-gel* activity of CO I and (G) CO IV, performed after BN-PAGE (n=4). (G) Western blots for the steady-state levels of individual MRC subunits from total protein extracts of heart, SkM and liver.

We detected a strong deregulation of *de novo* protein synthesis in DARS2-deficient mitochondria from heart and skeletal muscle (Figure 3.8A). Figure 3.8B corresponds to the loading control for *in organello* gel. While the turnover rates seem to be rather slow compared to liver mitochondria and unchanged between the two tissues after 3 hours of cold-chase (Figures 3.8C-D). This analysis also revealed two interesting points: (1) ND2 subunit does not contain a single aspartate residue in its sequence, thus we see an upregulation; (2) ATP6 (ATP synthase F0 subunit 6) contains only one aspartate residue which is in its 244th amino acid – and it is a 246 amino acid long polypeptide. In our *in organello* gel, ATP6 presents an additional polypeptide with a slightly lower molecular mass than, which is likely a truncated form of this protein lacking the last two residues, (Fig 3.8A – highlighted box). The number, percentage and positions of aspartate residues mitochondrial-encoded MRC subunits contain can be reviewed in Table 3.1.

The observed strong upregulation of ND2 subunit (NADH dehydrogenase subunit 2) is likely a consequence of increased number of ribosomes inside DARS2-deficient mitochondria (Figure 3.8D). Remarkably, the upregulation of

(A) Representative gel of *in organello* translation in heart, SkM and liver mitochondria (n=4). *De novo* synthesized proteins are isolated immediately after labeling with ³⁵S-met (1h pulse). Positions of individual mitochondrial-encoded proteins are indicated. (B) Commassie Brilliant Blue stained gel used as loading control. (C) Turnover of the newly synthesized proteins after 3 hours of ‘cold chase’ in isolated heart, SkM and liver mitochondria. (F) Western blots of mitochondrial ribosomal subunits MRPS-35, MRPS-27, MRPL-13, MRPL-12 in heart and SkM. HSC70 (Ctr) and Ponceau S used as loading controls.

Table 3.1 Length of mitochondrial-encoded MRC subunits and the number, percentage and positions of aspartate residues

| Subunit | Length (amino acid) | Aspartate number | Aspartate percentage | Aspartate positions |
|---------------------------|---------------------|------------------|----------------------|--|
| <i>Complex I</i> | | | | |
| ND1 | 318 | 3 | 0.94 | 51, 199, 283 |
| ND2 | 345 | 0 | 0 | 0 |
| ND3 | 115 | 2 | 1.74 | 42, 66 |
| ND4 | 459 | 6 | 1.31 | 46, 59, 87, 187, 251, 281 |
| ND4L | 97 | 1 | 1.03 | 87 |
| ND5 | 607 | 12 | 1.98 | 83, 111, 163, 179, 208, 297, 352, 355, 393, 447, 449, 554 |
| ND6 | 172 | 6 | 3.49 | 110, 118, 122, 129, 130, 172 |
| <i>Complex III</i> | | | | |
| cytb | 381 | 11 | 2.89 | 20, 58, 72, 171, 214, 216, 228, 248, 252, 254, 374 |
| <i>Complex IV</i> | | | | |
| COXI | 514 | 16 | 3.11 | 14, 50, 51, 91, 144, 212, 221, 227, 298, 300, 364, 369, 406, 407, 442, 445 |
| COXII | 227 | 11 | 4.85 | 11, 25, 57, 88, 112, 115, 119, 127, 139, 158, 173 |
| COXIII | 261 | 4 | 1.53 | 60, 111, 190, 246 |
| <i>Complex V</i> | | | | |
| ATP6 | 226 | 1 | 0.44 | 224 |
| ATP8 | 67 | 1 | 1.49 | 5 |

As we showed that mitochondrial protein synthesis is strongly affected with DARS2 deficiency, we next analyzed mitochondrial transcripts. We detected a general upregulation of mitochondrial transcript levels (mt-mRNAs) primarily in DARS2-deficient hearts, while *Cyt b* levels were increased also in skeletal muscle mitochondria (Figure 3.9A-B). This upregulation might purely reflect the increased mitochondrial mass in cardiomyocytes.

Although pathogenic mutations in some aminoacyl-tRNA synthetases lead to a decrease in the level of cognate tRNAs (Belostotsky et al., 2011; Edvardson et al., 2007), we found no changes in the steady-state levels of mitochondrial tRNAs, including tRNA^{Asp} (Figure 3.9A-B).

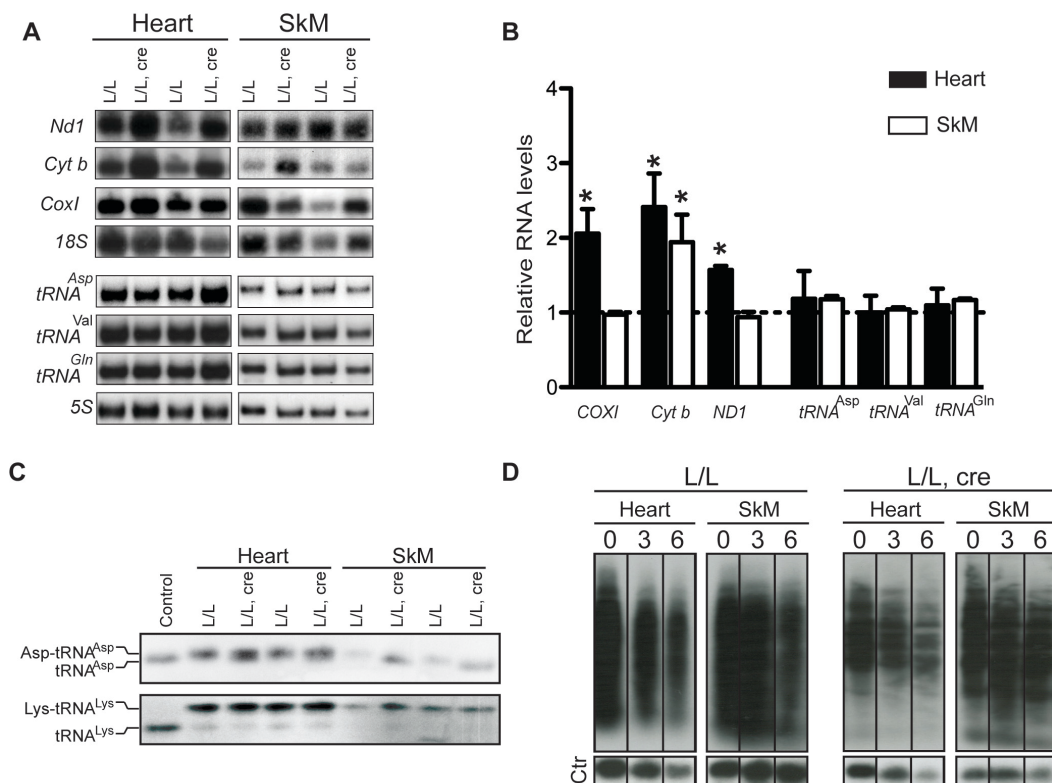


Figure 3.9 RNA-related assays (Northern blot, aminoacylation and *in organello* transcription).

(A) Northern blot analysis of mitochondrial mRNA and tRNA levels in heart. 18S rRNA and 5S rRNA are used as loading controls. (B) Quantification of mitochondrial mRNA and tRNA levels in heart and SkM presented as a percentage of control (n=5). (C) Aminoacylation assay for mitochondrial tRNA^{Asp} and tRNA^{Lys} in heart and SkM. Positions of charged (AA-tRNA^{AA}) and uncharged tRNAs (tRNA^{AA}) are indicated. (D) *In organello* transcription assay in heart and SkM mitochondria (n=5). Steady-state *CoxII* transcript levels are used as a loading control (Ctr). Bars represent mean ± S.E.M. Asterisks indicate level of statistical significance (Student's t-test, *p<0.05)

We also analyzed the level of tRNA aminoacylation by separation of charged and uncharged forms of tRNA^{Asp} under acidic conditions. While a full separation of the two forms, as shown for tRNA^{Lys}, cannot be achieved for tRNA^{Asp} (Enriquez and Attardi, 1996), we could observe minute, yet detectable shift in wild type samples compared to DARS2-deficient mitochondria (Figure 3.8C). This suggests that majority of tRNA^{Asp} in DARS2-deficient tissues is present in uncharged form, consistent with the predicted role of DARS2.

The question asked next was whether the rate of *de novo* transcription was affected. The analysis revealed similar *in organello* transcription rates but a slower turnover rate of skeletal muscle mitochondrial transcripts were observed (Figure 3.9D).

3.6. Mitochondrial stress responses are activated exclusively in DARS2-deficient heart

DARS2-deficient cardiomyocytes exhibited higher level of mitochondrial biogenesis. We were very intrigued by this observation and wanted to have an insight whether other mitochondrial stress responses were at work.

One of the hallmarks of mitochondrial dysfunction is the increased reactive oxygen species (ROS) production that leads to accumulation of oxidized proteins and upregulation of antioxidant responses in the cell. We performed oxyblot assay for protein carbonylation and Western blot for MnSOD (SOD2), the major mitochondrial ROS scavenging enzyme (Figure 3.10A). Quantified oxyblot assay can be found in Figure 3.10B. We found no differences between control and knockout mice for the parameters checked. This is in agreement with previous findings that general MRC deficiency does not affect ROS production (Trifunovic et al., 2005).

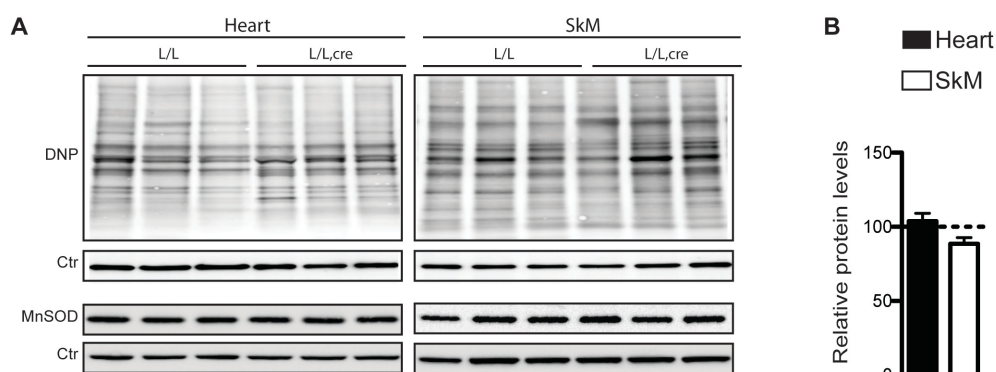


Figure 3.10 Antioxidant responses in DARS2-deficient heart and skeletal muscle.

(A) Oxidative stress levels via Western blot analysis of DNP (protein carbonylation) and MnSOD in heart and SkM. (B) Quantification of DNP levels presented as percentage of control.

Bars represent mean \pm S.E.M. (Student's t-test)

We have shown that DARS2-deficiency directly interferes with mitochondrial translation, and therefore, one would hypothesize that affected mitochondrial proteostasis might lead to the activation of mitochondrial unfolded protein response (UPR^{mt}). Indeed, in heart mitochondria, we detected increased levels of LON and AFG3L2, proteases involved in the turnover of misfolded proteins

(Figure 3.11A-B). Furthermore, two main mitochondrial chaperones mtHSP70 and HSP60 were upregulated, confirming the UPR^{mt} activation in 6-week-old hearts; however we did not observe any upregulation of CLPP, which is also one of the main players in UPR^{mt} (Figure 3.11A-B).

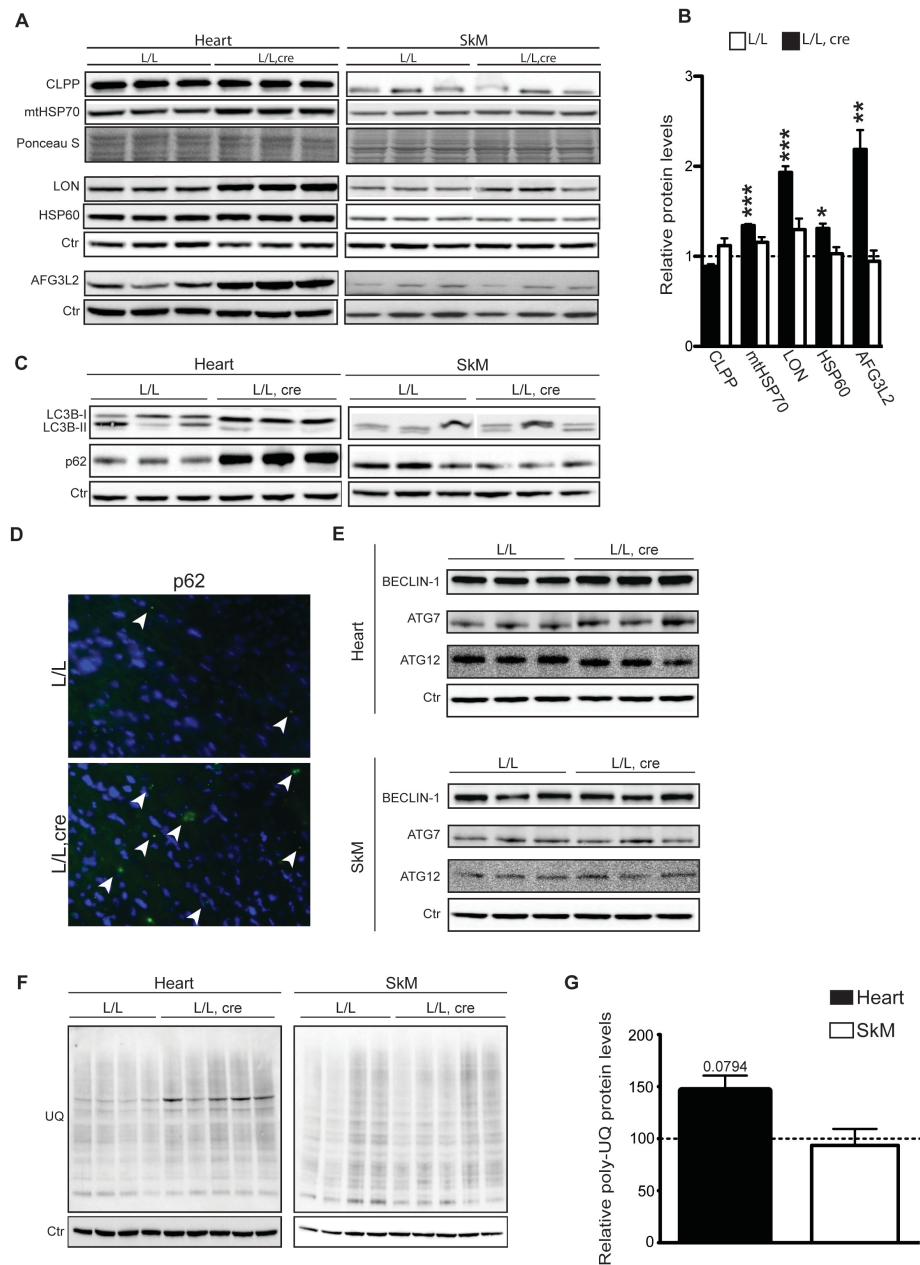


Figure 3.11 Mitochondrial unfolded protein response and autophagy in 6-week-old DARS2-deficient heart and skeletal muscle.

(A) Western blot analysis of CLPP, mtHSP70, LON, HSP60 and AFG3L2 levels in heart and SkM of control (L/L) and DARS2-deficient mice (L/L, cre). **(B)** Relative quantification of proteins involved in UPR^{mt} (CLPP, HSP60, LON, mtHSP70 and AFG3L2) in 6-week-old DARS2-deficient hearts and skeletal muscle normalized to respective controls. **(C)** Western blot analysis of LC3 and p62 levels in heart and SkM. **(D)** p62 (green) immunostaining of heart sections. DAPI (blue), (Scale bar: 100µm). **(E)** Western blot analysis of BECLIN-1, ATG7 and ATG12. **(D-E)** Western blot analysis **(D)** and quantification **(E)** of poly-UQ proteins in total protein extracts of heart and SkM. HSC70 (Ctr) is used as loading control. Bars represent mean ± S.E.M. Asterisks indicate level of statistical significance (Student's t-test, one p value is indicated over the error bar *p<0.05, **p<0.01, ***p<0.001) (n=5-8).

Another striking observation was the reduction in (macro)autophagy. In DARS2-deficient hearts, we observed the suppression of LC3B-I to LC3B-II conversion (Figure 3.11C) and accumulation of p62 (Figure 3.11C-D), suggesting a reduction in autophagy. This was further supported by the lack of autophagosomes on multiple heart section analyzed by TEM. Other components of the autophagy pathway, such as ATG7, ATG12 and BECLIN-1, were not affected (Figure 3.11E). In agreement with a reduction in autophagy and perturbations in protein folding environment, we detected somewhat higher levels of polyubiquitinated (poly-UQ) proteins (p value 0.0794) exclusively in DARS2-deficient hearts (Figure 3.11F-G).

Our observations so far proved the existence of MRC deficiency in both heart and skeletal muscle and upregulation of mitochondrial stress responses, such as UPR^{mt}, exclusively in heart. These posed the question whether MRC deficiency in DARS2-deficient skeletal muscle reached the threshold for the activation of stress responses observed in heart mitochondria. To test this, we analyzed DARS2-deficient heart mitochondria at 3 weeks of age that showed no obvious signs of mitochondrial cardiomyopathy (Figure 3.3B).

3.7. Early disturbance in mitochondrial proteostasis triggers stress responses in heart independent of MRC deficiency

Contrary to their 6-week-old counterparts, 3-week-old DARS2-deficient heart mitochondria only showed minor downregulation in MRC enzyme activities, CO IV being the only significantly affected one (Figure 3.12A).

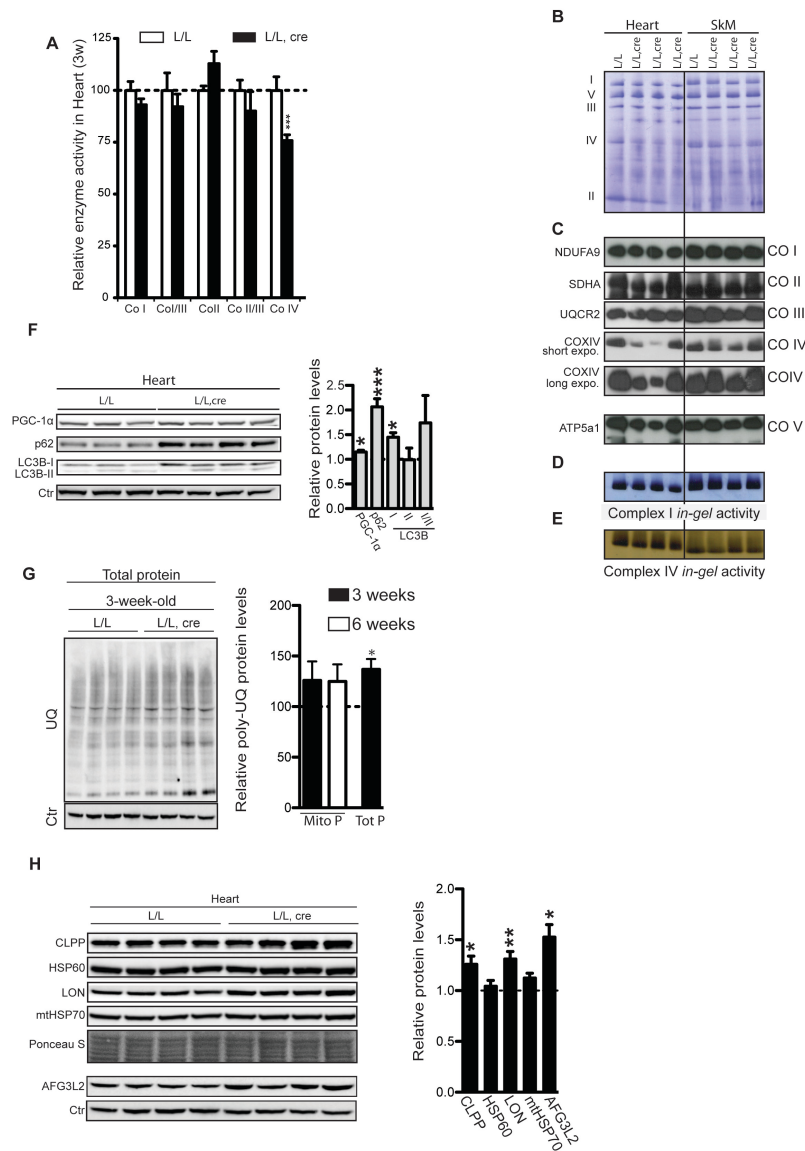


Figure 3.12 Characterization of mitochondrial dysfunction and stress responses in 3-week-old DARS2-deficient heart and skeletal muscle.

(A) Relative MRC complex activities in heart and SkM mitochondria of DARS2-deficient mice (L/L, cre) presented as a percentage of control (L/L) (n=5). **(B-E)** BN-PAGE analysis of respiratory chain complexes for 3- and 6-week-old mice. **(B)** Coomassie Brilliant Blue staining of BN-PAGE with indicated position of specific complexes. **(C)** Western blots for MRC complexes. Antibodies against individual MRC subunits (indicated on the left) and used to detect MRC complexes (indicated on the right). **(D)** In-gel activity of CO I and **(E)** CO IV, performed after BN-PAGE (n=4). **(F)** Western blot analysis with corresponding quantification of PGC-1 α , p62 and LC3 levels. HSC70 is used as loading control (Ctr). (n=5) **(G)** Western blots and corresponding quantification (n=4) of poly-UQ proteins from mitochondrial (Mito P) or total protein (Tot P) extracts in 3- and 6-week-old hearts. Results presented as fold-increase compared to the control (n=4). **(H)** Western blot analysis and quantification of CLPP, HSP60, LON, mtHSP70 and AFG3L2 levels in 3-week-old control (L/L) and DARS2-deficient (L/L, cre) hearts. Bars represent mean \pm S.E.M. Asterisks indicate level of statistical significance (Student's t-test, *p<0.05, **p<0.01, ***p<0.001).

BN-PAGE and Western blots for subunits of MRC complexes also revealed a mild-to-moderate change in knockout hearts, as well as no obvious change in the *in-gel* activities of CO I and CO IV (Figure 3.12B-E). Were the stress signals that were observed previously still persistent in 3-week-old DARS2-deficient hearts even if their mitochondrial function is barely changed? We found evidence for mitochondrial retrograde signaling via an increase in PGC1 α level (Figure 3.12F). Downregulated autophagy was still observed, illustrated by increased p62 levels and LC3B-I levels (Figure 3.12F). In agreement with a reduction in autophagy, we detected significantly higher levels of polyubiquitinated proteins in total tissue protein extracts and a tendency to increase in isolated mitochondrial extracts (Figure 3.12G). This suggests that mechanisms other than respiratory chain deficiency are the primary activators of adaptive changes in DARS2-deficient hearts.

We also checked the levels of mitochondrial proteases in 3-week-old animals as we performed for their 6-week-old counterparts. The levels of major mitochondrial proteases were up; this time including CLPP, which was not changed in 6-week-old hearts (Figure 3.12H). Interesting enough, those changes in proteases were not reflected in the levels of the two main mitochondrial

chaperones mtHSP70 and HSP60. None of these changes were observed in 3-week-old skeletal muscle from the same animals (data not shown).

These observations gave us hints that mitochondrial proteostasis could be the initial signal for the activation of different stress responses observed in DARS2-deficient heart mitochondria. We wanted further proof regarding the perturbed proteostasis.

In organello translation assay in 3-week-old heart mitochondria revealed higher *de novo* protein synthesis in knockouts, contrary to previous results (Figure 3.13A).

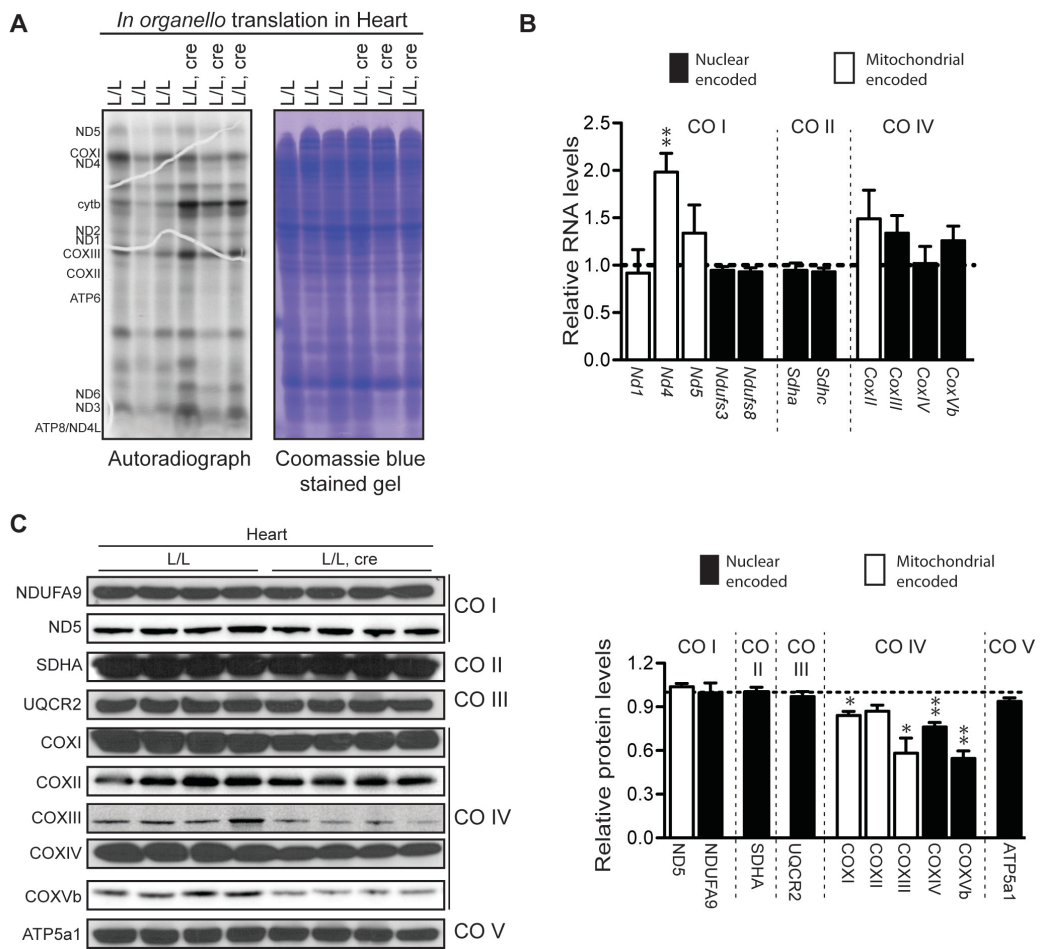


Figure 3.13 Proof on perturbed mitochondrial proteostasis in DARS2-deficient hearts.

(A) Representative gel of in organello translation in 3-week-old heart mitochondria and corresponding Coomassie Brilliant Blue stained gel used as loading control. (B) Relative expression levels of MRC subunits from 3-week-old hearts (n=5). (C) Western blot analysis and relative quantification of steady-state levels of MRC subunits in 3-week-old hearts (n=4).

Bars represent mean \pm S.E.M. Asterisks indicate level of statistical significance (Student's t-test, *p<0.05, **p<0.01).

Moreover, analysis of mRNA levels for MRC subunits revealed upregulation of transcripts for some nuclear- and mtDNA-encoded subunits (Figure 3.13B). Contrary to this, steady-state levels of different MRC subunits revealed a clear decrease in the level of CO IV subunits, both nuclear- and mtDNA-encoded (Figure 3.13C), in agreement with our previous results showing mild-to-moderate decrease in the level of fully assembled CO IV. Notably, the mRNA levels of CO IV were upregulated even if the protein levels were down. These findings identify an increased protein turnover of mtDNA- and nucleus-encoded MRC subunits, adding evidence for the disrupted protein-folding environment in DARS2-deficient hearts.

Recently, FGF21 was suggested as a novel marker of mitochondrial dysfunction. In skeletal muscle, MRC deficiency induced *Fgf21* transcription levels leading to a mitochondrial stress response with global changes (Tynjismaa et al., 2010). We wanted to check whether we would see a similar activation in *Fgf21* levels. What we found was an astonishing upregulation in the mRNA levels of *Fgf21* (250-fold) in both 3- and 6-week-old DARS2-deficient cardiomyocytes (Figure 3.14A).

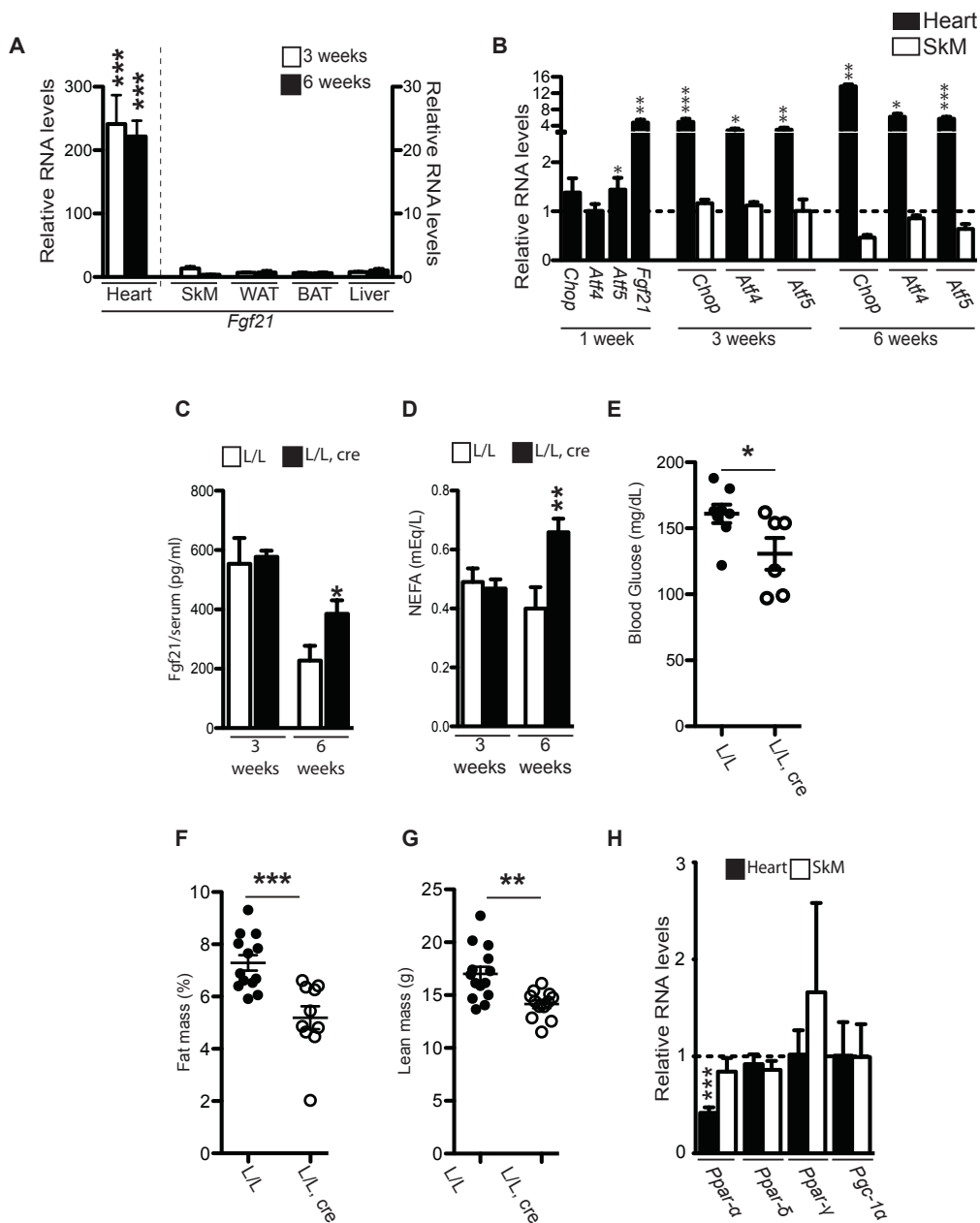


Figure 3.14 Fibroblast growth factor 21 (FGF21) levels and related adaptive systemic changes in DARS2 knockout mice.

(A) *Fgf21* expression levels in heart, SkM, white adipose tissue (WAT), brown adipose tissue (BAT) and liver of 3- and 6-week-old mice control (L/L) and DARS2-deficient mice (L/L, cre) (n=6). (B) Relative expression levels *Atf4*, *Atf5* and *Chop* in heart and SkM of 1-, 3- and 6-week-old mice, including *Fgf21* levels in 1-week-old mice (n=5). Results represent fold-increase compared to control. (C) FGF21 levels in serum from at 3- and 6-week-old age. (D) Circulating free fatty acid levels in 3- (n=3) and 6-week-old (n=12) control and knockout mice. (E) Blood glucose concentrations in 6-week-old

animals (n=6). **(F)** Percentage of body fat and **(G)** absolute lean mass in 6-week-old animals measured by NMR (n=10-12). **(H)** Relative expression levels of members of *Ppar* family (α , σ and γ) and *Pgc-1 α* in heart and SkM of 6-week-old animals (n=6). Results presented as fold-increase compared to the control. Bars represent mean \pm S.E.M. Asterisks indicate level of statistical significance (* $p \leq 0.05$; ** $p \leq 0.01$; *** $p < 0.001$; Student's t-test).

This increase in mRNA levels was also reflected in circulating levels of FGF21 in the serum of 6-week-old knockout mice (Figure 3.14C). Liver, skeletal muscle, white adipose tissue (WAT) and brown adipose tissue (BAT) are the main sources of FGF21 (Potthoff et al., 2012). Thus, all those tissues were checked for any signs of *Fgf21* upregulation. RT-PCR analysis confirmed that the increase in circulating FGF21 levels comes exclusively from the *Fgf21* upregulation in heart (Figure 3.14A). In animal models of diabetes, administration or overexpression of FGF21 caused reductions in body weight, blood glucose and lipid concentrations and liver fat content, as well as insulin resistance enhancement (Kharitonov et al., 2005). In agreement with those observations, we detected higher circulating free fatty acid levels, lower blood glucose and decreased fat mass in 6-week-old DARS2-deficient animals (Figures 3.14D-G). Therefore, mitochondrial dysfunction in heart, through increased cardiac *Fgf21* expression, seems to be acting as a global signal that changes the metabolism of the animal. *Fgf21* expression is shown to be regulated by two transcription factors: PPAR α and ATF4 (Potthoff et al., 2012; Kim et al., 2013). PPAR α , by directly binding to the *Fgf21* promoter, is responsible for fatty acid catabolism in the liver (Inagaki et al. 2007). We detected downregulation of *Ppar α* but high upregulation of *Atf4* (Figure 3.14H). Moreover, the levels of additional bZIP transcription factors that mediate protein homeostasis, *Chop* and *Atf5* (Wek and Cavener, 2007), were increased (Figure 3.14H).

These interesting results prompted us to look for additional support for our theory for the fact that impaired mitochondrial proteostasis is acting as an initial signal

for different mitochondrial stress responses, not MRC dysfunction *per se*. Thus, we wanted to check some of the parameters also in 1-week-old mice. The very first changes observed in 1-week-old DARS2-deficient hearts are mild upregulation of UPR^{mt} transcription activators ATF5 and CHOP, and a 6-fold increase in *Fgf21* levels (Figure 3.14B). On the contrary, Western blots for different proteases, autophagy markers, and the steady-state levels of MRC subunits did not reveal any changes between control and knockout mice (Figure 3.15). These results indicate that loss of proteostasis is a very early event that upregulates the UPR^{mt} transcription regulator(s).

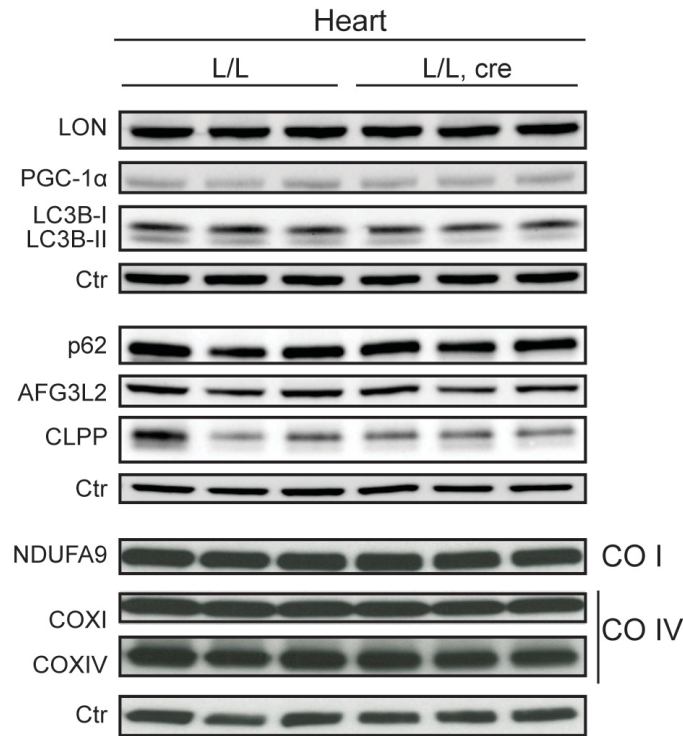


Figure 3.15 Western blots analysis of 1-week-old hearts.

Western blots analysis of 1-week-old hearts for the levels of individual MRC subunits (NDUFA9, COXI and COXIV); LON, CLPP and AFG3L2 protease; and markers of autophagy – p62 and LC3B. HSC70 (Ctr) was used as loading control (n=3).

Moreover, the upregulation of FGF21 expression coincides with the increase in the UPR^{mt} transcription activators. Our results indicate that, FGF21 can be one of the early markers of mitochondrial dysfunction and it might be a direct target of UPR^{mt}.

Together, our data show that accumulation of unfolded/unassembled proteins acts as the primary signal that leads the activation of mitochondrial stress responses. Those responses arise independently of respiratory chain deficiency and give rise to adaptive cell-intrinsic changes, and systemic shifts in metabolism.

3.8. DARS2 deficiency in forebrain neurons, hippocampus and striatum

Disclaimer: Some parts and figures of the remaining sections were published as part of Master of Science thesis of Stephan Lotter, who is supervised by Prof. Dr. Aleksandra Trifunovic and the author, Sukru Anil Dogan (Lotter, 2013).

The second mouse model generated was *Dars2*^{L/L, +/CaMKII α -Cre}, in which *Dars2* gene was disrupted in forebrain neurons, hippocampus and striatum by mating floxed (L/L) mice with mice expressing the cre-recombinase under the control of the Ca²⁺/calmodulin-dependent kinase II alpha promoter (CaMKII α -Cre). As in the previous model, the control mice are denoted as L/L and tissue-specific knockout mice as L/L, cre in the figures. The Ca²⁺/calmodulin-dependent kinase II alpha promoter is active from postnatal day 14 (P14), and maximal recombination occurs at P29 (Xu et al., 2000). Cerebellum is not affected, which is used as a negative control throughout the experiments.

Knockout mice were born in Mendelian proportions. They appeared normal, however, after weaning, they started to lose weight, which became more apparent when they become 12-16 weeks of age (Figure 3.16A-B).

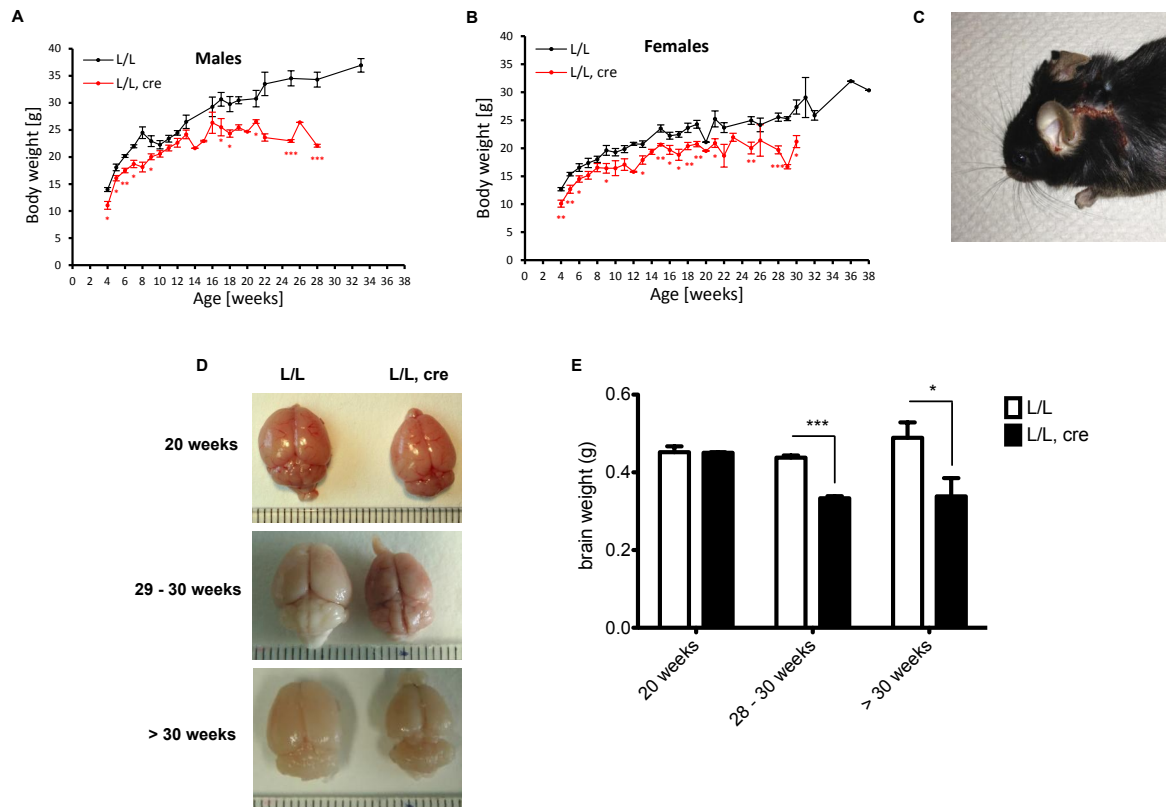


Figure 3.16 Phenotypic characterization of tissue-specific DARS2-deficiency in forebrain neurons, hippocampus and striatum.

(A-B) Body weight vs. age graph for (A) male, and (B) female control (L/L; black) and *Dars2*^{L/L, +/CaMKII α -Cre} mice (L/L, cre; red). (C) Self-inflicted injuries as a result of excessive scratching in *Dars2*^{L/L, +/CaMKII α -Cre} mice. (D) Representative brain pictures and (E) brain weight graph of control and *Dars2*^{L/L, +/CaMKII α -Cre} mice. Ages are indicated on the left of the panel D. n=16.

Bars represent mean \pm S.E.M. Asterisks indicate level of statistical significance (Student's t-test, *p<0.05; **p<0.01; ***p<0.001).

The mice showed no behavioral abnormalities until 28 weeks of age, when they started scratching their necks and face, leading to occurrence of self-inflicted wounds (Figure 3.16C). They had to be sacrificed when their wounds become

severe. For example, some knockout mice did not show any scratching behavior until they were in their early 30-weeks. Therefore, due to increased morbidity, majority of *Dars2*^{L/L, +/CaMKII α -Cre} mice had average lifespans of 32 weeks.

The first thing we analyzed was the brain size and morphology. When the knockout mice were 20-week-old, the gross morphology of their brains was indistinguishable from the control mice. However, in a short span of 2 months, the forebrain atrophied, which was even more severe in older mice, such as 32-week-old mice (Figure 3.16D-E). Taking these data into consideration, we have decided to group the mice in three different time points for the experiments: (i) 20-week-old, (ii) 28-30-week-old, and (iii) >30-week-old.

3.9. DARS2 deficiency in forebrain cause respiratory chain deficiency

After gross morphological analysis, we wanted to analyze biochemical consequences of DARS2 deficiency in forebrain neurons, as we did for the heart and skeletal muscle specific mice. First, we measured the levels of MRC enzyme activities (Figure 3.17A).

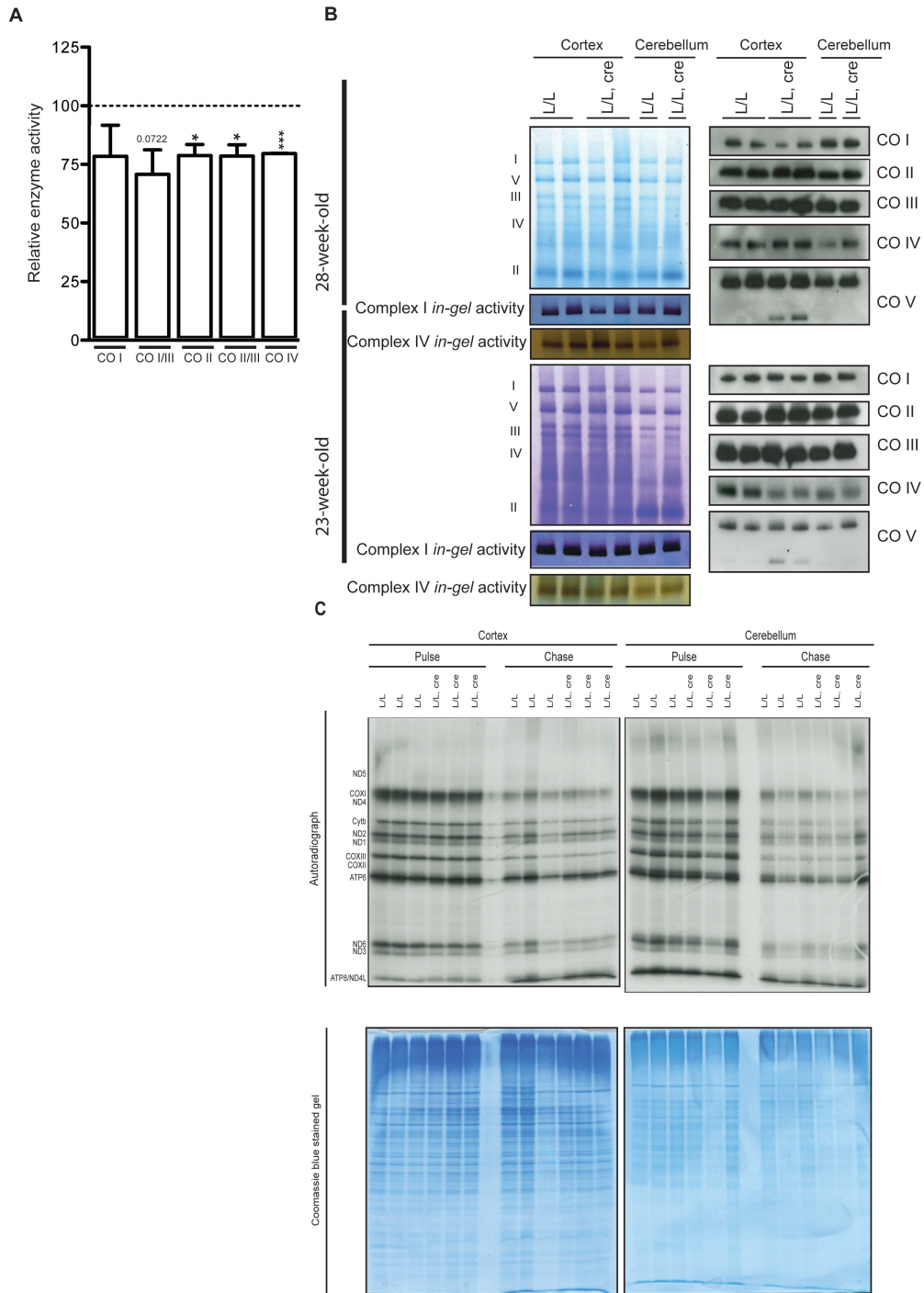


Figure 3.17 Characterization of mitochondrial dysfunction in 28- (and 23-) week-old *Dars2*^{L/L}, ^{+/CaMKII α -Cre} mice (L/L, cre) presented as a percentage of control (L/L). Bars represent

(A) Relative MRC complex activities in isolated cortex mitochondria of *Dars2*^{L/L}, ^{+/CaMKII α -Cre} mice (L/L, cre) presented as a percentage of control (L/L). Bars represent

mean \pm S.E.M. Number on the error bar and asterisks indicate level of statistical significance (* $p \leq 0.05$; ** $p \leq 0.01$; Student's t-test; $n=3$). **(B)** Representative Coomassie Brilliant Blue stained BN-PAGE gel (with indicated position of specific complexes), Western blots for MRC complexes and *in-gel* activity of CO I and CO IV, performed after BN-PAGE for 23- and 28-week-old control (L/L) and *Dars2*^{L/L, +/CaMKII α -Cre} (L/L, cre) mice. Cerebellum is used as negative control. **(C)** Representative gel of *in organello* translation of 28-week-old mice cortex and cerebellum mitochondria ($n=3$). *De novo* synthesized proteins are isolated immediately after labeling with ³⁵S-met (1h pulse). Positions of individual mitochondrial-encoded proteins are indicated. Coomassie Brilliant Blue stained gel used as loading control. Turnover of the newly synthesized proteins are assessed after 3 hours of 'cold chase'.

Significant decreases in CO III and IV was apparent, as well as a decline in CO I activity. Interestingly, we observed a decreased activity of CO II, in which all subunits of which are nuclear DNA encoded. This suggests that defective mitochondrial translation is exerting an adverse effect on CO II activity, which needs further experimental addressing.

BN-PAGE analysis did not reveal any abnormalities in the amount of fully assembled MRC complexes in both cortex and cerebellum when *Dars2*^{L/L, +/CaMKII α -Cre} mice were 28-week-old (Figure 3.17B). The Western blots to detect the MRC subunits from the corresponding BN-PAGE analysis also showed a similar pattern, as well as the *in-gel* activities (Figure 3.17B). However, the F1 subcomplex of CO V was visible in Western blots, indicating a translational problem. On the contrary, 23-week-old *Dars2*^{L/L, +/CaMKII α -Cre} mice showed decreased CO IV levels when BN-PAGE and the Western blots were performed (Figure 3.17B). However, this change was not reflected in CO IV *in gel* activity.

We did not detect a strong deregulation of *de novo* protein synthesis in DARS2-deficient mitochondria from cortex and cerebellum of 28-week-old *Dars2*^{L/L, +/CaMKII α -Cre} mice (Figure 3.17C). The turnover rate of mtDNA-encoded proteins, after 3 hours of cold-chase, was also not significantly different in *Dars2*^{L/L, +/CaMKII α -Cre} mice. As observed in heart and skeletal muscle specific DARS2

knockout mice, ND2 subunit, which does not contain a single aspartate residue, was still upregulated. Moreover, ATP6 showed an additional polypeptide with a slightly lower molecular mass, which is likely a truncated form of this protein (Fig 3.17C).

For these experiments, we were using cortex mitochondria and this mixed tissue contains not only neurons but also other cell types, i.e. glial cells. The lack of severe effects in BN-PAGE, *in organello* translation assay and *in-gel* activities can be attributed to the existence of cell types that are not affected by cre recombination and thus still contains DARS2. Another explanation could be the neurons that had DARS2 deficiency might have been lost as a result of cell death and the analyzed ones were the remaining, healthy ones.

To further investigate the respiratory chain dysfunction in *Dars2*^{L/L, +/CaMKII α -Cre} mice, we have performed COX-SDH staining on the group of 28-30 weeks of age mice (Figure 3.18A).

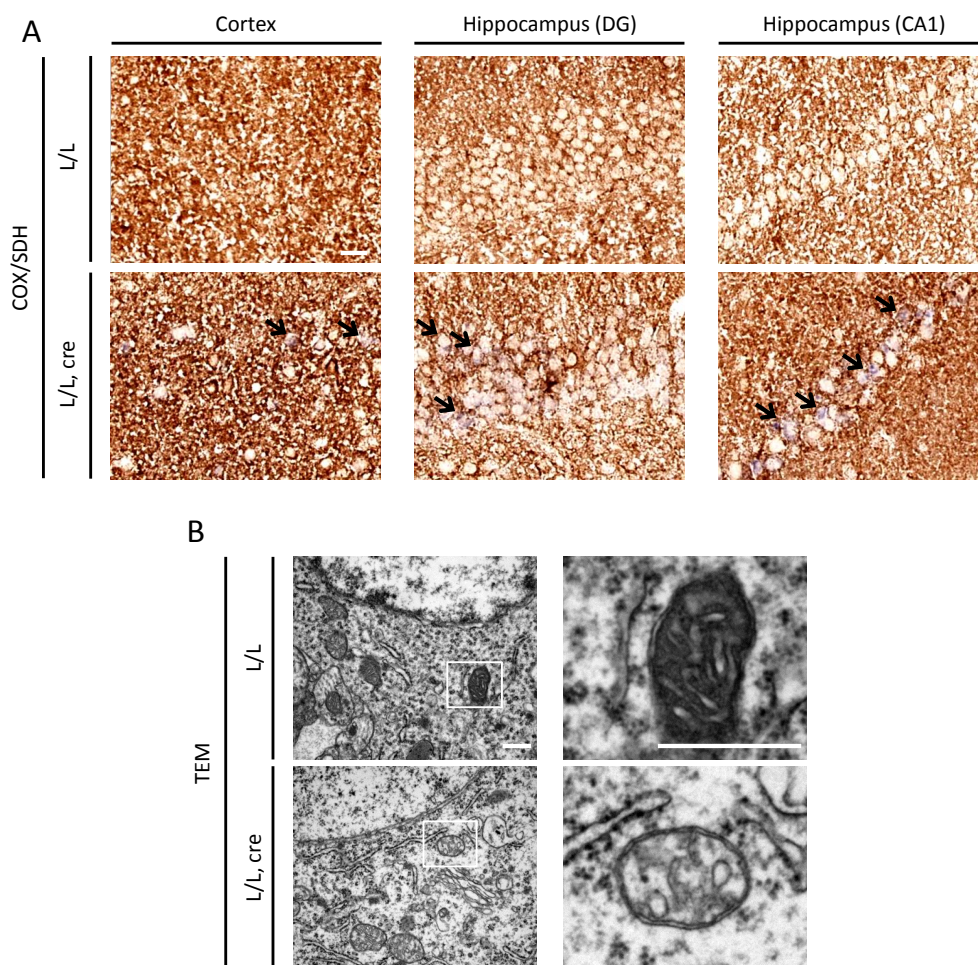


Figure 3.18 Further characterization of mitochondrial dysfunction by COX-SDH staining and TEM in 28/30-week-old mice.

(A) COX-SDH - Enzyme histochemical double staining for COX and SDH activities (Scale bars: 20 μm). Arrows indicate COX deficiency. **(B)** Transmission Electron Micrographs (Scale bar: 0.5 μm) of control (L/L) and *Dars2*^{L/L, +/CaMKII α -Cre} (L/L, cre) mice hippocampus and cortex (n=3).

Observed blue staining, indicating COX-deficiency, was apparent in cortex and to a higher extent in the stratum pyramidale of the cornu ammonis 1 (CA1) and the stratum granulosum of the dentate gyrus (DG) regions of hippocampus (Figure 3.18A, arrows).

Furthermore, we performed ultrastructural analysis of hippocampus in *Dars2*^{L/L, +/CaMKII α -Cre} mice (Figure 3.18B). Loss of cristae structure, which we did not observe in heart and skeletal muscle of the previous model, was apparent in hippocampal region, as well as accumulation of swollen and degenerating mitochondria, suggesting different tissue-specific responses might be responsible for the observed differences in TEM (Figure 3.18B).

Taken together, these results indicate that even if some techniques might not be sensitive enough to observe the extent of mitochondrial dysfunction in DARS2-deficient brains; enzymatic activities, histochemical and ultrastructural analyses provide enough evidence for the MRC deficiency.

3.10. DARS2 deficiency causes progressive neuronal degeneration

Intrigued by our observations so far, we wanted to assess the degree and reasons of atrophy in our mouse model. H&E staining for the microanatomical features of cell bodies and Nissl staining for the details in the perikaryon, cytoplasm of neurons, were the first stainings we performed.

20-week-old *Dars2*^{L/L, +/CaMKII α -Cre} mice, which also did not show any differences in brain size compared to controls, revealed no apparent differences upon Nissl staining (Figure 3.19A).

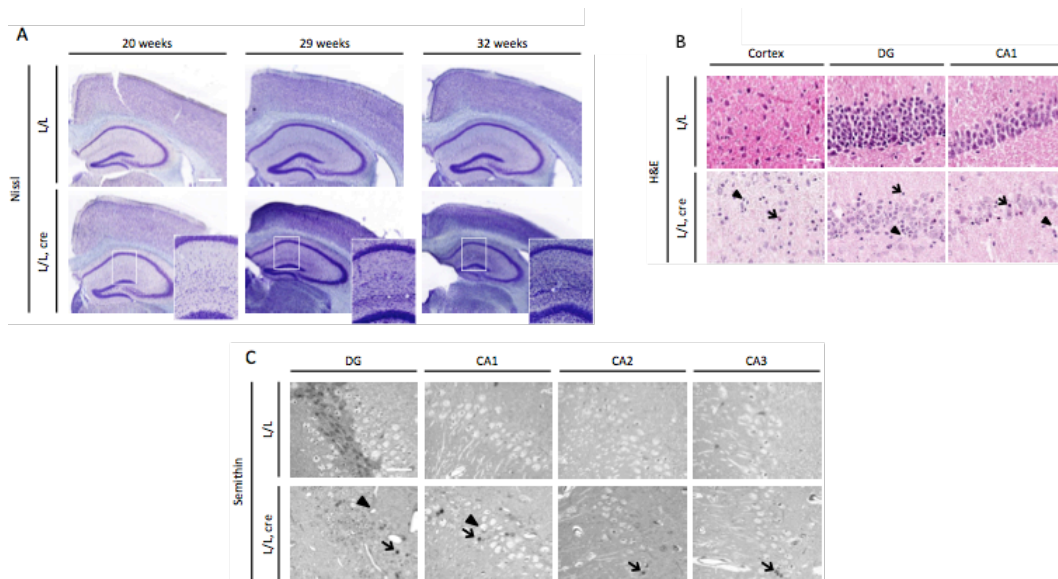


Figure 3.19 Neuronal degeneration in DARS2-deficient cortex and hippocampus.

(A) Representative Nissl staining (Scale bars: 500 μ m) of hippocampal regions of 20-, 29- and 32-week-old control (L/L) and *Dars2*^{L/L, +/CaMKII α -Cre} (L/L, cre) mice. Close-ups are for the indicated areas. (B) H&E staining of 29-week-old control and *Dars2*^{L/L, +/CaMKII α -Cre} mice for cortex, DG and CA1 regions (Scale bars: 500 μ m). Arrows indicate pyknosis, whereas arrowheads show vacuolar abnormalities. (C) Semithin sections for DG and CA regions of hippocampus for 29-week-old mice (Scale bars: 25 μ m).

On the other hand, with increasing age, considerable degeneration in cortex and severe disruption of cortical organization were observed (Figure 3.19A). We observed reduced cortical and hippocampal thickness, especially in the DG regions of 29- and 32-week-old *Dars2*^{L/L, +/CaMKII α -Cre} mice. Progressive cellular infiltration within the hippocampus (Figure 3.19A – close-ups) was seen in 29 and 32-week-old mice, which we hypothesized to be the result of an immune response. We concluded that the atrophy observed in knockout brains is due to the degeneration of neuronal cells in cortex and hippocampus.

H&E staining comprises of a blue color staining the nuclear chromatin, and thus nucleus, and shades of pink for the rest. When our mid-time point, 28-30-week-old mice, were analyzed, a decrease in neuron numbers were observed, most

prominently in CA1, CA2 and DG regions of hippocampus (Figure 3.19B). The cortical and hippocampal organization of the cells were disrupted, with occasional pyknotic nuclei, an indicator of apoptosis (Figure 3.19B – arrows). Another observation that was revealed by H&E staining was the abnormal vacuolar structures, which are signs of neuronal degeneration (Figure 3.19B – arrowheads).

Next, we wanted to confirm these results with semithin sections of the hippocampal DG and CA regions of 29-week-old mice. Both vacuolar lesions (Figure 3.19C - arrowheads) and signs of pyknosis, condensations of chromatin as a result of apoptosis/necrosis, (Figure 3.19C – arrows) were also observed. Semithin sections showed a substantial loss of pyramidal neurons, mostly in the DG and CA1 fields (Fig. 20 D), whereas neurons in the CA2 and CA3 regions were present more or less in normal numbers, although some pyknotic nuclei were observed.

Our results show that the atrophy of the brain size coincides with the decreased number of neurons and disorganized neuronal structure. We concluded that neurodegeneration observed in *Dars2*^{L/L, +/CaMKII α -Cre} mouse is progressive and affecting the specific regions of hippocampus more than the other neurons.

3.11. Corticohippocampal nerve cell loss was highly likely to be caused by apoptosis

The presence of pyknosis and loss of neurons prompted us to look for types of cell death by which neurons in *Dars2*^{L/L, +/CaMKII α -Cre} mice die. To assess apoptosis, TUNEL staining was performed on different regions of cortex and hippocampus (Figure 3.20A-D).

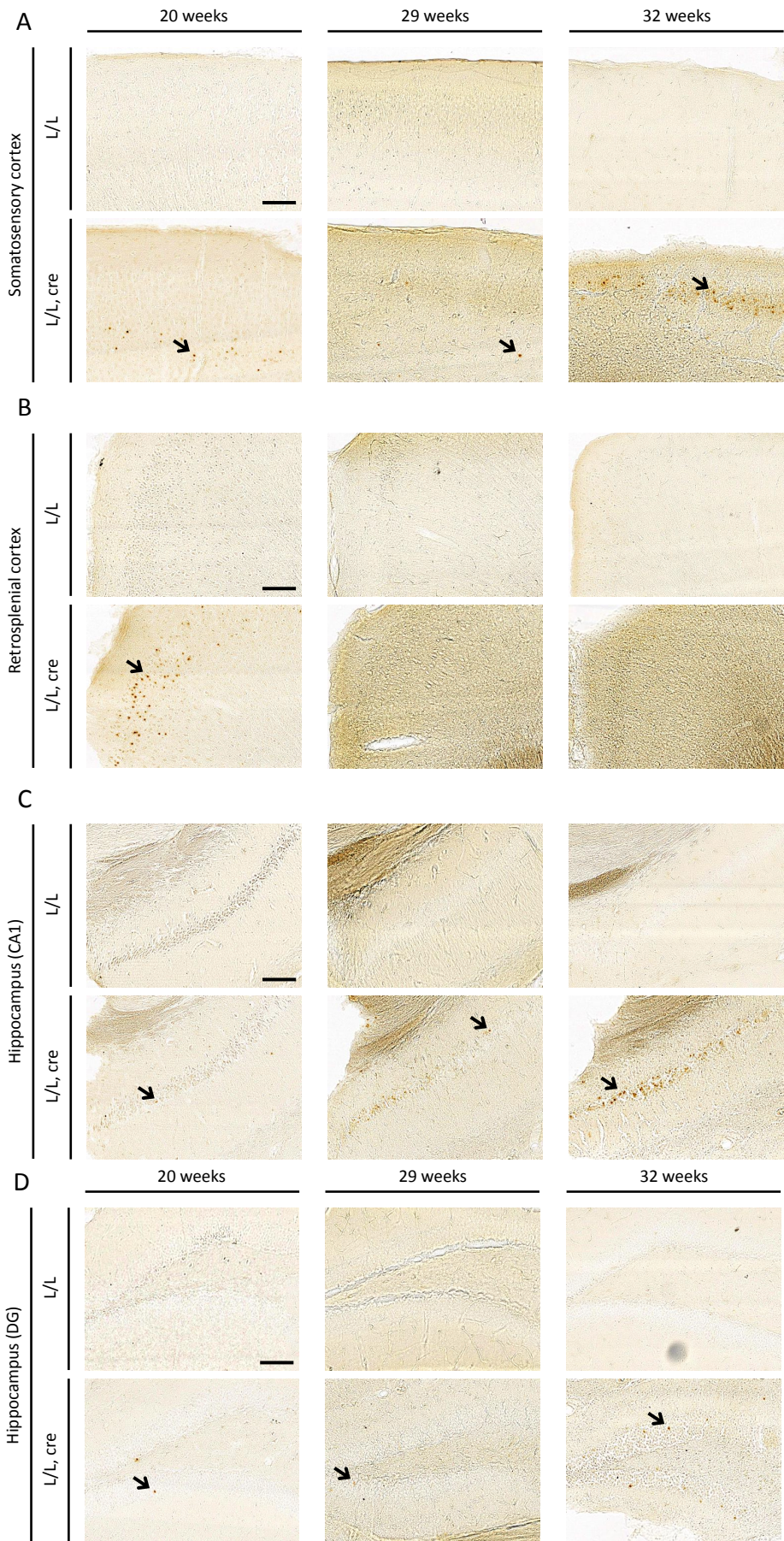


Figure 3.20 TUNEL staining in DARS2-deficient cortical and hippocampal regions.

(A-D) TUNEL staining for apoptosis in (A) the somatosensory cortex, (B) the retrosplenial cortex, (C) the hippocampal CA1 region, and (D) the hippocampal DG region of 20-, 29-, and 32-week-old control (L/L) and *Dars2*^{L/L, +/CaMKII α -Cre} (L/L, cre) mice (Scale bars: 100 μ m). Arrows indicate apoptotic neurons.

When *Dars2*^{L/L, +/CaMKII α -Cre} mice were 20-week-old, the somatosensory cortex, retrosplenial cortex, CA1 and DG regions of hippocampus showed increased numbers of apoptotic cells (brownish dots) when compared to the control mice (Figure 3.20A-D). Retrosplenial cortex was the region that affected the most (Figure 3.20B). When different regions in our second time point (29-week-old mice) were examined, we detected apoptosis in all the regions except retrosplenial cortex (Figure 3.20B). Somatosensory cortex (Figure 3.20A) and DG region (Figure 3.20 D) showed somewhat similar numbers of TUNEL-positive cells when compared to 20-week-old *Dars2*^{L/L, +/CaMKII α -Cre} mice. However, in CA1 region, the number of apoptotic neurons increased (Figure 3.20C). In our last time point (32-week-old mice), retrosplenial cortex also did not show apoptotic cells (Figure 3.20B). On the contrary, apoptosis increased progressively in somatosensory cortex (Figure 3.20A) and CA1 region of hippocampus (Figure 3.20C) and to a lesser extent in DG region (Figure 3.20D). These results were puzzling. TUNEL-positive cells in 20-week-old mice, seen especially in cortical regions, did not coincide with our observations of neuronal cell loss and disorganization as evident by Nissl staining of the same-aged mice. Moreover, when *Dars2*^{L/L, +/CaMKII α -Cre} mice were 29 weeks of age, brain atrophy indicated massive neuronal cell loss, which was not the case when TUNEL-positive nuclei were considered. We hypothesized that vast amount of apoptosis might be occurring during the 8-9 weeks of time when mice showed no microanatomical differences (20 weeks of age) to when they have lost most of their cortex (29 weeks of age). Thus, at this middle time point (29 weeks of age) we do not observe many TUNEL-positive nuclei while they have already been lost. When *Dars2*^{L/L, +/CaMKII α -Cre} mice were around 32 weeks of age, we again observed

massive apoptotic cells, especially in somatosensory cortex and CA1 region. This might be explained by the fact that when we decreased the time interval, we managed to observe the death of the previously ‘healthy’ neurons when the mice are 29-week-old.

Another interesting point to be mentioned was the differential regional involvement of neuronal loss as evidenced by apoptosis. Why some regions are more prone to mitochondrial dysfunction is an interesting question that should be addressed via further experimental addressing. Apoptosis should be checked at different time points and shorter time intervals (i.e before 20 weeks of age, between 20 and 29 weeks of age, etc.) to further investigate the differential regional loss of neurons. Moreover, cleaved caspase 3 staining, as well as RT-PCR should be performed to confirm our apoptosis-related results.

To sum up, we observed massive cell loss due to apoptosis in different regions of DARS2-deficient brain. It is still possible that other types of cell death pathways, such as necrosis, can contribute to the observed cell loss, however this still awaits experimental confirmation.

3.12. Increased immune response and gliosis in DARS2-deficient mice

The cellular infiltration we observed by Nissl staining was a hint for us that, maybe, those cells might be the activated microglia. Immunohistochemistry, specifically IBA1 staining, showed the presence of an inflammatory response in *Dars2*^{L/L, +/CaMKII α -Cre} mice. IBA1 is a calcium binding protein that is upregulated during the activation of microglia/macrophages. As the endogenous brain defense cells, microglia can be found in ‘resting’ and ‘activated’ forms (Emerit et al., 2004). ‘Resting’ microglia has smaller cell bodies and a lot of protrusions;

whereas ‘activated’ form retract their protrusions and increase the size of their cell bodies; this happens when there is some sort of ‘insult’ to the brain.

Both somatosensory and retrosplenial cortical areas, previously analyzed by TUNEL staining showed increased IBA1 staining and, thus, activated microglia in three different time points (20, 29, and 32 weeks of age) (Figure 3.21A-D). An age-dependent decrease in activated microglia was apparent in the somatosensory and retrosplenial cortex (Figure 3.21A-B), in contrast to hippocampal regions, where we saw increased number of activated microglia with increasing age (Figure 3.21C-D). This temporal decrease was interesting for us. We think that when *Dars2*^{L/L, +/CaMKII α -Cre} mice are 20-week-old, number of activated microglia are increased as the brain experiences some sort of ‘insult’. However, when the other later time points were considered, the inflammatory response in somatosensory and retrosplenial cortex were decreased due to the possibility that the ‘insult’ was also reduced in these regions. The increased numbers of activated microglia in hippocampal regions, on the other hand, might point out the ‘insult’ in play was still present and DARS-deficient hippocampus further upregulated the defense system against the ‘insult’.

Furthermore, in hippocampal regions and retrosplenial cortex, TUNEL-positive nuclei and the activated microglia overlapped, suggesting that increased apoptosis was mainly responsible for the activation of microglia and promoting an immune response in the affected regions. However, somatosensory cortex of 32-week-old *Dars2*^{L/L, +/CaMKII α -Cre} mice showed decreased levels of activated microglia compared to its 20-week-old counterpart. 32-week-old was the time point when we observed the most increased levels of apoptotic nuclei in somatosensory cortex. We concluded that different stress responses might be in play when neurons of different regions were taken into consideration. For example, a stress response other than the activation of microglia might be more active in the somatosensory cortex when neurodegeneration progresses.

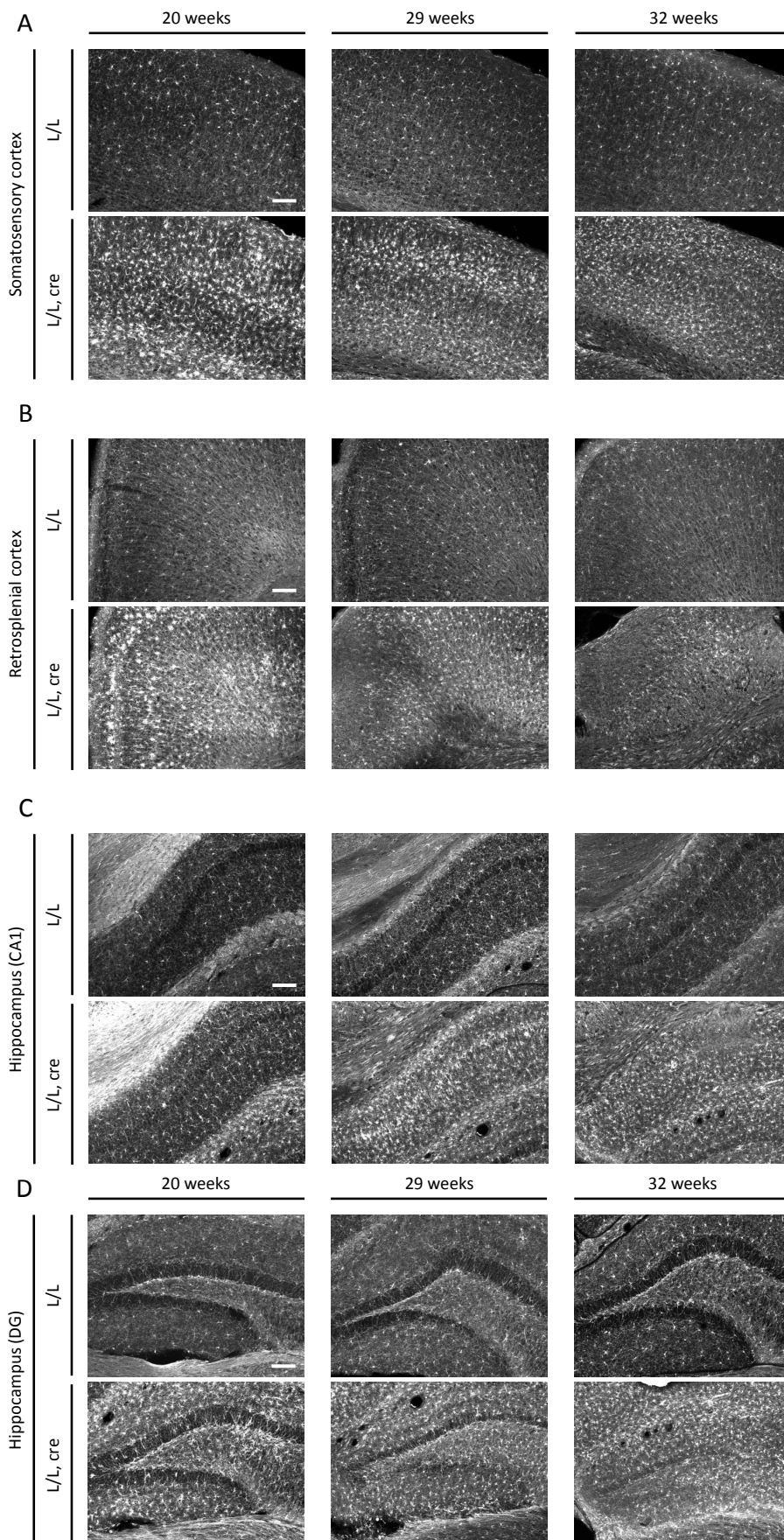


Figure 3.21 IBA1 staining in DARS2-deficient cortical and hippocampal regions.

(A-D) IBA1 staining for resting and activated microglia in **(A)** the somatosensory cortex, **(B)** the retrosplenial cortex, **(C)** the hippocampal CA1 region, and **(D)** the hippocampal DG region of 20-, 29-, and 32-week-old control (L/L) and knockout (L/L, cre) mice (Scale bars: 100 μ m).

During times of inflammation, microglia interact with astrocytes, the non-neuronal macroglial cells of central nervous system. We demonstrated the presence of gliosis by using GFAP staining to detect reactive astrocytes (Figure 3.22A-D).

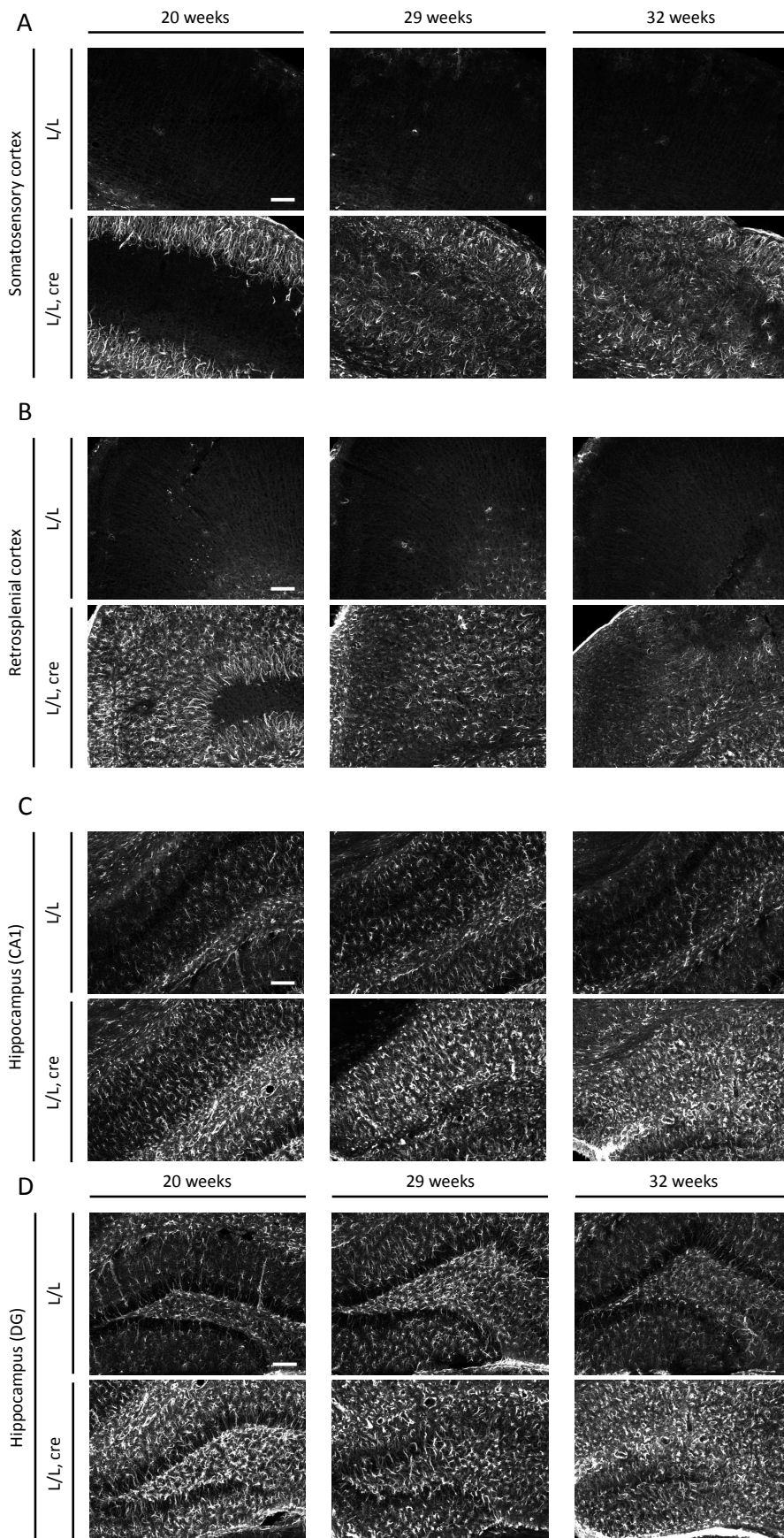


Figure 3.22 GFAP staining in DARS2-deficient cortical and hippocampal regions.

(A-D) GFAP staining for astrocytes in (A) the somatosensory cortex, (B) the retrosplenial cortex, (C) the hippocampal CA1 region, and (D) the hippocampal DG region of 20-, 29-, and 32-week-old control (L/L) and knockout (L/L, cre) mice (Scale bars: 100 μ m).

When *Dars2*^{L/L, +/CaMKII α -Cre} mice were 20-week-old, they had a vast increase of GFAP-immunoreactive cells in the outer layers of somatosensory cortex, which later diffuses to the other layers with increasing age (Figure 3.22A). These layers coincide with the TUNEL-positive nuclei. The retrosplenial cortex of knockout mice also exhibited reactive astrocytes in all of the ages examined (Figure 3.22B) and their number seemed to be decreased with increasing age of animals, similar to activated microglia. So, we concluded that many astrocytes were having protrusions directed into the degenerating neocortex. Hippocampal regions also showed high number of GFAP-positive astrocytes in knockout mice (Figure 3.22C-D). The progressive infiltration as observed by activated microglia was also observed in activated astrocytes. Reactive astrogliosis increased with increasing age in CA1 (Figure 3.22C) and DG (Figure 3.22D) regions of hippocampus.

It would be very interesting to repeat these experiments in different age and time intervals of *Dars2*^{L/L, +/CaMKII α -Cre} mice, i.e younger mice, to see whether activated microglia and/or astrocytes were also available in different regions of DARS2-deficient brain regions.

4. Discussion

You would think that, as Vogons from 'Hitchhiker's Guide to the Galaxy' would say, "Resistance is useless!" when you are in a teen slasher movie. However, there are some rules that should be mentioned and you would be safe if you follow them:

First, you should not sin, not during the movie and not ever! Any sins in the past would have the potential to break out and destroy you.

Second, you should not use sentences like 'Hello?', 'Who is there?', and 'I'll be right back' -especially, when wondering around in dark, scary places! They are bound to decrease your chance of survival next to zero.

The last and the most important rule is never, ever, under any circumstances assume the killer is dead!

Mitochondrial disorders are very heterogeneous from a clinical, genetical, biochemical and molecular point of view (Schaefer et al., 2004). This can be exemplified by the fact that mitochondrial diseases can be caused by mutations in genes either encoded by nuclear DNA or mitochondrial DNA. Moreover, mitochondrial diseases can manifest in any organ and the age-onset also varies from childhood to adulthood. Eased by the advantages in whole genome sequencing, mutations causing mitochondrial diseases were never easier to pinpoint as they are today. However, the molecular consequences of mitochondrial dysfunction and impaired oxidative phosphorylation in cellular and/or organismal level are still far from being completely understood. Especially when it comes to the question how similar mutations are presenting themselves as different organ/disease manifestations or how different mutations are causing the

same mitochondrial diseases, we have no satisfactory answer. Similarly, the tissue-specificity of mitochondrial aminoacyl-tRNA synthetase-related diseases has been an unforeseen phenomenon. Mutations in nuclear encoded proteins that obey the laws of Mendelian genetics and therefore have the same type of defect in all different cell types, i.e. aminoacyl-tRNA synthetases, should give rise to similar failure in all cells/organs but this is not the case. In determining the extent of tissue-specific defects, a pivotal role can be attributed to the different kinds of, and largely unknown, compensatory mechanisms that are employed by cells against OXPHOS deficiency. Given mitochondrial functions in the cell and organism, those mechanisms are bound to be complex.

In this study, we generated the first mouse model that is deficient for mitochondrial aspartyl-tRNA synthetase (DARS2). The idea behind was not to mimic the clinical presentations of a disease but generating a mouse model with strong respiratory chain deficiency as observed in majority of mitochondrial diseases. Tissue-specific manifestations and various stress signals/compensatory mechanisms activated were examined with different tissue-specific DARS2-deficient models. We have generated three mouse models: a full body knockout (by ACTB-cre mediated recombination), heart and skeletal muscle deficient (by Ckmm-cre mediated recombination) and forebrain neurons, striatum and hippocampus deficient (by CaMKII α -cre mediated recombination). These tissues are highly dependent on the OXPHOS for energy production; therefore, more involved in mitochondrial diseases (Dogan and Trifunovic, 2011). Moreover, heart and skeletal muscle are of a common origin.

4.1. Mitochondrial aspartyl-tRNA synthetase (DARS2) is essential for embryonic development and one copy of the gene is enough for survival in mouse

Our results demonstrate that DARS2 is an essential protein needed for early mammalian development as complete lack of DARS2 leads to developmental arrest around time of organogenesis, which is consistent with results obtained from mice deficient in other genes essential for mtDNA maintenance and/or expression, such as TFAM (Larsson et al., 1998), POLGA (Hance et al., 2005), MTERF3 (Park et al., 2007) and TFB1M (Metodiev et al., 2009). *Tfam*^{-/-} embryos had a mutant appearance with smaller sizes, delayed neuronal development, cardiovascular malformations, and lack of mtDNA when examined between E8.5 and E10.5 (Larsson et al., 1998). TFAM loss caused embryonic arrest after implementation. Similarly, disruption of *PolgA* also resulted in embryonic lethality at the time of late gastrulation and before early organogenesis, between E7.5 and E8.5 (Hance et al., 2005). After gastrulation, organogenesis starts in mouse embryos at E7.5, the time when increased mtDNA replication is needed for the activation of aerobic metabolism (John, 2013). Failure to expand mtDNA molecules causes embryonic lethality due to the lack of organogenesis. Lessons from TFAM, indispensable for mtDNA maintenance, and POLGA, the only DNA polymerase in mitochondria, knockout mice emphasized the critical importance of mtDNA maintenance and replication during organogenesis.

Some mitochondrial aminoacyl-tRNA synthetases can show misacetylation, i.e. mt-tRNA^{Gln} can be acetylated by both EARS2 and SARS2 (Nagao et al., 2009). We were wondering whether some other mitochondrial synthetases can also compensate for the lack of DARS2 but our results suggest that such compensation is unlikely due to the embryonic lethality of DARS2-deficient whole body knockout mice.

Our results clearly show that one working copy of *Dars2* gene is sufficient for survival of the mouse. This observation is in agreement with data from human heterozygous carriers of mutations in *DARS2* gene (Isohanni et al., 2010; Scheper et al., 2007). Notably, carrier frequency for the common *DARS2* mutation is found to be relatively high in general Finnish population (1:95) and is thought to be quite common in other European derived populations (Isohanni et al., 2010).

4.2. DARS2 deficiency in heart and skeletal muscle causes comparable mitochondrial dysfunction in both tissues but activates mitochondrial stress responses exclusively in heart

DARS2 deficiency in heart and skeletal muscle gave rise to strong mitochondrial respiratory chain dysfunction in both tissues when the mice are 6-week-old. Further, we observed activation of various kinds of mitochondrial stress responses, only in DARS2-deficient cardiomyocytes.

Mitochondrial dysfunction in LBSL patients carrying DARS2 mutations is also somewhat a matter of controversy (Scheper et al., 2007). Lactate elevation commonly detected in white matter of LBSL patients is a hallmark of mitochondrial dysfunction, thus suggesting a role of mitochondria in disease onset; however, a defect in MRC activities or levels of individual complexes could not be confirmed in patient fibroblasts and lymphoblasts (Scheper et al., 2007). This most probably reflects the tissue-specificity of the observed defect. Recently, it was shown that the splicing of DARS2 exon 3, giving rise to the common mutation in LBSL patients, is regulated in a cell-type-specific manner and is less efficient in neuronal cells (van Berge et al., 2012). Furthermore, efforts to correlate missense mutations in LBSL patients with the severity of the disease progression did not reveal any connection. For example, the mild disease manifestation of one of the LBSL missense mutations do not coincide with the

substantial effects the mutation exerts on the catalytic activity when cell culture studies were performed (van Berge et al., 2013).

Mitochondrial aminoacyl-tRNA synthetases seem to be involved in tRNA maintenance. For example, mutations in both RARS2 and SARS2 cause remarkable reduction in the amounts of the corresponding tRNAs (Edvardson et al., 2007; Belostotsky et al., 2011). However, this is not a general observation. When MARS2 is depleted in *Drosophila*, no effect was observed on the steady-state levels of mitochondrial tRNA^{Met} (Bayat et al., 2012). Moreover, the common mutation in LBSL patients does not affect the stability of tRNA^{Asp} (van Berge et al., 2012). Similarly, our results show that tRNA^{Asp} levels do not change upon DARS2 depletion, which further suggests that, the level of aminoacylation or binding to DARS2 does not determine stability of tRNA^{Asp}.

Expression of Cre-recombinase from the muscle creatine kinase (*Ckmm*) promoter is a commonly used method to disrupt genes *in vivo*. *Ckmm-Cre* mediated deletion of mitochondrial maintenance/transcription genes were proven to be useful tools to unravel the functions and consequences of defective mtDNA replication or transcription. Two different TFAM tissue-specific knockouts have been generated so far. *Tfam*^{L/L, +/Ckmm-cre} mouse shows dilated cardiomyopathy, atrioventricular heart conduction blocks, and death at 2–4 weeks of age (Wang et al., 1999). Weight loss and increased mitochondrial dysfunction due to mtDNA loss are some of the hallmarks of this animal, which are consistent with our results. Even if a moderate reduction is observed in mtDNA levels, skeletal muscle does not show any signs of respiratory chain dysfunction and myopathic symptoms (Wang et al., 1999). The second model for TFAM depletion in heart and skeletal muscle has been generated again using *Ckmm-Cre* but this time with nuclear localization signal (NLS) (Hansson et al., 2004). The usefulness of *Tfam*^{L/L, +/Ckmm-cre} was limited due to their short lifespan. *Tfam*^{L/L, +/Ckmm/NLS-cre} mice, on the other hand, had a longer life span of 10–12 weeks and showed similar

symptoms, such as progressive increasing heart size, depletion of mtDNA, and severe respiratory chain dysfunction in heart (Hansson et al., 2004). This mouse model also did not develop any skeletal muscle phenotypes. The *Ckmm-Cre* that was used in our study is also *Ckmm/NLS-Cre*. Another heart and skeletal muscle specific mouse model, MTERF3 knockout animals, had a life span of 18 weeks, increased heart sizes, abnormal mitochondria in heart consistent with severe respiratory chain deficiency (Park et al., 2007). Yet again, in this model, skeletal muscle had normal morphology and mitochondrial function, even in the final stages of their lives. Hence, even if depletion of TFAM and DARS2 leads to similar phenotypes, i.e. cardiac hypertrophy, severe respiratory chain dysfunction, etc., the strong mitochondrial respiratory chain dysfunction observed in DARS2-deficient skeletal muscle, makes our case intriguing. Moreover, the maximal lifespan of our mice is either half (Hansson et al., 2004) or 1/3rd (Park et al., 2007) of the mice models discussed. So, the age alone cannot account for the normal mitochondrial function in TFAM or MTERF3 knockout skeletal muscle. Our results suggest that skeletal muscle has an intrinsic protective mechanism relying primarily on the slow turnover of mitochondrial transcripts that is coupled with possible upregulation of muscle regeneration. This is very effective when mtDNA replication or transcription defects were considered (Hansson et al., 2004; Park et al., 2007). Although other factors, including complementation between nuclei due to the syncytial nature of skeletal muscle organization and post-transcriptional regulation were also proposed to play role in skeletal muscle ability to compensate for the mitochondrial deficiency (Wang et al., 1999), our results argue that low level turnover rate of mitochondrial transcripts is primary mechanism. It has been shown that both nuclear and mitochondrial mRNAs for MRC subunits are much more stable in skeletal muscle than in heart (Connor et al., 1996). Half-life of COXVIc (nuclear-encoded) and COXIII (mtDNA-encoded) mRNA in heart were 3.3h and 2.1h, respectively, compared to 16h and 23h in skeletal muscle (Connor et al., 1996). Similar differences have been observed for proteins that directly or indirectly regulate the stability of

mitochondrial protein synthesis like TFAM, PGC-1 α and NRF-2 α (D'souza et al., 2012). The observed difference seems to be specific for the MRC subunits, as the rates of decline for δ -aminolevulinic synthase (ALAs) mRNA did not differ in two tissues (Connor et al., 1996) arguing that this indeed is a very specific response.

In our DARS2-deficient heart and skeletal muscle mouse model, the signs of mitochondrial retrograde signaling in the form of mitochondrial biogenesis were observed only in heart. Increased mitochondrial mass is a common feature of mitochondrial dysfunction. For example, *Tfam*^{L/L, +/-Ckmm/NLS-cre} mice had increased mitochondrial mass (25%) when they were 8-week-old (Hansson et al., 2004) and a similar mitochondrial biogenesis was observed in 12- and 16-week-old *Mterf3*^{L/L, +/-Ckmm-cre} mice (Park et al., 2007). 'Myopathy mouse' with skeletal muscle-specific disruption of *Tfam* showed accumulation of abnormal mitochondria, decline of respiratory chain function and a maximal lifespan of 16-20 weeks (Wredenberg et al., 2002). Increased mitochondrial mass and 'ragged-red fibers' (RRF), indicative of abnormal mitochondria accumulation were observed when the mice are 15-week-old (Wredenberg et al., 2002). RRFs with COX deficiency are one of the important signs observed in human patients with mitochondrial myopathy. RRFs are seen in patients, who have impaired mitochondrial translation and ETC defects (Zeviani et al., 1993). In 'myopathy mouse', increased mitochondrial mass is thought to be beneficial by improving the energy homeostasis in skeletal muscle (Wredenberg et al., 2002). As opposed to 'myopathy mouse', in our mouse model, we did not detect any RRFs. Another mouse model with increased mitochondrial mass in skeletal muscle is the 'deletor mouse', expressing mutant mouse mitochondrial helicase Twinkle, which mimics late-onset mitochondrial myopathy (Tyynismaa et al., 2005). No signs of mitochondrial dysfunction were noted during the first year of the deletor mouse. At that age, respiratory chain dysfunction was observed without mitochondrial proliferation. However, when deletor mice were 18-month-old, mitochondrial

mass was also increase, suggesting mitochondrial dysfunction, as evident by COX deficient cells, preceded mitochondrial proliferation (Tyynismaa et al., 2005). Skeletal muscle is intrinsically much more equipped to cope with increased levels of unassembled proteins and mitochondrial dysfunction. This could be the reason that we do not observe increased mitochondrial mass in DARS2-deficient skeletal muscle. It is plausible to argue that, as in deleter mice, after a certain age, we would also see upregulation of mitochondrial biogenesis also in skeletal muscle. Unluckily, the short lifespan of DARS2-deficient mice makes it impossible to test this hypothesis.

Recently, FGF21 was suggested as a novel marker of mitochondrial dysfunction (Tyynismaa et al., 2010). FGF21 is a “starvation-hormone”, which has regulatory roles in glucose, lipid, phosphate and bile acid metabolism (Kharitonov et al., 2005). In ‘deleter mouse’, the expression of skeletal muscle *Fgf21* was increased 2.5 fold when the mice are 14-month-old and 3.5 fold when they are 20-24-month-old, which were also reflected in the mouse plasma FGF21 levels (Tyynismaa et al., 2010). Surprisingly, the levels of *Ppara* and *Pgc-1 α* levels were not changed. Upon starvation, it is known that the levels of *Fgf21* goes up ~200-fold (Kharitonov et al., 2005). In DARS2-deficient cardiomyocytes, however, we observed an astonishing upregulation of ~250-fold in *Fgf21* levels. This increase was evident also in 3-week-old mice. Circulating levels of FGF21 in the serum of 6-week-old knockout mice was 70% upregulated. Our results clearly show that the upregulation of FGF21 levels in mouse serum comes exclusively from DARS2-deficient cardiomyocytes, while we did not observe any upregulation of *Fgf21* levels in other tissues that are known to secrete this cytokine. In ‘deleter mouse’, upregulation of *Chop* was also observed (Tyynismaa et al., 2010). Not only *Chop*, but also other transcription factors, *Atf4* and *Atf5*, was highly upregulated in DARS2-deficient hearts. Those three transcription factors regulate the protein homeostasis in the cell (Wek and Cavener, 2007). As well, recently it was shown that skeletal muscle-specific deletion of *Atg7*

(autophagy-related 7) increased *Fgf21* expression through the induction of *Atf4* (Kim et al., 2013). Autophagy deficiency in the skeletal muscle of these mice caused mitochondrial dysfunction, which through *Atf4*, a master regulator of stress response, induced *Fgf21*, as well as the circulating FGF21 levels (Kim et al., 2013). This is in agreement with our results. Moreover, we can argue that not only ATF4 but also ATF5 and CHOP can be involved in the regulation of *Fgf21* levels. In accordance with ‘deletor mouse’, in our case, *Fgf21* levels were not induced by *Ppara* that is normally responsible for increased *Fgf21* expression in liver upon fasting, as we detected downregulation of *Ppara*. As the proposed role of FGF21 suggests, we observed systemic changes in DARS2-deficient animals. We detected changes in metabolism by rising lipolysis in fat tissues and increasing NEFA levels in blood (60%), as well as lower blood glucose levels in 6-week-old DARS2-deficient animals. Notably, when 1-week-old DARS2-deficient hearts were examined, we still observed a 6-fold increase in *Fgf21* levels, as well as mild upregulation of ATF5 and CHOP.

We also have implications that FGF21 might activate mitochondrial biogenesis by stabilising PGC1- α levels. It has been shown that FGF21 has a role to increase PGC1- α protein levels rather than *Pgc1- α* expression levels (Fisher et al., 2012). Additionally, absence of FGF21 caused decreased PGC1- α levels. In DARS2-deficient hearts, we also detected higher levels of PGC1- α protein levels both in 3- and 6-week old mice but not any changes in mRNA levels.

Moreover, the master regulator of mitochondrial biogenesis, PGC1- α , is known to be a negative regulator of autophagy (Sandri et al., 2006; Wenz et al., 2009). Cardiomyocytes further revealed another remarkable response, in the form of reduced (macro)autophagy. One of the best characterized substrates of selective autophagy is p62 (sequestosome 1/SQSTM1). p62 directly interacts with LC3 (microtubule-associated protein light chain 3) on the isolation membrane

(Weidberg et al., 2011). Decrease or impairment in autophagy is accompanied by accumulation of p62 and accumulation of polyubiquitinated proteins (Mizushima et al., 2010). In DARS2-deficient hearts, p62 and LC3B-I levels were upregulated as well as polyubiquitinated proteins. Furthermore, we did not observe any autophagosomes on TEM sections, strengthening our observation of decreased autophagy. As shown before (Kim et al., 2013), autophagy deficiency is enough to increase the expression of *Fgf21*, however it is still unclear whether FGF21 can perform the reverse and increased levels of FGF21 can also contribute to the observed decreased autophagy phenotype in DARS2-deficient hearts.

A specialized form of autophagy, mitophagy, acts on damaged mitochondria to eliminate damage at the organelle level. Much of our knowledge about mitophagy comes from *in vitro* studies. A very recent study pointed out that accumulation of misfolded proteins in the mitochondrial matrix could initiate mitophagy mediated by PINK1 and the E3 ubiquitin ligase PARK2/parkin by a mechanism independent of mitochondrial depolarization (Jin and Youle, 2013). They suggested that this leads to mitophagy, which is triggered by the accumulation of unfolded proteins in mitochondria. Even if this study is providing evidence that unfolded protein load is the main cause of mitophagy and suggesting the role of mitophagy as a quality control mechanism, they also used cell culture studies. We are in need of more *in vivo* studies to unravel the role of mitophagy as a quality control mechanism *in vivo*. For example, an *in vivo* study showed that depolarized mitochondria do not recruit Parkin in dopaminergic neurons (Sterky et al., 2011).

Due to deregulated mitochondrial translation, we saw activation of UPR^{mt} again exclusively in heart. Our results from 3- and 6-week-old DARS2-deficient hearts indicate that the activation of UPR^{mt} occurs very early and precedes any other changes. Moreover, in this study, we present strong evidence regarding the role of disturbed protein homeostasis in triggering the mitochondrial stress responses

activated in DARS2-deficient hearts, not respiratory chain dysfunction *per se*. The partial loss of MARS2 protein seems to lead to the accumulation of misfolded proteins in mitochondria, triggering UPR^{mt} in *Drosophila* (Bayat et al., 2012). Similarly, in *Drosophila* and human post-mortem samples, it is implied that higher levels of misfolded components of respiratory complexes lead to an increase in markers of the UPR^{mt} (Pimenta de Castro et al., 2012). Strikingly, a recent study found out in *C. elegans* that when mitochondrial translation is inhibited by RNAi knockdown of mitochondrial ribosomal protein S5 (*mrps-5*), worms live longer, even if their respiration rate is decreased (Houtkooper et al., 2013). The researchers found out that stoichiometric imbalance between nuclear DNA- and mtDNA-encoded oxidative phosphorylation proteins, or mitonuclear protein imbalance, activates UPR^{mt} that can account for the longevity of the worms. We also observed mitonuclear protein imbalance in 3- and 6-week old DARS2-deficient hearts. Moreover, the expression levels of nuclear DNA- and mtDNA-encoded CO IV subunits were slightly increased, even if the protein levels were decreased, which suggest an increased protein turnover. Furthermore, a higher *de novo* protein synthesis in 3-week-old DARS2-deficient hearts was observed. These results are the indicators of increased amount of unfolded and/or unassembled proteins accumulating in DARS2-deficient heart mitochondria.

It is generally believed that mitochondrial respiratory deficiency is the primary activator of compensatory responses. Our results show that adaptive responses activated in heart are independent from respiratory chain deficiency, but rather stemming from impaired mitochondrial proteostasis. A recent study indicated that mitochondrial translational stress causes defective cell proliferation and this occurs before any real OXPHOS defect (Richter et al., 2013). Therefore, mitochondrial protein synthesis appears to be an important checkpoint for the monitoring of mitochondrial homeostasis and seems to be independent of energy metabolism.

All those stress signals were only evident in DARS2-deficient cardiomyocytes, but not in skeletal muscle. Skeletal muscle, comprising of different cell and even mitochondrial subpopulations, has better capacity for folding and turnover of mitochondrial proteins. If you add mRNA and protein stability skeletal muscle possesses –as discussed before-, intrinsically it is much more equipped to cope with increased levels of unassembled proteins. When DARS2-deficient skeletal muscles were examined, increased stability of mitochondrial transcripts, moderate upregulation of ribosomes and a likely increase in regeneration were observed. Inactivated stress responses in skeletal muscle further strengthen the fact that these responses arise independently of respiratory deficiency, while the deficiency is as strong as in DARS2-deficient heart.

Notably, increased ribosomal subunits were observed in both tissues, even if it was less in skeletal muscle. We think that this is due to the increased number of stalled ribosomes due to lack of charged tRNA^{Asp} and therefore creation of “hungry codons” (Temperley et al., 2010).

Let's remember the last rule of teen slashers: “Never, ever, under any circumstances assume the killer is dead!” Is it possible that the serial killer is not dead and hiding for a second and cleverer killing-spree?

Heart is employing different stress responses in order to counteract respiratory chain deficiency. It is thought-provoking to argue that these responses might be adding to the progression of cardiomyopathy instead of ameliorating it. For example, increased expression of PGC-1 α in the neonatal heart is beneficial and increases mitochondrial biogenesis, while increased expression of PGC-1 α in the adult heart leads to cardiomyopathy (Lehman et al., 2000; Russell et al., 2004). It seems that those stress responses might cause a possible demise of the cells instead of improving the disease manifestations.

To sum up, our results clearly demonstrate that direct disruption of mitochondrial protein synthesis by deletion of *Dars2* gene leads to activation of cellular stress responses in a tissue-specific manner. DARS2-deficient heart reacts to defective translation at a very early stage by enacting a repertoire of mitochondrial and extramitochondrial responses, including increased production of FGF21, activation of the UPR^{mt}, inhibition of autophagy and increased mitochondrial biogenesis. Strikingly, these specific responses arise before any real insult in respiratory chain. The triggering signal for these responses appears to be the accumulation of unfolded and/or unassembled respiratory chain subunits, resulting in mitonuclear imbalance.

On the other hand, we showed that skeletal muscle has increased stability of mitochondrial transcripts, moderate upregulation of ribosomes and a likely increase in regeneration. We think that if the lifespan of our animals were longer, we would have seen, at least some, of the stress responses not only in heart but also in skeletal muscle.

We propose that disrupted mitochondrial proteostasis upregulates stress-related transcriptional factors/activators like ATF4, ATF5 and CHOP, which further contribute to the upregulation of ‘mitokine’ FGF21 and UPR^{mt} (Figure 4.1). By increasing PGC1- α stability, FGF21 seems to be of great importance for increased mitochondrial biogenesis and decreased autophagy. Moreover, FGF21 mediates general metabolic changes in DARS2-deficient mice. Our results are of great importance while it is generally believed that mitochondrial respiratory deficiency is the primary activator of compensatory responses. However, we emphasize the importance of disrupted protein homeostasis that precedes respiratory chain deficiency as the driving force behind the activated stress responses. Changing this current view could present new therapeutic possibilities for mitochondrial diseases.

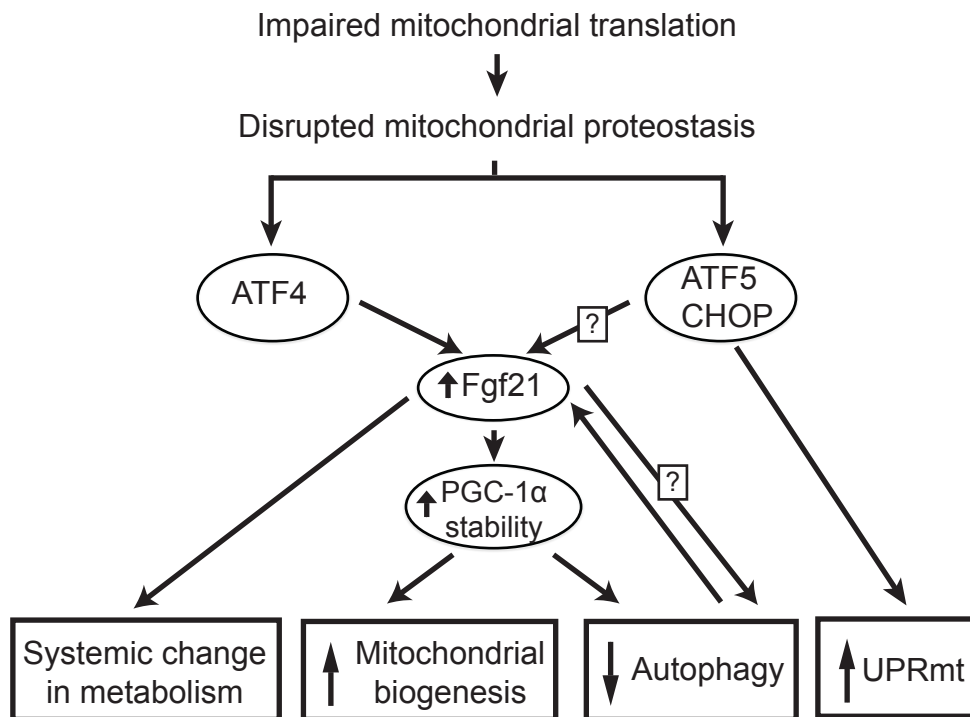


Figure 4.1 Proposed model for the heart-mediated stress responses to perturbed protein homeostasis caused by DARS2 deficiency.

Impaired proteostasis in mitochondria directs preferential upregulation of stress-related transcriptional activators like ATF4, ATF5 and CHOP, which in turn regulate FGF21 levels. The cascade activated leads to the upregulation of mitochondrial biogenesis and UPR^{mt} while downregulating autophagy and provide a systemic change in metabolism.

4.3. DARS2 deficiency in forebrain neurons, hippocampus and striatum causes progressive neuronal degeneration accompanied by an activation of inflammatory responses and reactive astrogliosis in an age- and region-dependent manner

In this study, we further wanted to examine forebrain neurons with respect to their responses to mitochondrial translation defect caused by DARS2 deficiency.

Mitochondrial dysfunction in *Dars2*^{L/L, +/CaMKII α -Cre} mice were not that apparent when some techniques were employed. This can be due to the fact that DARS2 deficiency was induced in forebrain neurons, and the tissue used for the experiments, cortex, included other cell types, i.e. different neuronal cell types and glial cells. Those cells were not affected by cre recombination and thus still contained DARS2. Moreover, severe DARS2-deficient neurons would have already been lost as a result of increased apoptosis and we were analyzing comparably ‘healthier’ neurons. To be able to conduct those experiments, a whole brain knockout, i.e. using Nestin-cre, would have been more useful. However, the fact that full body knockout of DARS2 was embryonic lethal and Nestin promoter was also active before birth, could also indicate that *Dars2*^{L/L, +/Nestin-Cre} mice might be embryonic lethal.

Progressively atrophied brain, abnormal behaviour exemplified via excessive scratching, mitochondrial dysfunction were the hallmarks of *Dars2*^{L/L, +/CaMKII α -Cre} mice. COX deficiency was more apparent in CA1 and DG regions of hippocampus. One interesting fact that should be mentioned is our observation for decreased activity for CO II in MRC enzyme activities. This suggests that defective mitochondrial translation is exerting an adverse effect on CO II activity, which needs further experimental addressing. TEM analysis revealed loss of cristae structure in DARS-2 deficient hippocampal regions, which we did not observe in heart and skeletal muscle of the previous model.

Those observations were also in accordance with the literature. Knockout mouse models using the CaMKII α promoter, such as TFAM (Sorensen et al., 2001), COX10 (Fukui et al., 2007), PHB2 (Merkwirth et al., 2012), Rieske iron–sulfur protein (RISP) (Diaz et al., 2012) and NDUFA5 (Peralta et al., 2013) revealed similar findings. For example, mitochondrial late-onset neurodegeneration (MILON) mice were generated after postnatal deletion of *Tfam* gene in forebrain neurons (Sorensen et al., 2001). MILON mice appeared perfectly normal and

showed no abnormalities until the age of 5-6 months, as in our mouse model. Following this time period, their physical condition deteriorated pretty rapidly and death occurred within 1-2 weeks. This was a very interesting observation indicating that after a threshold had been passed, the mice could no longer carry the burdens of TFAM depletion. In our case, however, animals do not die but have to be sacrificed due to the excessive scratching. The onset of abnormalities seem to be similar, even though mitochondrial translation defect due to DARS2-depletion appear to be handled better compared to mitochondrial maintenance/transcription defect. As *Dars2*^{L/L, +/CaMKII α -Cre} mice, MILON mice displayed a progressive, marked neuronal cell loss, degeneration, severe disruption of cortical organization and axonal degeneration in neocortex and hippocampus, which successfully mimics the late-onset and progressive nature of human neurodegenerative diseases (Dogan and Trifunovic, 2011). In *Phb2*^{NKO} mice, however, aging-related phenotypes, such as weight loss and kyphosis, were observed around 12-14 weeks of age (Merkwirth et al., 2012). Scratching behavior was detected around this time, and the mice died between the ages of 14 and 22 weeks. Similarly to our study, progressive forebrain atrophy and neuronal loss accompanied with increased astrogliosis and mitochondria with almost complete absence of cristae. In a recent study, NDUFA5 subunit of CO I was selectively ablated in neurons (Peralta et al., 2013). The mice showed mild chronic encephalopathy at the age of 11 months, but neuronal death or gliosis were not detected. As can be seen from these examples and current study, the age onset of mitochondrial dysfunction/behavioral abnormalities varies between these mouse models. This could be due to the different roles of different proteins knocked out in each mouse model but also as a result of the CaMKII α -cre mice used. For example, Merkwirth et al. used a different CaMKII α -cre mice (Dragatsis and Zeitlin, 2000) but in our and Sorensen et al.'s study another cre mice was used (Xu et al., 2000). Even if it is not clear why, the onset of symptoms are earlier in Dragatsis and Zeitlin's CaMKII α -cre mice. This could be the result of different strategies used when these cre lines were generated. Both lines

included a nuclear localization signal but the CaMKII α gene promoter fragments were coming from different labs. Finally Dragatsis and Zeitlin's CaMKII α -cre transgene expression vector was shorter compared to Xu et al.'s. It would be very useful to mate these two different CaMKII α -cre mice to a reporter strain to see whether the expression patterns and onset of effects differ from each other.

Our results revealed considerable degeneration in cortex and severe disruption of cortical and hippocampal organization in an age-dependent progressive manner. The interesting fact was the occurrence of apoptosis in different brain regions in different ages. When mice are 20-week-old, retrosplenial cortex showed signs of apoptosis but as the age increased, no TUNEL-positive nuclei were found. CA1 region displayed high occurrence of progressive apoptotic cells with increased age whereas DG region of hippocampus, showing the highest signs of COX deficiency, displayed very minute amounts of apoptosis. It seems that vast amount of apoptosis might be occurring between 20 and 29 weeks of age. Thus, at 29 weeks of age we do not observe many TUNEL-positive nuclei while they have already been lost. Apoptosis should be checked at different time points and shorter time intervals (i.e before 20 weeks of age, between 20 and 29 weeks of age, etc.) to further investigate the differential regional loss of neurons.

Our results indicate that different regions of brain seem to react differently to defective mitochondrial translation, which can be a result of their ability to cope with mitochondrial dysfunction. Why some regions are more prone to mitochondrial dysfunction is an exciting question that should be further experimentally addressed. Neurons are extraordinary in being able to survive even with dysfunctional mitochondria. Neurons were found to survive for at least 1 month after shutting off oxidative phosphorylation in *Tfam*^{L/L, +/CaMKII α -Cre} mice and that neuronal cell death barely activated defense mechanisms against reactive oxygen species (Sorensen et al., 2001). Increased glycolysis and support from other neuronal cell types have been proposed to account for this fact (Koopman et

al., 2012). Brain is known to utilize glucose as fuel. Both neurons and astrocytes rely on OXPHOS for ATP generation but it has been experimentally proven that astrocytes can also utilize glycogen. It appears that when glycolysis is stimulated, the released lactate can be taken up by neurons and can be used, which indicates astrocytes and neurons are metabolically linked by lactate shuttling (Koopman et al., 2012).

DARS2-deficient knockout mice showed increased levels of activated microglia and reactive astrocytes. The progressive infiltration as observed by activated microglia was also available in activated astrocytes. Occurrence of neuroinflammatory reactions were a common aspect of neurodegenerative disorders such as Alzheimer's disease (AD), Parkinson's disease (PD), Multiple sclerosis (MS), Huntington's disease (HD) and Amyotrophic Lateral Sclerosis (ALS). Normally, in those diseases, microglia and astrocytes are activated in response to apoptosis (Vidal-Taboada et al., 2011).

Microglial cells, resident macrophages of central nervous system (CNS), are of mesenchymal origin and comprise 10-20% of the adult glia (Ransohoff and Perry, 2009). Reactive gliosis, or neuroinflammation, is the aggressive response of glia to the activating stimuli such as neuronal death, toxins or mechanical injury (Block et al., 2007). Microglia transforms and gets activated to form the first line of defense against these stimuli, and that is observed nearly in all of the neurological disorders. Reactive microglia are necessary for neuronal survival, i.e. phagocytosis to clear toxic and cellular debris. They also release anti-inflammatory factors, to guide the migration of stem cells to the site of inflammation and injury. Astrocytes, on the other hand, ectodermal cells and they provide support for surrounding neurons and take part in physical structuring of the brain, maintaining ion homeostasis and even promotion of myelination (Sofroniew and Vinters, 2010). Not being immune cells *per se*, astrocytes

contribute to the immune response by influencing microglial behavior (Farina et al., 2007).

In our knockout mouse model, both somatosensory and retrosplenial cortical areas showed activated microglia in three different time points (20, 29, and 32 weeks of age) but there existed an age-dependent decrease, in contrast to hippocampal regions, where we saw increased number of activated microglia with increasing age. This temporal decrease is interesting. The somatosensory cortex is an area of the brain that processes input from the various systems in the body that are sensitive to touch, including pain and temperature, whereas retrosplenial cortex is a region that supports a range of cognitive functions, including episodic memory, navigation, imagination and planning for the future (Vann et al., 2009). Moreover, retrosplenial cortex is consistently compromised in the most common neurological disorders that impair memory. The decline of activated microglia with advanced age could suggest that at early age, the ‘insult’ to the retrosplenial cortex and the somatosensory cortex is greater. It is provoking to argue that this ‘insult’ could be pain –in case of somatosensory cortex- and decline in memory and navigation –in case of retrosplenial cortex-. When later time points were considered, the inflammatory response might be decreased due to the possibility that the ‘insult’ was also reduced in these regions.

Reactive astrogliosis patterns coincided with the apoptotic neuronal loss. We can also conclude that not only apoptosis but also severe diffuse reactive astrogliosis and the microglial activation may have contributed further to neuronal degeneration. It is known that this innate immune response can also be potentially add to the progression of neurodegeneration while microgliosis can provoke amyloid- β plaque formation, dystrophic neurite growth, and excessive tau phosphorylation (Vidal-Taboada et al., 2011). As the microgliosis and astrogliosis become chronic, similar to our case, the initial neuroprotective effect can transform into a cytotoxic one. This would explain the worsening of the

phenotype between the ages of 29 weeks and 32 weeks. It would also be very interesting to look for those markers in nonsymptomatic younger mice brains and compare apoptosis with the activation of immune response.

Neurodegenerative diseases cause the activation of microglia when misfolded proteins accumulate, i.e. the amyloid- β peptides are known to activate microglia in AD and in the case of ALS and HD, the misfolded proteins, this time accumulated intracellularly, are also responsible for microgliosis (Perry et al., 2010). This is of interest due to the fact that in heart and skeletal muscle specific DARS2 knockout mouse, unfolded/misfolded proteins are the first signal that causes the systemic changes and activation of stress signals. These specific responses precede respiratory chain deficiency. This observation might be also true in *Dars2*^{L/L, +/CaMKII α -Cre} mice. Buildup of unfolded and/or unassembled respiratory chain subunits due to the imbalance between the increased levels of *de novo* protein synthesis and decreased folding capacity could be directing the upregulation of stress-related signals. We have also checked the markers for UPR^{mt} both in brain and other tissues in *Dars2*^{L/L, +/CaMKII α -Cre} mice, as suggested by the ‘cell-nonautonomous’ theory (Durieux et al., 2011), but we could not detect any changes in the levels of mtHSP70 and HSP60 (Lotter, 2013). More experimental data concentrating on disturbed proteostasis should be gathered as had been done for *Dars2*^{L/L, +/Ckmm-Cre} mice, i.e. levels of different proteases.

To sum up, defective mitochondrial translation in *Dars2*^{L/L, +/CaMKII α -Cre} mice caused weight loss, abnormal behavior, and severe forebrain atrophy, which is caused by neuronal cell apoptosis and accompanied by activation of inflammatory responses such as microgliosis and reactive astrogliosis. Surprisingly, neurodegeneration occurred in an age-dependent manner and affected cortex and hippocampal regions differently. The mechanisms and exact pattern of observed phenotypes still waits experimental addressing.

4.4. Summary and perspectives

The mechanisms leading to the tissue-specific manifestations of mitochondrial diseases are still largely unknown. In this study, we compared three different highly-energy demanding tissues, heart, skeletal muscle and forebrain neurons, which are commonly affected in mitochondrial diseases. Our results indicate the existence of different intrinsic and extrinsic coping mechanisms each tissue possesses. Heart reacts to defective mitochondrial translation by enacting a repertoire of mitochondrial and extramitochondrial responses; skeletal muscle is intrinsically much more equipped to cope with increased levels of unassembled/unfolded proteins and mitochondrial dysfunction; neurons employ defense/inflammatory systems and rely on the fact that they can live up to 1 month after OXPHOS is turned off. However, all these responses might be adding to the progression of observed phenotypes instead of ameliorating them.

To further strengthen the findings of this study, two new mouse models could be very useful. First, generating a double knockout mouse by deletion of *Dars2* in heart and skeletal muscle, as used in this study, in combination with *Fgf21* knockout mouse would be very interesting. By this, we could experimentally prove the pivotal role of FGF21 in activation of the stress responses and pinpoint which of the observed responses are due to FGF21.

Second, generation of a *Dars2*^{L/L, +/Plp-Cre} mouse could give us further insights about the disease LBSL. Plp1 promoter is tamoxifen-inducible (Leone et al., 2003). It has been shown that injecting the lactating mothers with 1 mg of tamoxifen daily during 5 days starting at postnatal day 1 (P1) induces recombination only in brain areas that start myelination between P1 and P5, which includes the medulla, the pontine fibers, and white matter tracts in the cerebellum. This model might, to some extent, mimic the human disease LBSL, while MRIs of LBSL patients show signal abnormalities in the cerebral white matter and

specific brain stem and spinal cord tracts (van der Knaap et al., 2003). Therefore, *Dars2*^{L/L, +/Plp-Cre} could have given insight to the observed phenotypes in patients. Moreover, we could compare how neurons, by using the *Dars2*^{L/L, +/CaMKII α -Cre} mice of this study, and mature oligodendrocytes, two different cell types, react to defective mitochondrial protein synthesis.

References

- Acin-Perez, R., Fernandez-Silva, P., Peleato, M. L., Perez-Martos, A., & Enriquez, J. A. (2008). Respiratory active mitochondrial supercomplexes. *Mol Cell*, 32(4), 529-539.
- Aldridge, J. E., Horibe, T., & Hoogenraad, N. J. (2007). Discovery of genes activated by the mitochondrial unfolded protein response (mtUPR) and cognate promoter elements. *PLoS One*, 2(9), e874.
- Almajan, E. R., Richter, R., Paeger, L., Martinelli, P., Barth, E., Decker, T., Larsson, N. G., Kloppenburg, P., Langer, T., & Rugarli, E. I. (2012). AFG3L2 supports mitochondrial protein synthesis and Purkinje cell survival. *J Clin Invest*, 122(11), 4048-58.
- Antonellis, A., & Green, E. D. (2008). The role of aminoacyl-tRNA synthetases in genetic diseases. *Annu Rev Genomics Hum Genet*, 9, 87-107.
- Barel, O., Shorer, Z., Flusser, H., Ofir, R., Narkis, G., Finer, G., Shalev, H., Nasasra, A., Saada, A., & Birk, O. S. (2008). Mitochondrial complex III deficiency associated with a homozygous mutation in UQCRQ. *Am J Hum Genet*, 82(5), 1211-1216.
- Bayat, V., Thiffault, I., Jaiswal, M., Tetreault, M., Donti, T., Sasarman, F., Bernard, G., Demers-Lamarche, J., Dicaire, M. J., Mathieu, J., Vanasse, M., Bouchard, J. P., Rioux, M. F., Lourenco, C. M., Li, Z., Haueter, C., Shoubridge, E. A., Graham, B. H., Brais, B., & Bellen, H. J. (2012). Mutations in the Mitochondrial Methionyl-tRNA Synthetase Cause a Neurodegenerative Phenotype in Flies and a Recessive Ataxia (ARSAL) in Humans. *PLoS Biol*, 10(3), e1001288.
- Belostotsky, R., Ben-Shalom, E., Rinat, C., Becker-Cohen, R., Feinstein, S., Zeligson, S., Segel, R., Elpeleg, O., Nassar, S., & Frishberg, Y. (2011). Mutations in the mitochondrial seryl-tRNA synthetase cause hyperuricemia, pulmonary hypertension, renal failure in infancy and alkalosis, HUPRA syndrome. *Am J Hum Genet*, 88(2), 193-200.
- Berthonneau, E., & Mirande, M. (2000). A gene fusion event in the evolution of aminoacyl-tRNA synthetases. *FEBS Lett*, 470(3), 300-304.
- Block, M. L., Zecca, L., & Hong, J. S. (2007). Microglia-mediated neurotoxicity: uncovering the molecular mechanisms. *Nat Rev Neurosci*, 8(1), 57-69.

- Bourgeron, T., Chretien, D., Rotig, A., Munnich, A., & Rustin, P. (1993). Fate and expression of the deleted mitochondrial DNA differ between human heteroplasmic skin fibroblast and Epstein-Barr virus-transformed lymphocyte cultures. *J Biol Chem*, 268(26), 19369-19376.
- Buck, C. A., & Nass, M. M. (1969). Studies on mitochondrial tRNA from animal cells. I. A comparison of mitochondrial and cytoplasmic trna and aminoacyl-tRNA synthetases. *J Mol Biol*, 41(1), 67-82.
- Burdon, R. H. (1996). Control of cell proliferation by reactive oxygen species. *Biochem Soc Trans*, 24(4), 1028-1032.
- Butow, R. A., & Avadhani, N. G. (2004). Mitochondrial signaling: the retrograde response. *Mol Cell*, 14(1), 1-15.
- Choi, K. H., & Licht, S. (2005). Control of peptide product sizes by the energy-dependent protease ClpAP. *Biochemistry*, 44(42), 13921-13931.
- Chomyn, A., Martinuzzi, A., Yoneda, M., Daga, A., Hurko, O., Johns, D., Lai, S. T., Nonaka, I., Angelini, C., & Attardi, G. (1992). MELAS mutation in mtDNA binding site for transcription termination factor causes defects in protein synthesis and in respiration but no change in levels of upstream and downstream mature transcripts. *Proc Natl Acad Sci U S A*, 89(10), 4221-4225.
- Clement, M. V., & Pervaiz, S. (1999). Reactive oxygen intermediates regulate cellular response to apoptotic stimuli: an hypothesis. *Free Radic Res*, 30(4), 247-252.
- Connor, M. K., Takahashi, M., & Hood, D. A. (1996). Tissue-specific stability of nuclear- and mitochondrially encoded mRNAs. *Arch Biochem Biophys*, 333(1), 103-108.
- D'souza, D. M., Lai, R. Y., Shuen, M., & Hood, D. A. (2012). mRNA Stability as a Function of Striated Muscle Oxidative Capacity. *Am J Physiol Regul Integr Comp Physiol*.
- De Meirleir, L., Seneca, S., Damis, E., Sepulchre, B., Hoorens, A., Gerlo, E., Garcia Silva, M. T., Hernandez, E. M., Lissens, W., & Van Coster, R. (2003). Clinical and diagnostic characteristics of complex III deficiency due to mutations in the BCS1L gene. *Am J Med Genet A*, 121A(2), 126-131.
- Delarue, M. (1995). Aminoacyl-tRNA synthetases. *Curr Opin Struct Biol*, 5(1), 48-55.

- Diaz, F., Garcia, S., Padgett, K. R., & Moraes, C. T. (2012). A defect in the mitochondrial complex III, but not complex IV, triggers early ROS-dependent damage in defined brain regions. *Hum Mol Genet*, *21*(23), 5066-5077.
- DiMauro, S., Bonilla, E., Zeviani, M., Nakagawa, M., & DeVivo, D. C. (1985). Mitochondrial myopathies. *Ann Neurol*, *17*(6), 521-538.
- DiMauro, S., & Schon, E. A. (2008). Mitochondrial disorders in the nervous system. *Annu Rev Neurosci*, *31*, 91-123.
- Dogan, S. A., & Trifunovic, A. (2011). Modelling mitochondrial dysfunction in mice. *Physiol Res*, *60 Suppl 1*, S61-S70.
- Dragatsis, I., & Zeitlin, S. (2000). CaMKIIalpha-Cre transgene expression and recombination patterns in the mouse brain. *Genesis*, *26*(2), 133-135.
- Droge, W. (2002). Free radicals in the physiological control of cell function. *Physiol Rev*, *82*(1), 47-95.
- Dubourg, O., Azzedine, H., Yaou, R. B., Pouget, J., Barois, A., Meininger, V., Bouteiller, D., Ruberg, M., Brice, A., & LeGuern, E. (2006). The G526R glycyI-tRNA synthetase gene mutation in distal hereditary motor neuropathy type V. *Neurology*, *66*(11), 1721-1726.
- Durieux, J., Wolff, S., & Dillin, A. (2011). The cell-non-autonomous nature of electron transport chain-mediated longevity. *Cell*, *144*(1), 79-91.
- Edgar, D., Shabalina, I., Camara, Y., Wredenberg, A., Calvaruso, M. A., Nijtmans, L., Nedergaard, J., Cannon, B., Larsson, N. G., & Trifunovic, A. (2009). Random point mutations with major effects on protein-coding genes are the driving force behind premature aging in mtDNA mutator mice. *Cell Metab*, *10*(2), 131-138.
- Edvardson, S., Shaag, A., Kolesnikova, O., Gomori, J. M., Tarassov, I., Einbinder, T., Saada, A., & Elpeleg, O. (2007). Deleterious mutation in the mitochondrial arginyl-transfer RNA synthetase gene is associated with pontocerebellar hypoplasia. *Am J Hum Genet*, *81*(4), 857-862.
- Elo, J. M., Yadavalli, S. S., Euro, L., Isohanni, P., Gotz, A., Carroll, C., Valanne, L., Alkuraya, F. S., Uusimaa, J., Paetau, A., Caruso, E. M., Pihko, H., Ibba, M., Tyynismaa, H., & Suomalainen, A. (2012). Mitochondrial phenylalanyl-tRNA synthetase mutations underlie fatal infantile Alpers encephalopathy. *Hum Mol Genet*. *21*(20), 4521-9.

- Emerit, J., Edeas, M., & Bricaire, F. (2004). Neurodegenerative diseases and oxidative stress. *Biomed Pharmacother*, 58(1), 39-46.
- Enriquez, J. A., & Attardi, G. (1996). Analysis of aminoacylation of human mitochondrial tRNAs. *Methods Enzymol*, 264, 183-196.
- Farina, C., Aloisi, F., & Meinl, E. (2007). Astrocytes are active players in cerebral innate immunity. *Trends Immunol*, 28(3), 138-145.
- Finsterer, J. (2008). Leigh and Leigh-like syndrome in children and adults. *Pediatr Neurol*, 39(4), 223-235.
- Fisher, F. M., Kleiner, S., Douris, N., Fox, E. C., Mepani, R. J., Verdeguer, F., Wu, J., Kharitonov, A., Flier, J. S., Maratos-Flier, E., & Spiegelman, B. M. (2012). FGF21 regulates PGC-1alpha and browning of white adipose tissues in adaptive thermogenesis. *Genes Dev*, 26(3), 271-281.
- Fukui, H., Diaz, F., Garcia, S., & Moraes, C. T. (2007). Cytochrome c oxidase deficiency in neurons decreases both oxidative stress and amyloid formation in a mouse model of Alzheimer's disease. *Proc Natl Acad Sci U S A*, 104(35), 14163-14168.
- Gotz, A., Tynismaa, H., Euro, L., Ellonen, P., Hyotylainen, T., Ojala, T., Hamalainen, R. H., Tommiska, J., Raivio, T., Oresic, M., Karikoski, R., Tammela, O., Simola, K. O., Paetau, A., Tyni, T., & Suomalainen, A. (2011). Exome Sequencing Identifies Mitochondrial Alanine-tRNA Synthetase Mutations in Infantile Mitochondrial Cardiomyopathy. *Am J Hum Genet*, 88(5), 635-642.
- Hackenbrock, C. R., Chazotte, B., & Gupte, S. S. (1986). The random collision model and a critical assessment of diffusion and collision in mitochondrial electron transport. *J Bioenerg Biomembr*, 18(5), 331-368.
- Han, J. M., Kim, J. Y., & Kim, S. (2003). Molecular network and functional implications of macromolecular tRNA synthetase complex. *Biochem Biophys Res Commun*, 303(4), 985-993.
- Hance, N., Ekstrand, M. I., & Trifunovic, A. (2005). Mitochondrial DNA polymerase gamma is essential for mammalian embryogenesis. *Hum Mol Genet*, 14(13), 1775-1783.
- Hanna, M. G., Nelson, I. P., Morgan-Hughes, J. A., & Harding, A. E. (1995). Impaired mitochondrial translation in human myoblasts harbouring the mitochondrial DNA tRNA lysine 8344 A-->G (MERRF) mutation: relationship to proportion of mutant mitochondrial DNA. *J Neurol Sci*, 130(2), 154-160.

Hansson, A., Hance, N., Dufour, E., Rantanen, A., Hultenby, K., Clayton, D. A., Wibom, R., & Larsson, N. G. (2004). A switch in metabolism precedes increased mitochondrial biogenesis in respiratory chain-deficient mouse hearts. *Proc Natl Acad Sci U S A*, *101*(9), 3136-3141.

Hatefi, Y., Haavik, A. G., Fowler, L. R., & Griffiths, D. E. (1962). Studies on the electron transfer system: XLII. Reconstitution of the electron transfer system. *J Biol Chem* *237*, 2661–2669.

Haut, S., Brivet, M., Touati, G., Rustin, P., Lebon, S., Garcia-Cazorla, A., Saudubray, J. M., Boutron, A., Legrand, A., & Slama, A. (2003). A deletion in the human QP-C gene causes a complex III deficiency resulting in hypoglycaemia and lactic acidosis. *Hum Genet*, *113*(2), 118-122.

Haynes, C. M., Fiorese, C. J., & Lin, Y. F. (2013). Evaluating and responding to mitochondrial dysfunction: the mitochondrial unfolded-protein response and beyond. *Trends Cell Biol*, *23*(7), 311-318.

Haynes, C. M., Yang, Y., Blais, S. P., Neubert, T. A., & Ron, D. (2010). The matrix peptide exporter HAF-1 signals a mitochondrial UPR by activating the transcription factor ZC376.7 in *C. elegans*. *Mol Cell*, *37*(4), 529-540.

Holt, I. J., Harding, A. E., Petty, R. K., & Morgan-Hughes, J. A. (1990). A new mitochondrial disease associated with mitochondrial DNA heteroplasmy. *Am J Hum Genet*, *46*(3), 428-433.

Horibe, T., & Hoogenraad, N. J. (2007). The chop gene contains an element for the positive regulation of the mitochondrial unfolded protein response. *PLoS One*, *2*(9), e835.

Houtkooper, R. H., Mouchiroud, L., Ryu, D., Moullan, N., Katsyuba, E., Knott, G., Williams, R. W., & Auwerx, J. (2013). Mitonuclear protein imbalance as a conserved longevity mechanism. *Nature*, *497*(7450), 451-457.

Ibba, M., & Soll, D. (2000). Aminoacyl-tRNA synthesis. *Annu Rev Biochem*, *69*, 617-650.

Inagaki, T, P Dutchak, G Zhao, X Ding, L Gautron, V Parameswara, Y Li, R Goetz, M Mohammadi, V Esser, JK Elmquist, RD Gerard, SC Burgess, RE Hammer, DJ Mangelsdorf, & SA Kliewer. (2007). Endocrine regulation of the fasting response by PPARalpha-mediated induction of fibroblast growth factor 21. *Cell Metab* *5*, 415–25.

Isohanni, P., Linnankivi, T., Buzkova, J., Lonqvist, T., Pihko, H., Valanne, L., Tienari, P. J., Elovaara, I., Pirttila, T., Reunanen, M., Koivisto, K., Marjavaara, S., & Suomalainen, A. (2010). DARS2 mutations in mitochondrial leucoencephalopathy and multiple sclerosis. *J Med Genet*, 47(1), 66-70.

Jin, S. M., & Youle, R. J. (2013). The accumulation of misfolded proteins in the mitochondrial matrix is sensed by PINK1 to induce PARK2/Parkin-mediated mitophagy of polarized mitochondria. *Autophagy*, 9(11), 1750-1757.

John, J. C. S. (2013). Mitochondrial DNA, Mitochondria, Disease and Stem Cells. Humana Press.

Karamanlidis, G., Lee, C. F., Garcia-Menendez, L., Kolwicz, S. C. J., Suthammarak, W., Gong, G., Sedensky, M. M., Morgan, P. G., Wang, W., & Tian, R. (2013). Mitochondrial complex I deficiency increases protein acetylation and accelerates heart failure. *Cell Metab*, 18(2), 239-250.

Kaufmann, P., Engelstad, K., Wei, Y., Kulikova, R., Oskoui, M., Sproule, D. M., Battista, V., Koenigsberger, D. Y., Pascual, J. M., Shanske, S., Sano, M., Mao, X., Hirano, M., Shungu, D. C., Dimauro, S., & De Vivo, D. C. (2011). Natural history of MELAS associated with mitochondrial DNA m.3243A>G genotype. *Neurology*, 77(22), 1965-1971.

Kearns, T. P., & Sayre, G. P. (1958). Retinitis pigmentosa, external ophthalmoplegia, and complete heart block: unusual syndrome with histologic study in one of two cases. *AMA Arch Ophthalmol*, 60(2), 280-289.

Kelly, D. P., & Scarpulla, R. C. (2004). Transcriptional regulatory circuits controlling mitochondrial biogenesis and function. *Genes Dev*, 18(4), 357-368.

Kharitonov, A., Shiyanova, T. L., Koester, A., Ford, A. M., Micanovic, R., Galbreath, E. J., Sandusky, G. E., Hammond, L. J., Moyers, J. S., Owens, R. A., Gromada, J., Brozinick, J. T., Hawkins, E. D., Wroblewski, V. J., Li, D. S., Mehrbod, F., Jaskunas, S. R., & Shanafelt, A. B. (2005). FGF-21 as a novel metabolic regulator. *J Clin Invest*, 115(6), 1627-1635.

Kim, K. H., Jeong, Y. T., Oh, H., Kim, S. H., Cho, J. M., Kim, Y. N., Kim, S. S., Kim do, H., Hur, K. Y., Kim, H. K., Ko, T., Han, J., Kim, H. L., Kim, J., Back, S. H., Komatsu, M., Chen, H., Chan, D. C., Konishi, M., Itoh, N., Choi, C. S., & Lee, M. S. (2013). Autophagy deficiency leads to protection from obesity and insulin resistance by inducing Fgf21 as a mitokine. *Nat Med*, 19(1), 83-92.

- Ko, Y. G., Kang, Y. S., Kim, E. K., Park, S. G., & Kim, S. (2000). Nucleolar localization of human methionyl-tRNA synthetase and its role in ribosomal RNA synthesis. *J Cell Biol*, 149(3), 567-574.
- Ko, Y. G., Kim, E. Y., Kim, T., Park, H., Park, H. S., Choi, E. J., & Kim, S. (2001). Glutamine-dependent antiapoptotic interaction of human glutaminyl-tRNA synthetase with apoptosis signal-regulating kinase 1. *J Biol Chem*, 276(8), 6030-6036.
- Koopman, W. J., Distelmaier, F., Smeitink, J. A., & Willems, P. H. (2013). OXPHOS mutations and neurodegeneration. *EMBO J*. 32(1), 9-29.
- Kukat, C. & Larsson, N. G. (2013) mtDNA makes a U-turn for the mitochondrial nucleoid. *Trends Cell Biol* 23(9), 457-63.
- Kuznetsov, A. V., Veksler, V., Gellerich, F. N., Saks, V., Margreiter, R., & Kunz, W. S. (2008). Analysis of mitochondrial function in situ in permeabilized muscle fibers, tissues and cells. *Nat Protoc*, 3(6), 965-976.
- Larsson, N. G. (2010). Somatic mitochondrial DNA mutations in mammalian aging. *Annu Rev Biochem*, 79, 683-706.
- Larsson, N. G., Wang, J., Wilhelmsson, H., Oldfors, A., Rustin, P., Lewandoski, M., Barsh, G. S., & Clayton, D. A. (1998). Mitochondrial transcription factor A is necessary for mtDNA maintenance and embryogenesis in mice. *Nat Genet*, 18(3), 231-236.
- Lehman, J. J., Barger, P. M., Kovacs, A., Saffitz, J. E., Medeiros, D. M., & Kelly, D. P. (2000). Peroxisome proliferator-activated receptor gamma coactivator-1 promotes cardiac mitochondrial biogenesis. *J Clin Invest*, 106(7), 847-856.
- Leigh, D. (1951). Subacute necrotizing encephalomyelopathy in an infant. *J Neurol Neurosurg Psychiatry*, 14(3), 216-221.
- Leone, D. P., Genoud, S., Atanasoski, S., Grausenburger, R., Berger, P., Metzger, D., Macklin, W. B., Chambon, P., & Suter, U. (2003). Tamoxifen-inducible gli-specific Cre mice for somatic mutagenesis in oligodendrocytes and Schwann cells. *Mol Cell Neurosci*, 22(4), 430-440.
- Lin, J., Puigserver, P., Donovan, J., Tarr, P., & Spiegelman, B. M. (2002). Peroxisome proliferator-activated receptor gamma coactivator 1beta (PGC-1beta), a novel PGC-1-related transcription coactivator associated with host cell factor. *J Biol Chem*, 277(3), 1645-1648.

- Ling, J., Reynolds, N., & Ibba, M. (2009). Aminoacyl-tRNA synthesis and translational quality control. *Annu Rev Microbiol*, *63*, 61-78.
- Linnankivi, T., Lundbom, N., Autti, T., Hakkinen, A. M., Koillinen, H., Kuusi, T., Lonnqvist, T., Sainio, K., Valanne, L., Aarimaa, T., & Pihko, H. (2004). Five new cases of a recently described leukoencephalopathy with high brain lactate. *Neurology*, *63*(4), 688-692.
- Longatti, A., & Tooze, S. A. (2009). Vesicular trafficking and autophagosome formation. *Cell Death Differ*, *16*(7), 956-965.
- Lotter, S. (2013). Mitochondrial aspartyl-tRNA synthetase (DARS2) deficiency in brain-specific knockout mice (Master's Thesis, University of Cologne).
- Luft, R., Ikkos, D., Pakmieri, G., Ernster, L., & Afzelius, B. (1962). A case of severe hypermetabolism of nonthyroid origin with a defect in the maintenance of mitochondrial respiratory control: a correlated clinical, biochemical, and morphological study. *J Clin Invest*, *41*, 1776-1804.
- Lyons, G. E., Muhlebach, S., Moser, A., Masood, R., Paterson, B. M., Buckingham, M. E., & Perriard, J. C. (1991). Developmental regulation of creatine kinase gene expression by myogenic factors in embryonic mouse and chick skeletal muscle. *Development*, *113*(3), 1017-1029.
- Madrazo, J. A., & Kelly, D. P. (2008). The PPAR trio: regulators of myocardial energy metabolism in health and disease. *J Mol Cell Cardiol*, *44*(6), 968-975.
- Man, P. Y., Turnbull, D. M., & Chinnery, P. F. (2002). Leber hereditary optic neuropathy. *J Med Genet*, *39*(3), 162-169.
- Margulis, L. (1975). Symbiotic theory of the origin of eukaryotic organelles; criteria for proof. *Symp Soc Exp Biol*, *29*, 21-38.
- Matsushima, Y., & Kaguni, L. S. (2012). Matrix proteases in mitochondrial DNA function. *Biochim Biophys Acta*, *1819*(9-10), 1080-1087.
- McBride, H. M., Neuspiel, M., & Wasiak, S. (2006). Mitochondria: more than just a powerhouse. *Curr Biol*, *16*, R551-R560.
- Merkwirth, C., Martinelli, P., Korwitz, A., Morbin, M., Bronneke, H. S., Jordan, S. D., Rugarli, E. I., & Langer, T. (2012). Loss of prohibitin membrane scaffolds impairs mitochondrial architecture and leads to tau hyperphosphorylation and neurodegeneration. *PLoS Genet*, *8*(11), e1003021.

Metodiev, M. D., Lesko, N., Park, C. B., Camara, Y., Shi, Y., Wibom, R., Hultenby, K., Gustafsson, C. M., & Larsson, N. G. (2009). Methylation of 12S rRNA is necessary for in vivo stability of the small subunit of the mammalian mitochondrial ribosome. *Cell Metab*, 9(4), 386-397.

Miyake, N., Yamashita, S., Kurosawa, K., Miyatake, S., Tsurusaki, Y., Doi, H., Saito, H., & Matsumoto, N. (2011). A novel homozygous mutation of DARS2 may cause a severe LBSL variant. *Clin Genet*, 80(3), 293-296.

Mizushima, N., & Komatsu, M. (2011). Autophagy: renovation of cells and tissues. *Cell*, 147(4), 728-741.

Mizushima, N., Yamamoto, A., Matsui, M., Yoshimori, T., & Ohsumi, Y. (2004). In vivo analysis of autophagy in response to nutrient starvation using transgenic mice expressing a fluorescent autophagosome marker. *Mol Biol Cell*, 15(3), 1101-1111.

Mizushima, N., Yoshimori, T., & Levine, B. (2010). Methods in mammalian autophagy research. *Cell*, 140(3), 313-326.

Moraes, C. T., Ciacci, F., Bonilla, E., Jansen, C., Hirano, M., Rao, N., Lovelace, R. E., Rowland, L. P., Schon, E. A., & DiMauro, S. (1993). Two novel pathogenic mitochondrial DNA mutations affecting organelle number and protein synthesis. Is the tRNA(Leu(UUR)) gene an etiologic hot spot? *J Clin Invest*, 92(6), 2906-2915.

Moraes, C. T., DiMauro, S., Zeviani, M., Lombes, A., Shanske, S., Miranda, A. F., Nakase, H., Bonilla, E., Werneck, L. C., Servidei, S., & et, a. (1989). Mitochondrial DNA deletions in progressive external ophthalmoplegia and Kearns-Sayre syndrome. *N Engl J Med*, 320(20), 1293-1299.

Mori, K., Ma, W., Gething, M. J., & Sambrook, J. (1993). A transmembrane protein with a cdc2+/CDC28-related kinase activity is required for signaling from the ER to the nucleus. *Cell*, 74(4), 743-756.

Motley, W. W., Seburn, K. L., Nawaz, M. H., Miers, K. E., Cheng, J., Antonellis, A., Green, E. D., Talbot, K., Yang, X. L., Fischbeck, K. H., & Burgess, R. W. (2011). Charcot-Marie-Tooth-linked mutant GARS is toxic to peripheral neurons independent of wild-type GARS levels. *PLoS Genet*, 7(12), e1002399.

Nagao, A., Suzuki, T., Katoh, T., Sakaguchi, Y., & Suzuki, T. (2009). Biogenesis of glutaminyl-mt tRNA^{Gln} in human mitochondria. *Proc Natl Acad Sci U S A*, 106(38), 16209-16214.

- Nargund, A. M., Pellegrino, M. W., Fiorese, C. J., Baker, B. M., & Haynes, C. M. (2012). Mitochondrial Import Efficiency of ATFS-1 Regulates Mitochondrial UPR Activation. *Science*, *337*(6094), 587-90.
- Naviaux, R. K., & Nguyen, K. V. (2004). POLG mutations associated with Alpers' syndrome and mitochondrial DNA depletion. *Ann Neurol*, *55*(5), 706-712.
- Ngo, J. K., & Davies, K. J. (2007). Importance of the lon protease in mitochondrial maintenance and the significance of declining lon in aging. *Ann N Y Acad Sci*, *1119*, 78-87.
- Nordberg, J., & Arner, E. S. (2001). Reactive oxygen species, antioxidants, and the mammalian thioredoxin system. *Free Radic Biol Med*, *31*(11), 1287-1312.
- Okamoto, K., Kondo-Okamoto, N., & Ohsumi, Y. (2009). Mitochondria-anchored receptor Atg32 mediates degradation of mitochondria via selective autophagy. *Dev Cell*, *17*(1), 87-97.
- Park, C. B., Asin-Cayuela, J., Camara, Y., Shi, Y., Pellegrini, M., Gaspari, M., Wibom, R., Hultenby, K., Erdjument-Bromage, H., Tempst, P., Falkenberg, M., Gustafsson, C. M., & Larsson, N. G. (2007). MTERF3 is a negative regulator of mammalian mtDNA transcription. *Cell*, *130*(2), 273-285.
- Park, S. G., Ewalt, K. L., & Kim, S. (2005). Functional expansion of aminoacyl-tRNA synthetases and their interacting factors: new perspectives on housekeepers. *Trends Biochem Sci*, *30*(10), 569-574.
- Pearson, H. A., Lobel, J. S., Kocoshis, S. A., Naiman, J. L., Windmiller, J., Lammi, A. T., Hoffman, R., & Marsh, J. C. (1979). A new syndrome of refractory sideroblastic anemia with vacuolization of marrow precursors and exocrine pancreatic dysfunction. *J Pediatr*, *95*(6), 976-984.
- Peralta, S., Torraco, A., Wenz, T., Garcia, S., Diaz, F., & Moraes, C. T. (2013). Partial complex I deficiency due to the CNS conditional ablation of Ndufa5 results in a mild chronic encephalopathy but no increase in oxidative damage. *Hum Mol Genet*. [Epub ahead of print].
- Perry, V. H., Nicoll, J. A., & Holmes, C. (2010). Microglia in neurodegenerative disease. *Nat Rev Neurol*, *6*(4), 193-201.
- Pierce, S. B., Chisholm, K. M., Lynch, E. D., Lee, M. K., Walsh, T., Opitz, J. M., Li, W., Klevit, R. E., & King, M. C. (2011). Mutations in mitochondrial histidyl tRNA synthetase HARS2 cause ovarian dysgenesis and sensorineural hearing loss of Perrault syndrome. *Proc Natl Acad Sci U S A*, *108*(16), 6543-8.

Pierce, S. B., Gersak, K., Michaelson-Cohen, R., Walsh, T., Lee, M. K., Malach, D., Klevit, R. E., King, M. C., & Levy-Lahad, E. (2013). Mutations in LARS2, Encoding Mitochondrial Leucyl-tRNA Synthetase, Lead to Premature Ovarian Failure and Hearing Loss in Perrault Syndrome. *Am J Hum Genet.* 92(4), 605-13.

Pimenta de Castro, I., Costa, A. C., Lam, D., Tufi, R., Fedele, V., Moiso, N., Dinsdale, D., Deas, E., Loh, S. H. Y., & Martins, L. M. (2012). Genetic analysis of mitochondrial protein misfolding in *Drosophila melanogaster*. *Cell Death Differ.*

Potthoff, M. J., Klierer, S. A., & Mangelsdorf, D. J. (2012). Endocrine fibroblast growth factors 15/19 and 21: from feast to famine. *Genes Dev.* 26(4), 312-324.

Puigserver, P., Wu, Z., Park, C. W., Graves, R., Wright, M., & Spiegelman, B. M. (1998). A cold-inducible coactivator of nuclear receptors linked to adaptive thermogenesis. *Cell*, 92(6), 829-839.

Ransohoff, R. M., & Perry, V. H. (2009). Microglial physiology: unique stimuli, specialized responses. *Annu Rev Immunol*, 27, 119-145.

Richter, U., Lahtinen, T., Marttinen, P., Myohanen, M., Greco, D., Cannino, G., Jacobs, H. T., Lietzen, N., Nyman, T. A., & Battersby, B. J. (2013). A mitochondrial ribosomal and RNA decay pathway blocks cell proliferation. *Curr Biol*, 23(6), 535-541.

Riehle, C., Wende, A. R., Zaha, V. G., Pires, K. M., Wayment, B., Olsen, C., Bugger, H., Buchanan, J., Wang, X., Moreira, A. B., Doenst, T., Medina-Gomez, G., Litwin, S. E., Lelliott, C. J., Vidal-Puig, A., & Abel, E. D. (2011). PGC-1beta deficiency accelerates the transition to heart failure in pressure overload hypertrophy. *Circ Res*, 109(7), 783-793.

Riley, L. G., Cooper, S., Hickey, P., Rudinger-Thirion, J., McKenzie, M., Compton, A., Lim, S. C., Thorburn, D., Ryan, M. T., Giege, R., Bahlo, M., & Christodoulou, J. (2010). Mutation of the mitochondrial tyrosyl-tRNA synthetase gene, YARS2, causes myopathy, lactic acidosis, and sideroblastic anemia--MLASA syndrome. *Am J Hum Genet*, 87(1), 52-59.

Robinson, J. C., Kerjan, P., & Mirande, M. (2000). Macromolecular assemblage of aminoacyl-tRNA synthetases: quantitative analysis of protein-protein interactions and mechanism of complex assembly. *J Mol Biol*, 304(5), 983-994.

Russell, L. K., Mansfield, C. M., Lehman, J. J., Kovacs, A., Courtois, M., Saffitz, J. E., Medeiros, D. M., Valencik, M. L., McDonald, J. A., & Kelly, D. P. (2004). Cardiac-specific induction of the transcriptional coactivator peroxisome proliferator-activated receptor gamma coactivator-1alpha promotes mitochondrial biogenesis and reversible cardiomyopathy in a developmental stage-dependent manner. *Circ Res*, *94*(4), 525-533.

Ryan, M. T., & Hoogenraad, N. J. (2007). Mitochondrial-nuclear communications. *Annu Rev Biochem*, *76*, 701-722.

Ryan, M. T., Naylor, D. J., Hoj, P. B., Clark, M. S., & Hoogenraad, N. J. (1997). The role of molecular chaperones in mitochondrial protein import and folding. *Int Rev Cytol*, *174*, 127-193.

Sandri, M., Lin, J., Handschin, C., Yang, W., Arany, Z. P., Lecker, S. H., Goldberg, A. L., & Spiegelman, B. M. (2006). PGC-1alpha protects skeletal muscle from atrophy by suppressing FoxO3 action and atrophy-specific gene transcription. *Proc Natl Acad Sci U S A*, *103*(44), 16260-16265.

Santos-Cortez, R. L., Lee, K., Azeem, Z., Antonellis, P. J., Pollock, L. M., Khan, S., Irfanullah, Andrade-Elizondo, P. B., Chiu, I., Adams, M. D., Basit, S., Smith, J. D., Nickerson, D. A., McDermott, B. M. J., Ahmad, W., & Leal, S. M. (2013). Mutations in KARS, encoding lysyl-tRNA synthetase, cause autosomal-recessive nonsyndromic hearing impairment DFNB89. *Am J Hum Genet*, *93*(1), 132-140.

Sasarman, F., Nishimura, T., Thiffault, I., & Shoubridge, E. A. (2012). A novel mutation in YARS2 causes myopathy with lactic acidosis and sideroblastic anemia. *Hum Mutat*. *33*(8), 1201-6.

Scarpulla, R. C. (2012). Nucleus-encoded regulators of mitochondrial function: integration of respiratory chain expression, nutrient sensing and metabolic stress. *Biochim Biophys Acta*, *1819*(9-10), 1088-1097.

Scarpulla, R. C., Vega, R. B., & Kelly, D. P. (2012). Transcriptional integration of mitochondrial biogenesis. *Trends Endocrinol Metab*, *23*(9), 459-466.

Schaefer, A. M., Taylor, R. W., Turnbull, D. M., & Chinnery, P. F. (2004). The epidemiology of mitochondrial disorders--past, present and future. *Biochim Biophys Acta*, *1659*(2-3), 115-120.

Scheper, G. C., van der Klok, T., van Anandel, R. J., van Berkel, C. G., Sissler, M., Smet, J., Muravina, T. I., Serkov, S. V., Uziel, G., Bugiani, M., Schiffmann, R., Krageloh-Mann, I., Smeitink, J. A., Florentz, C., Van Coster, R., Pronk, J. C., & van der Knaap, M. S. (2007). Mitochondrial aspartyl-tRNA synthetase deficiency causes leukoencephalopathy with brain stem and spinal cord involvement and lactate elevation. *Nat Genet*, *39*(4), 534-539.

Schlame, M., & Ren, M. (2006). Barth syndrome, a human disorder of cardiolipin metabolism. *FEBS Lett*, *580*(23), 5450-5455.

Seburn, K. L., Nangle, L. A., Cox, G. A., Schimmel, P., & Burgess, R. W. (2006). An active dominant mutation of glycyl-tRNA synthetase causes neuropathy in a Charcot-Marie-Tooth 2D mouse model. *Neuron*, *51*(6), 715-726.

Shapira, Y., Harel, S., & Russell, A. (1977). Mitochondrial encephalomyopathies: a group of neuromuscular disorders with defects in oxidative metabolism. *Isr J Med Sci*, *13*(2), 161-164.

Silver, L. M. (1995). *Mouse genetics: concepts and applications*. Oxford University Press.

Sofroniew, M. V., & Vinters, H. V. (2010). Astrocytes: biology and pathology. *Acta Neuropathol*, *119*(1), 7-35.

Sorensen, L., Ekstrand, M., Silva, J. P., Lindqvist, E., Xu, B., Rustin, P., Olson, L., & Larsson, N. G. (2001). Late-onset corticohippocampal neurodepletion attributable to catastrophic failure of oxidative phosphorylation in MILON mice. *J Neurosci*, *21*(20), 8082-8090.

Steenweg, M. E., Ghezzi, D., Haack, T., Abbink, T. E., Martinelli, D., van Berkel, C. G., Bley, A., Diogo, L., Grillo, E., Te Water Naude, J., Strom, T. M., Bertini, E., Prokisch, H., van der Knaap, M. S., & Zeviani, M. (2012). Leukoencephalopathy with thalamus and brainstem involvement and high lactate 'LTBL' caused by EARS2 mutations. *Brain*, *135*(Pt 5), 1387-1394.

Sterky, F. H., Lee, S., Wibom, R., Olson, L., & Larsson, N. G. (2011). Impaired mitochondrial transport and Parkin-independent degeneration of respiratory chain-deficient dopamine neurons in vivo. *Proc Natl Acad Sci U S A*.

Suzuki, T., Nagao, A., & Suzuki, T. (2011). Human mitochondrial diseases caused by lack of taurine modification in mitochondrial tRNAs. *Wiley Interdiscip Rev RNA*, *2*(3), 376-386.

Synofzik, M., Schicks, J., Lindig, T., Biskup, S., Schmidt, T., Hansel, J., Lehmann-Horn, F., & Schols, L. (2011). Acetazolamide-responsive exercise-induced episodic ataxia associated with a novel homozygous DARS2 mutation. *J Med Genet.* 48(10), 713-5.

Tatsuta, T., & Langer, T. (2008). Quality control of mitochondria: protection against neurodegeneration and ageing. *EMBO J*, 27(2), 306-314.

Tatuch, Y., Christodoulou, J., Feigenbaum, A., Clarke, J. T., Wherret, J., Smith, C., Rudd, N., Petrova-Benedict, R., & Robinson, B. H. (1992). Heteroplasmic mtDNA mutation (T----G) at 8993 can cause Leigh disease when the percentage of abnormal mtDNA is high. *Am J Hum Genet*, 50(4), 852-858.

Temperley, R., Richter, R., Dennerlein, S., Lightowers, R. N., & Chrzanowska-Lightowers, Z. M. (2010). Hungry codons promote frameshifting in human mitochondrial ribosomes. *Science*, 327(5963), 301.

Testa, G., Schaft, J., van der Hoeven, F., Glaser, S., Anastassiadis, K., Zhang, Y., Hermann, T., Stremmel, W., & Stewart, A. F. (2004). A reliable lacZ expression reporter cassette for multipurpose, knockout-first alleles. *Genesis*, 38(3), 151-158.

Tiranti, V., Galimberti, C., Nijtmans, L., Bovolenta, S., Perini, M. P., & Zeviani, M. (1999). Characterization of SURF-1 expression and Surf-1p function in normal and disease conditions. *Hum Mol Genet*, 8(13), 2533-2540.

Trifunovic, A., Hansson, A., Wredenberg, A., Rovio, A. T., Dufour, E., Khvorostov, I., Spelbrink, J. N., Wibom, R., Jacobs, H. T., & Larsson, N. G. (2005). Somatic mtDNA mutations cause aging phenotypes without affecting reactive oxygen species production. *Proc Natl Acad Sci U S A*, 102(50), 17993-17998.

Tyynismaa, H., Mjosund, K. P., Wanrooij, S., Lappalainen, I., Ylikallio, E., Jalanko, A., Spelbrink, J. N., Paetau, A., & Suomalainen, A. (2005). Mutant mitochondrial helicase Twinkle causes multiple mtDNA deletions and a late-onset mitochondrial disease in mice. *Proc Natl Acad Sci U S A*, 102(49), 17687-17692.

Tyynismaa, H., Carroll, C. J., Raimundo, N., Ahola-Erkkila, S., Wenz, T., Ruhanen, H., Guse, K., Hemminki, A., Peltola-Mjosund, K. E., Tulkki, V., Oresic, M., Moraes, C. T., Pietilainen, K., Hovatta, I., & Suomalainen, A. (2010). Mitochondrial myopathy induces a starvation-like response. *Hum Mol Genet.* 19(20), 3948-58.

Tzoulis, C., Tran, G. T., Gjerde, I. O., Aasly, J., Neckelmann, G., Rydland, J., Varga, V., Wadel-Andersen, P., & Bindoff, L. A. (2011). Leukoencephalopathy with brainstem and spinal cord involvement caused by a novel mutation in the DARS2 gene. *J Neurol.* 259(2), 292-6.

Vafai, S. B., & Mootha, V. K. (2012). Mitochondrial disorders as windows into an ancient organelle. *Nature*, 491(7424), 374-383.

van Berge, L, S Dooves, CG van Berkel, E Polder, MS van der Knaap, and GC Scheper. (2012). Leukoencephalopathy with brain stem and spinal cord involvement and lactate elevation is associated with cell-type-dependent splicing of mtAspRS mRNA. *Biochem J.* 441, 955–62.

van Berge, L, J Kevenaar, E Polder, A Gaudry, C Florentz, M Sissler, MS van der Knaap, and GC Scheper. (2013). Pathogenic mutations causing LBSL affect mitochondrial aspartyl-tRNA synthetase in diverse ways. *Biochem J.* 450, 345–50.

van der Knaap, M. S., van der Voorn, P., Barkhof, F., Van Coster, R., Krageloh-Mann, I., Feigenbaum, A., Blaser, S., Vles, J. S., Rieckmann, P., & Pouwels, P. J. (2003). A new leukoencephalopathy with brainstem and spinal cord involvement and high lactate. *Ann Neurol*, 53(2), 252-258.

Van Goethem, G., Dermaut, B., Lofgren, A., Martin, J. J., & Van Broeckhoven, C. (2001). Mutation of POLG is associated with progressive external ophthalmoplegia characterized by mtDNA deletions. *Nat Genet*, 28(3), 211-212.

Van Goethem, G., Martin, J. J., Dermaut, B., Lofgren, A., Wibail, A., Ververken, D., Tack, P., Dehaene, I., Van Zandijcke, M., Moonen, M., Ceuterick, C., De Jonghe, P., & Van Broeckhoven, C. (2003). Recessive POLG mutations presenting with sensory and ataxic neuropathy in compound heterozygote patients with progressive external ophthalmoplegia. *Neuromuscul Disord*, 13(2), 133-142.

Van Goethem, G., Schwartz, M., Lofgren, A., Dermaut, B., Van Broeckhoven, C., & Vissing, J. (2003). Novel POLG mutations in progressive external ophthalmoplegia mimicking mitochondrial neurogastrointestinal encephalomyopathy. *Eur J Hum Genet*, 11(7), 547-549.

Vann, S. D., Aggleton, J. P., & Maguire, E. A. (2009). What does the retrosplenial cortex do? *Nat Rev Neurosci.* 10(11):792-802.

Vidal-Taboada, J. M., Mahy, N., & Rodríguez, M. J. (2011). Microglia, Calcification and Neurodegenerative Diseases. In R. Chuen-Chung Chang (Ed.), *Neurodegenerative Diseases - Processes, Prevention, Protection and Monitoring*

(pp. 301-322). InTech.

Wakasugi, K., Slike, B. M., Hood, J., Ewalt, K. L., Cheresch, D. A., & Schimmel, P. (2002a). Induction of angiogenesis by a fragment of human tyrosyl-tRNA synthetase. *J Biol Chem*, *277*(23), 20124-20126.

Wakasugi, K., Slike, B. M., Hood, J., Otani, A., Ewalt, K. L., Friedlander, M., Cheresch, D. A., & Schimmel, P. (2002b). A human aminoacyl-tRNA synthetase as a regulator of angiogenesis. *Proc Natl Acad Sci U S A*, *99*(1), 173-177.

Wallace, D. C. (2005). A mitochondrial paradigm of metabolic and degenerative diseases, aging, and cancer: a dawn for evolutionary medicine. *Annu Rev Genet*, *39*, 359-407.

Wang, J., Wilhelmsson, H., Graff, C., Li, H., Oldfors, A., Rustin, P., Bruning, J. C., Kahn, C. R., Clayton, D. A., Barsh, G. S., Thoren, P., & Larsson, N. G. (1999). Dilated cardiomyopathy and atrioventricular conduction blocks induced by heart-specific inactivation of mitochondrial DNA gene expression. *Nat Genet*, *21*(1), 133-137.

Weidberg, H., Shvets, E., & Elazar, Z. (2011). Biogenesis and cargo selectivity of autophagosomes. *Annu Rev Biochem*, *80*, 125-156.

Weisiger, R. A., & Fridovich, I. (1973). Mitochondrial superoxide simutase. Site of synthesis and intramitochondrial localization. *J Biol Chem*, *248*(13), 4793-4796.

Wek, R. C., & Cavener, D. R. (2007). Translational control and the unfolded protein response. *Antioxid Redox Signal*, *9*(12), 2357-2371.

Wenz, T., Rossi, S. G., Rotundo, R. L., Spiegelman, B. M., & Moraes, C. T. (2009). Increased muscle PGC-1 {alpha} expression protects from sarcopenia and metabolic disease during aging. *Proc Natl Acad Sci U S A*. *106*(48), 20405-10.

Wibom, R., Hagenfeldt, L., & von Döbeln, U. (2002). Measurement of ATP production and respiratory chain enzyme activities in mitochondria isolated from small muscle biopsy samples. *Anal Biochem*, *311*(2), 139-151.

Wolstenholme, D. R., Macfarlane, J. L., Okimoto, R., Clary, D. O., & Wahleithner, J. A. (1987). Bizarre tRNAs inferred from DNA sequences of mitochondrial genomes of nematode worms. *Proc Natl Acad Sci U S A*, *84*(5), 1324-1328.

Wredenberg, A., Wibom, R., Wilhelmsson, H., Graff, C., Wiener, H. H., Burden, S. J., Oldfors, A., Westerblad, H., & Larsson, N. G. (2002). Increased mitochondrial mass in mitochondrial myopathy mice. *Proc Natl Acad Sci U S A*, *99*(23), 15066-15071.

Xu, B., Zang, K., Ruff, N. L., Zhang, Y. A., McConnell, S. K., Stryker, M. P., & Reichardt, L. F. (2000). Cortical degeneration in the absence of neurotrophin signaling: dendritic retraction and neuronal loss after removal of the receptor TrkB. *Neuron*, *26*(1), 233-245.

Xu, J., Lloyd, D. J., Hale, C., Stanislaus, S., Chen, M., Sivits, G., Vonderfecht, S., Hecht, R., Li, Y. S., Lindberg, R. A., Chen, J. L., Jung, D. Y., Zhang, Z., Ko, H. J., Kim, J. K., & Veniant, M. M. (2009). Fibroblast growth factor 21 reverses hepatic steatosis, increases energy expenditure, and improves insulin sensitivity in diet-induced obese mice. *Diabetes*, *58*(1), 250-259.

Yang, Z., & Klionsky, D. J. (2010). Eaten alive: a history of macroautophagy. *Nat Cell Biol*, *12*(9), 814-822.

Yoneda, T., Benedetti, C., Urano, F., Clark, S. G., Harding, H. P., & Ron, D. (2004). Compartment-specific perturbation of protein handling activates genes encoding mitochondrial chaperones. *J Cell Sci*, *117*(Pt 18), 4055-4066.

Young, J. C., Hoogenraad, N. J., & Hartl, F. U. (2003). Molecular chaperones Hsp90 and Hsp70 deliver preproteins to the mitochondrial import receptor Tom70. *Cell*, *112*(1), 41-50.

Zeviani, M., Muntoni, F., Savarese, N., Serra, G., Tiranti, V., Carrara, F., Mariotti, C., & DiDonato, S. (1993). A MERRF/MELAS overlap syndrome associated with a new point mutation in the mitochondrial DNA tRNA(Lys) gene. *Eur J Hum Genet*, *1*(1), 80-87.

Zhang, M., Mileyskoykaya, E., & Dowhan, W. (2005). Cardiolipin is essential for organization of complexes III and IV into a supercomplex in intact yeast mitochondria. *J Biol Chem*, *280*(33), 29403-29408.

Zhao, Q., Wang, J., Levichkin, I. V., Stasinopoulos, S., Ryan, M. T., & Hoogenraad, N. J. (2002). A mitochondrial specific stress response in mammalian cells. *EMBO J*, *21*(17), 4411-4419.

Zong, H., Ren, J. M., Young, L. H., Pypaert, M., Mu, J., Birnbaum, M. J., & Shulman, G. I. (2002). AMP kinase is required for mitochondrial biogenesis in skeletal muscle in response to chronic energy deprivation. *Proc Natl Acad Sci U S A*, *99*(25), 15983-15987.

Acknowledgements

It was a fascinating journey; that is for sure! Getting used to a different country, a different culture, basically different everything! This time, you also don't have your parents and your friends to help you through this crazy ride but apparently you can get used to anything and you can make new friends and family wherever you are!

The person I should be thankful the most is Sandra. Our story began years before, exactly on 13.10.2006 at 22:18:51 –more than 7 years!- when I sent her this email:

“Dear Dr. Trifunovic,

This is Anil Dogan, a 2nd - and last - year master's student at Biological Sciences Department, Middle East Technical University, Ankara, Turkey. (I had my BSc degree at Molecular Biology and Genetics Department of the same university)...

...I had the opportunity to listen to Nils-Göran Larsson at 5th European Congress of Biogerontology (September 16 - 20), Istanbul, Turkey, where I had a poster presentation. I was also very interested in his research beforehand. He mentioned about you and your research a lot during his speech. You are exactly conducting my dream research. I could not find satisfactory information about you, your lab, etc. in the Mitochondrial Medicine Center's website. So, I decided to write to you about the Ph.D opportunities. I am checking the website www.mitomed.se for vacancies but - if it is not going to be rude - would like to ask you if you are planning to have a Ph.D student for Fall 2007. If you do so, should I apply to Karolinska or your center directly? Or should I just keep checking on the announcements on your website?

I have asked quite a lot of questions. If you could find time and answer them, I would really appreciate.”

I was a hopeful, and as you can see extremely kind, master's student at that time, wishing his studies would finish soon :) That was not the case. Anyways, she replied to me 3 days later:

“Dear Anil,

I am glad that you are interested in my research. I am currently on maternity leave and I will start working again from January next year. At the moment I have two PhD students and I am hoping to get another post-doc very soon. I could be interested in your application. I think that you should come and visit us sometimes during spring and meet people in the lab. I am also starting a big project on *C. elegans* and your experience would be just an advantage. Please send me your CV and we will keep in touch.

Best,

Aleksandra”

The day I received this email, I knew that I would go to Sandra's lab and work for her; nothing would stop me. After this, I started to look for ways to be able to visit her lab and 'meet the people' as she suggested. Thanks to my journalism past, I found a great scholarship and went to Sweden as a science journalist visiting Karolinska Institutet (see dear PIs, you should be careful about what you are writing to prospective students :)) I was there for a week during 25.05.2008-01.06.2008 and the last day, Sandra took me aside and asked me what I would like to do with my life. I said 'This is what I want!' She told me that she would be very happy to have me as her PhD student but that they are moving to Germany :) I guess, till today, it was the best day of my life. One more year passed till I managed to be a part of her lab but finally I was there on 09.11.2009 [So, dear reader, as you can see, stalking sometimes pays :)] Now, more than four years later, and if you ask me whether I would do something differently, my answer will be 'NO'! I always knew the time I would spend in her lab would be great, and it was. I consider myself one of the lucky ones who had the opportunity to be trained by the master herself :) Sandra is not only a great scientist and the smartest

person I know, but also the nicest, the best cook, the know-it-all (the subject can be TV series or opera, does not matter) person ever. My friends know that sometimes I refer to myself as ‘perfection in human form’: that might not be true for myself but for sure for Sandra! One day, even if I am lucky enough to have my own lab, Trifunovic lab will always be ‘my lab’, where I belong and of where I will always carry the honor of being a graduate of (of course till then Sandra will be the greatest mitochondrial researcher ever).

Second, I would like to pay my regards to my mother Ayla İlaslan, my grandmother Fatma İlaslan, my brother Arda Doğan, my aunt Zehra Kıran and my uncle Eyüp İlaslan for their reliance on me. Especially, my mother who never gave up believing in me... I could not succeed without you.

Throughout this PhD marathon, my dear friends were always there. This time, we were miles apart but still they found a way to be a part of my life. Davut Onur Dağlıoğlu-Esin Kömez, Evren-Ceyda Poyraz, Vefizoom-İpek Karaege, Gizem Kolbaşı, Aslı Torun, Hakan Demirbilek, Çağlayan-Feride Irmak, Ercüment-Altınay Yörük, Hüseyin Yıldırım, Alten Oskay, Güneş Gökmen... I don’t see you as friends anymore but as my extended family. I don’t know how to thank for everything we have ever shared. I am dreaming of being close to you again, every day!

Another huge ‘Thank you’ goes to my family in Cologne: Özlem Karalay, Mehmet Deniz Akyüz, Melek Emine Akyüz and Ömer Oğul Öncel. I do not know how my life would be without you guys. It is amazing to have you in my life.

My lab mates Dr. Alexandra Kukat, Dr. Ivana Bratic-Hench, Dr. Marija Herholz, Dr. Karolina Szczepanowska, Dr. Rozina Kardakari, Priyanka Maiti, Estela Cepeda, Christina Becker, Dominic Seiferling, Marijana Aradjanski, Linda Baumann, Katharina Senft... To be able to work with you was really nice;

especially with my crazy, and at the same time great, student Stephan Lotter, who is gonna have to deal with me a bit more till I leave.

I had this idea that after some age it is impossible to make new friends, apparently I was dead wrong! My dearest Claire Pujol, my bro Victor Pavlenko and my kiro Steffen Hermans... Thank you for everything, without you Cologne would be impossible to bear:

I have learned so much from Claire: about science, music, art, and being nice. It was just my luck and privilege to be able to work with you and be your friend; without you I would not be the person I am today. Unfortunately, you are also the person who suffered from my mood swings the most; well, I was not that bad, was I?

My bro Victor: I have bothered you a lot but it is all because I truly enjoy your company. Your 'dostluk' (in Turkish we differentiate friend and 'dost') and our talks over a coffee or a beer were, most of the time, what kept me from being completely depressed. You are basically the only reason why I wanna earn more than a million dollars/year (Canadian of course!), so I can hire you. I hope everything is going to turn out great for you because your golden heart deserves the best (I had to put a touchy sentence here to annoy you)!

Steffen, without you, I would not know whom to hug. I am also grateful that, together, we made Germany to learn the word 'kiro'.

Other friends from various labs (mostly Brüning people) also made the life bearable with their constant energy, coffee breaks and helping hands –either with experiments or hugs-. I truly enjoyed sharing our floor and life for 4 years.

I would like to thank Prof. Dr. Elena Rugarli, Prof. Dr. Matthias Hammerschmidt, Prof. Dr. Thomas Langer, Dr. Tina Wenz, Prof. Dr. Nils-Göran Larsson and amazing people in their labs for all the discussions, valuable insights, help and friendship throughout my PhD period.

Erklärung

Ich versichere, dass ich die von mir vorgelegte Dissertation selbständig angefertigt, die benutzten Quellen und Hilfsmittel vollständig angegeben und die Stellen der Arbeit - einschließlich Tabellen, Karten und Abbildungen -, die anderen Werken im Wortlaut oder dem Sinn nach entnommen sind, in jedem Einzelfall als Entlehnung kenntlich gemacht habe; dass diese Dissertation noch keiner anderen Fakultät oder Universität zur Prüfung vorgelegen hat; dass sie - abgesehen von unten angegebenen Teilpublikationen - noch nicht veröffentlicht worden ist sowie, dass ich eine solche Veröffentlichung vor Abschluss des Promotionsverfahrens nicht vornehmen werde.

Die Bestimmungen der Promotionsordnung sind mir bekannt. Die von mir vorgelegte Dissertation ist von Prof. Dr. Aleksandra Trifunovic betreut worden.

Köln, den 27.03.2014

(Şükrü Anıl Doğan)

Teilpublikationen

Artikel

Dogan, S. A., Pujol, C., Maiti, P., Kukat, A., Wang, S., Hermans, S., Senft, K., Wibom, R., Rugarli, E. I., & Trifunovic, A. (2014). Tissue-Specific Loss of DARS2 Activates Stress Responses Independently of Respiratory Chain Deficiency in the Heart. *Cell Metab*, 19(3), 458-469

Curriculum Vitae

Sukru Anil Dogan

PERSÖNLICHE DATEN

Adresse CECAD, Universität zu Köln, Institut für Genetik, Zülpicher Str. 47a,
50674, Köln, Deutschland
Email anil.dogan@uni-koeln.de
Geburtsdatum / -ort Oktober 06, 1982 / Malatya, Türkei
Staatsangehörigkeit Türkisch

AUSBILDUNG

10/2009 – 01/2014 – **Doktorarbeit** am Cologne Cluster of Excellence on Cellular Stress Responses in Aging-associated Diseases (CECAD), Köln, Deutschland
Prof. Dr. Aleksandra Trifunovic
Mitochondrial aspartyl-tRNA synthetase (DARS2) Deficiency in Mice

09/2005 – 02/2009 – **Diplomarbeit** der Molekulare Biologie und Genetik an der Orta Dogu Teknik Universitesi (ODTU), Ankara, Türkei
Prof. Dr. Inci Togan
Reassessment of Genetic Diversity in Native Turkish Sheep Breeds with Large Numbers of Microsatellite Markers and Mitochondrial DNA (mtDNA)

09/2000 – 08/2005 – **Studium** der Molekulare Biologie und Genetik an der Orta Dogu Teknik Universitesi (ODTU), Ankara, Türkei

PUBLIKATIONEN

- Kukat, A., **Dogan, S. A.**, Edgar, D., Mourier, A., Jacoby, C., Maiti, P., Mauer, J., Becker, C., Senft, K., Wibom, R., Kudin, A. P., Hultenby, K., Flogel, U., Rosenkranz, S., Ricquier, D., Kunz, W. S., Trifunovic, A. UCP2 attenuates mitochondrial dysfunction independently of ROS production and uncoupling activity. *PLoS Genetics*, *in press*.
- **Dogan, S. A.***, Pujol, C. *, Maiti, P., Kukat, A., Wang, S., Hermans, S., Wibom, R., Rugarli, E. I., Trifunovic, A. (2014) Tissue-specific loss of DARS2 activates stress responses independently of respiratory chain deficiency in the heart. *Cell Metabolism* 19(3), 458–469. * *Equal contribution*

- Demirci, S., Koban Bastanlar, E., Dagtas, N. D., Piskin, E., Engin, A., Ozer, F., Yuncu, E., **Dogan, S. A.**, Togan, I. (2013). Mitochondrial DNA Diversity of Modern, Ancient and Wild Sheep (*Ovis gmelinii anatolica*) from Turkey: New Insights on the Evolutionary History of Sheep. *PLoS One*, 8(12), e81952.
- Yuncu, E., Demirci, S., Koban-Bastanlar, E., **Dogan, S. A.**, Tasdemir, U., Togan, I. (2013). Comparative study of three simple molecular approaches in search of mtDNA haplogroup identification of domestic sheep. *Small Ruminant Res*, 114(1), 64-71.
- **Dogan, S. A.**, & Trifunovic, A. (2011). Modelling mitochondrial dysfunction in mice. *Physiol Res*, 60 Suppl 1, S61-70.

VORTRÄGE

Mitochondrial aspartyl-tRNA Synthetase (DARS2) deficiency in mice

- Gordon Research Conferences on Bioenergetics (06/2013, Andover, NH, USA) (*Kurzer Vortrag*)
- 1st CECAD Graduate Symposium (11/2012, Cologne, Germany) (*Vortrag*)
- 16th Biennial Meeting of “Society for Free Radical Research International” (09/2012, London, UK)
- 11th International Symposium on Neurobiology and Neuroendocrinology of Aging (08/2012, Bregenz, Österreich)
- 8th European Meeting on Mitochondrial Pathology (06/2011, Zaragoza, Spainen)
- 61. Mosbacher Kolloquium - The Biology of Aging: Mechanisms and Intervention (04/2010, Mosbach/Baden, Deutschland)

Genetic Diversity in Turkish Native Sheep Breeds Based on Two Types of Genetic Markers

- 4th International Symposium on Health Informatics and Bioinformatics (04/2009, Ankara, Türkei)

Rescuing Larval Arrest Initiated by Mitochondrial DNA Deficiency in *C. elegans*

- 5th European Congress of Biogerontology (09/2006, Istanbul, Türkei)